UNIVERSITY OF SOUTHERN QUEENSLAND
AUSTRALIA

DETECTING BINARY STAR PLANETARY AND BROWN DWARF COMPANIONS FROM ANALYSIS OF ECLIPSE TIMING VARIATIONS

A Thesis Submitted by

Alan Kelvin Getley, M.Astron., B.Sc.

For the Award of

Doctor of Philosophy

2021

ABSTRACT

Binary stars have long been known to show mutual and precisely periodic eclipses, if their orbit is favourably inclined to our line of sight. However, more recently space telescope missions such as Kepler have provided long-term precision light-curves for thousands of stars, enabling analyses of binary star eclipse timing variations to search for perturbing low-mass sub-stellar companions, namely brown dwarfs and planets. This thesis thus comprises three interrelated studies, as follows.

(1) The extent to which eclipse time variations can detect binary star low-mass bodies is simulated for Kepler Eclipsing Binary Star Catalog stars using empirical data from the catalog as a starting point. The analysis finds that even planetary mass companions are readily detectable with eclipse time variations, although successful detection is strongly dependent on the orbital period of the host eclipsing binary star, and the orbital period and eccentricity of the third body. The detectable range of companion body masses and orbital periods also can be reliably estimated simply, using just two equations.

(2) In a study of orbital dynamics, for those binary stars found to produce complex eclipse timing variations, their evolving system orbital configuration is inferred, and their long-term dynamical stability is simulated. The analysis finds that even complex eclipse time variations are explainable by low-mass, even planetary, companions in stable orbits, and where highly eccentric third bodies around eccentric binary stars can explain a complex "flip-flop" feature seen in some observed-calculated diagrams. For some proposed new low-mass companions, the simulated orbits are expected to be stable over long dynamical timescales, with the companions remaining detectable.

(3) In terms of new planetary detections, in a study of KIC 5095269, a plan-

etary mass companion has been found in a highly inclined orbit relative to the orbit of the host stars. The eclipse time variation analysis for this system indicates a 7.70 Jupiter mass planet in a 237.7 day orbit, stable for at least ten million years.

In conclusion, this thesis has established the feasibility of eclipsing timing variations as a way to survey binary stars for brown dwarf and planetary companions. In the future, space telescope surveys such as those being done by the Transiting Exoplanet Survey Satellite (TESS) will accrue additional useful eclipsing binary star light curves, and enable more extensive searches for binary star low-mass companions.

CERTIFICATION OF THESIS

This Thesis is the work of Alan Kelvin Getley except where otherwise acknowledged, with the majority of the authorship of the papers presented as a Thesis by Publication undertaken by the Student. The work is original and has not previously been submitted for any other award, except where acknowledged.

Doctor Bradley Carter
Principal Supervisor

Doctor Rachel King
Associate Supervisor

Doctor Simon O'Toole
Associate Supervisor

Student and supervisors signatures of endorsement are held at the University.

LIST OF CONTRIBUTIONS FROM PUBLICATION CO-AUTHORS

This section details contributions by the various authors for each of the papers presented in this thesis by publication.

Chapter 2, Getley et al. (2021):

Getley, A. K., B. Carter, R. King, and S. O'Toole (2021). "The detectability of binary star planetary and brown dwarf companions from eclipse timing variations". *Monthly Notices of the Royal Astronomical Society* 504.3, pp. 4291–4301.

Author	Percent Contribution	Tasks Performed
A. K. Getley	85	Performed target selection, simulations, analysis, interpretation, wrote all drafts of paper, conception of project.
B. Carter R. King S. O'Toole	15	Conception of project, interpretation, suggested edits to manuscript.

Chapter 3, Getley et al. (2020):

Getley, A. K., B. Carter, R. King, and S. O'Toole (2020). "Stability of planetary, single M dwarf, and binary star companions to Kepler detached eclipsing binaries and a possible five-body system". *Monthly Notices of the Royal Astronomical Society* 498.3, pp. 4356–4364.

Author	Percent Contribution	Tasks Performed
A. K. Getley	85	Performed target selection, simulations, analysis, interpretation, wrote all drafts of paper, conception of project.
B. Carter R. King S. O'Toole	15	Conception of project, interpretation, suggested edits to manuscript.

Chapter 4, Getley et al. (2017):

Getley, A. K., B. Carter, R. King, and S. O'Toole (2017). "Evidence for a planetary mass third body orbiting the binary star KIC 5095269". *Monthly Notices of the Royal Astronomical Society* 468, pp. 2932–2937.

Author	Percent Contribution	Tasks Performed
A. K. Getley	85	Performed target selection, wrote code, analysis, interpretation, wrote all drafts of paper, conception of project.
B. Carter R. King S. O'Toole	15	Conception of project, interpretation, suggested edits to manuscript.

ACKNOWLEDGEMENTS

This research was supported by an Australian Government Research Training Program (RTP) Scholarship.

My thanks go out to the University of Southern Queensland. It wasn't easy finding a university willing to take on an off-campus PhD student. The University of Southern Queensland embraces and supports remote learning options so that achievements like this are increasingly available to those who would otherwise miss out.

A big thanks to my supervisors (and co-authors), Drs Brad Carter, Rachel King and Simon O'Toole. I can't imagine a better, more supportive, supervisory team than mine. Without their guidance, support and understanding I wouldn't have made it this far.

I would also like to thank my friends and family. In particular my mum, Lorna-Mary, and my dad, Alan. They are always there when I need them, supporting me in every way possible and it would have been impossible for me to do this without them. For those who I've lost along the way, I carry you with me every day.

Finally, I would like to specifically acknowledge and thank my grandad, Neville Timothy Bush (Tim; 1924 - 2016). I've been interested in astronomy for as long as I can remember and that's all thanks to his interest in astronomy. I was reading his collection of astronomy books for as long as I've been able to read. Without him, I wouldn't be here.

CONTENTS

LIST OF FIGURES

LIST OF TABLES

CHAPTER 1

INTRODUCTION

Binary stars are systems composed of two stars that orbit a common centre of gravity and are an excellent source of information on fundamental stellar properties. The orbits of the component stars and Kepler's laws can be used to determine properties, such as the mass, of the binary star components. Binary stars thus can provide precise physical measurements difficult or impossible to obtain from observing single stars.

Often the distance and separation are such that the two components cannot be resolved and appear as a single point of light. As such, binary stars are classified into a number of different types, usually based on the method of detection (Carroll and Ostlie 2007; Jain 2015). The classifications are 1) visual, 2) spectroscopic, 3) astrometric and 4) eclipsing.

Visual binary stars are when two bound stars are separated enough for the individual stars to be resolved using a telescope (Kovaleva et al. 2016) and have a visual orbit. The brightness of the individual stars may affect the identification of a visual binary star. If one star is significantly brighter than the other, the second star may be obscured and visually unidentifiable. Without viewing the orbit of the binary, two stars may appear visually close however may not be gravitationally bound.

Spectroscopic binaries are identified by the periodic variations of the Doppler shift in the spectral lines of the light from the component stars (Kopal 1979). The spectral lines from a star shifts towards the blue as the star moves towards us and then shifts towards the red as the star moves away. It is possible for the spectral lines from both stars to be observed, resulting in a double-lined spectroscopic binary, or just one star, resulting in a single-lined spectroscopic binary (Konacki et al. 2010).

Astrometric binaries are identified when one star can be seen to orbit around centre of mass with a secondary, unseen, star. The secondary star may be too small or too faint to be observed or may possibly be a black hole or neutron star (Andrews, Breivik, and Chatterjee 2019). By using properties from the observable star and Kepler's laws, the properties of the secondary star, and the system as a whole, are able to be determined (Descamps 2005).

Eclipsing binaries, and the timing of the eclipses, are the focus of this thesis and are discussed in section 1.1.

More detail on these binary star classifications can be found in Carroll and Ostlie (2007).

1.1 Eclipsing Binary Stars

Eclipsing binaries are identified when the orbital plane of the two component stars align with the Earth so that the stars eclipse each other. As one star passes in front of the other some, or all, of the light from the other star is blocked. This dimming of the light can be measured from Earth to determine some of the orbital characteristics of the system, such as the orbital period of the binary star and the relative sizes of the component stars (Kopal 1979). A detailed review in determining the various properties of the individual stars found in eclipsing binaries is presented in Southworth (2012).

Eclipsing binary stars can provide valuable information about the component stars such as details on the system and component mass and radii. With this information, stellar evolution models can be tested (Kirk et al. 2016). Of the more than 200,000 targets observed by the Kepler mission, only 2,878 targets (or $\sim$1.3%) were found to be eclipsing binaries. As such while eclipsing binaries are extremely useful to gather information the necessary geometrical requirements to observe eclipses makes them rare occurrences.

A primary eclipse occurs when the hotter primary star eclipses the cooler secondary star, while a secondary eclipse occurs when the cooler secondary star eclipses the hotter primary star (figure 1.1). For main sequence stars, the primary star is larger than the secondary star. However, an evolved star can be larger and cooler than a hotter, smaller, main sequence star. Depending on the inclination of the system, secondary eclipses may be shallow or may not be observable at all.

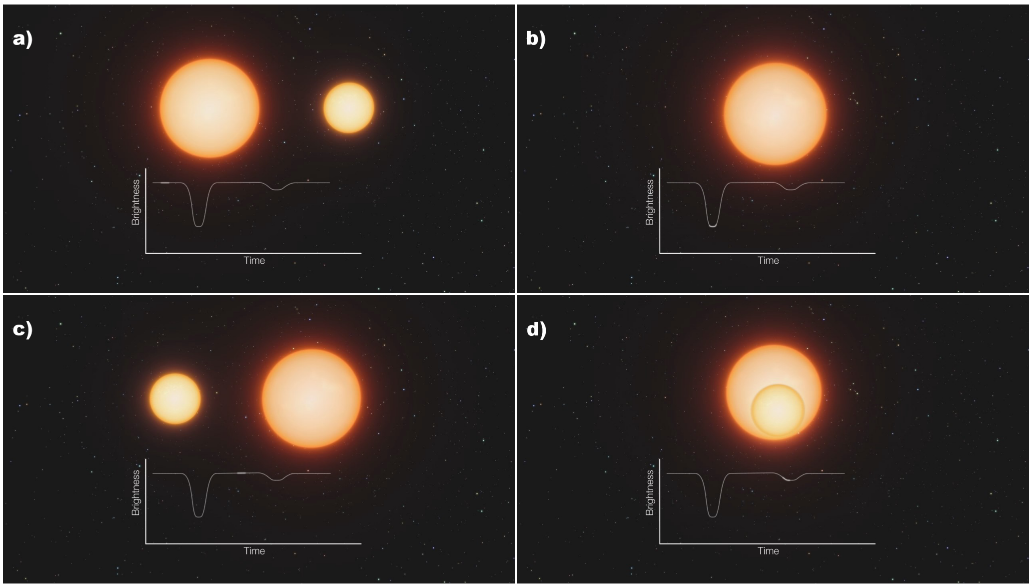

Figure 1.1: Frames from a video showing an artist's impression of an eclipsing binary. Video by ESO/L. Calçada (https://www.eso.org/public/videos/eso1311b/; retrieved 3 December 2020.). a) The two stellar components of the system are completely separated. As a result, the brightness of the system is at its maximum. b) The evolved, larger but cooler, star completely covers the hotter star resulting in the brightness of the system being at its minimum. c) After half an orbit, the two stellar components are completely separated again and the brightness returns to a maximum. d) The hotter star partially covers the evolved, larger but cooler, star. The brightness of the system decreases from its maximum (but not as much as its minimum).

In systems that consist of just the two stars, in the simplest case the times between minima will be consistent and can be accurately predicted. The times of the nth eclipse, t_n, can be determined by from the period, p and the first eclipse time, t_0:

$$t_n = pn + t_0 \tag{1.1}$$

As eclipse times can be accurately predicted, the actual (or observed) eclipse times can be compared to the predicted time to look for eclipse time variations.

1.1.1 Eclipse Time Variations

In systems where there is a third body, the gravitational effects of the third body on the binary stars will lead to variations in the times of the minima. As such variations in the eclipse timings of binary stars may alert us to the presence of previously unknown or unseen third bodies. Third bodies could be planets, brown dwarfs or a third stellar companion. The variations in the times of the minima can be seen by plotting Observed (O) eclipses times minus Calculated (C) eclipse times vs time, forming an O-C diagram. Deviations from a linear ephemeris can then be easily viewed (figure 1.2).

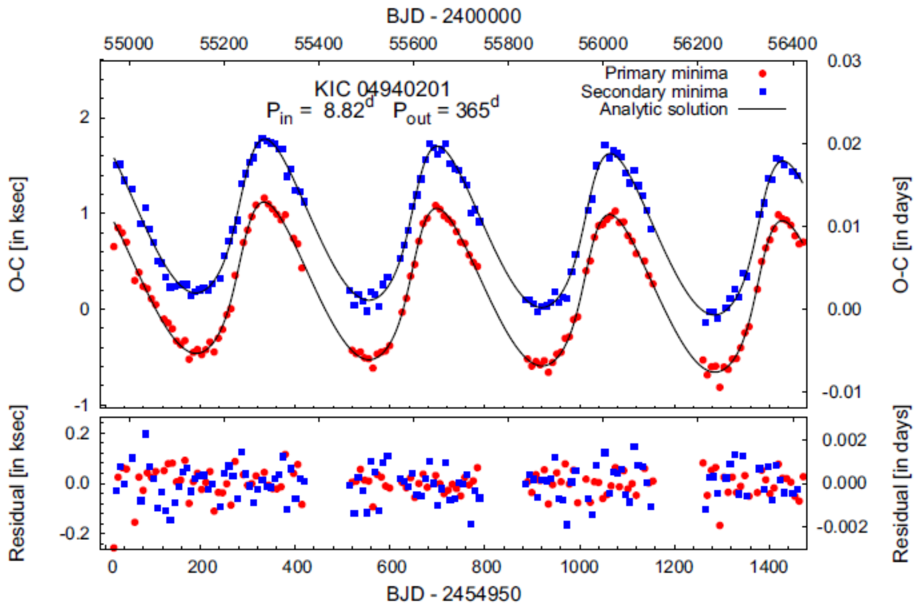

Figure 1.2: O-C diagram for KIC 04940201. Primary eclipse variations are shown by the red circles while the secondary eclipse variations are shown by the blue squares. Periodic deviations from a linear ephemeris can be seen. Image reproduced from Borkovits et al. (2015).

While periodic variations may be the result of a third body within the system, there are a number of other sources of variability that need to be considered when comparing eclipse times. Variations may also be caused by 1) star spots, 2) apsidal motion or precession (discussed in more detail in section 1.1.2) or 3) tidal deformations. Star spots crossing the surface of the stars can distort the shape and depth of eclipses which may lead to systematic trends in the eclipse times (Orosz et al. 2012). Star spots also appear as quasi-periodic modulation in the light curve outside the eclipse regions.

Binary stars that are in a close pair exert tidal effects on the component stars (Hilditch 2001). These effects distort the shape of the component stars and affect the orbit of the close binary star and may explain the variations seen in some O-C diagrams (Borkovits et al. 2003).

1.1.2 Apsidal Motion

Apsidal motion is the rotation of the axis within its own plane (Hilditch 2001). For purely circular orbits, i.e. when all points in an orbit are at periastron, there can be no apsidal motion. As such, only eccentric orbits can exhibit apsidal motion. Apsidal motion may be due to a third body within a system (Bozkurt and Değirmenci 2007) or entirely independent of a third body.

Apsidal motion that is independent of a third body may be due to relativistic effects, mutual tidal deformations or deformations of the components due to axial rotation (Petrova and Orlov 2002; Orosz 2015). When general relativity or tidal effects are the cause of apsidal motion, eclipse time variations will appear sinusoidal with the primary and secondary eclipse time variations being "out of phase" by approximately 180 degrees. Classical apsidal motion produces a sinusoidally varying time shift (Beuermann et al. 2010) with ranges from a few years to a few centuries.

As general relativity and tidal effects produce distinctive timing signatures, the source of apsidal motion (i.e. third body induced or natural to the system) can be assumed. If a third body is determined to be the cause of apsidal motion, the rate of apsidal motion caused by a third body is able to be calculated (Bozkurt and Değirmenci 2007).

1.2 Planet Formation

Where the periodic variations are due to the effects of third bodies, characterisation of the planet properties are of key interest. Planet formation is considered to be dominated by core accretion, however the alternative disc instability mechanism has been proposed to explain gas giant planets and brown dwarfs. In core accretion, a rocky core is formed when rocky particles collide and stick together.

The rocky core is then able to accrete gaseous material to form larger planets (Liu et al. 2018). With disc instability, a protoplanetary disc breaks up due to gravitational instability forming clumps of gas which evolve in to planets (Boss 2012; Chabrier et al. 2014). It is also argued (Nordlund 2011) that the separation of planets and brown dwarfs would be more physically meaningful if separated by formation method rather than a convenient mass divide of 13 Jupiter masses.

A key way to constrain formation models and to help understand formation and classification of third bodies is to locate more third bodies so that frequency, masses, orbits and stability predictions can be tested and, if necessary, refined. There have been a large number of planets orbiting other stars other than our own, however very few of these have been orbiting around binary stars. As of March 2021, there are more than 4,300 exoplanets known listed in the NASA Exoplanet Archive[1]. However, of these there are only around 12 or so confirmed circumbinary planets (Doyle 2019). The galactic population of circumbinary planets is calculated to be at least several million (Welsh et al. 2012).

1.3 The Kepler Mission

In 2009, the Kepler space telescope was launched with the aim of surveying our region of the Milky Way galaxy to locate planets of Earth's size or smaller and to explore the structure and diversity of planetary systems. The Kepler field of view was required to never be blocked at any point throughout the year. As such the field of view was outside the ecliptic plane to avoid the Sun. To maximise efficiency, as many stars as possible needed to be observable in the field of view. More than 150,000 stars were observed in the hopes of observing planetary transits (Borucki et al. 2010). One of the benefits of observing so many stars with high precision is finding a large number of eclipsing binary stars.

The loss of two of the four reaction wheels on the Kepler spacecraft in 2013 resulted in the ending of the Kepler mission and the start of the K2 mission in 2014 (Howell et al. 2014). Despite the loss of the reaction wheels, the K2 mission has a photometric precision approaching the level of the original Kepler mission (Libralato et al. 2016) and as such still provides high precision observations for

[1] https://exoplanetarchive.ipac.caltech.edu/index.html

the targets. However, fields were limited to the ecliptic and observations were limited to ~ 60 days. No K2 Data was used in this thesis.

1.4 Detecting Third Bodies

There are two types of planetary bodies that can be part of binary star systems. The first type is the S-type planet, where a planet orbits just one of the two stars. The second type is the P-type planet where a planet orbits both of the stars. This is illustrated in figure 1.3. Eclipse timing variation studies have successfully detected P-type planets (Schwarz et al. 2011).

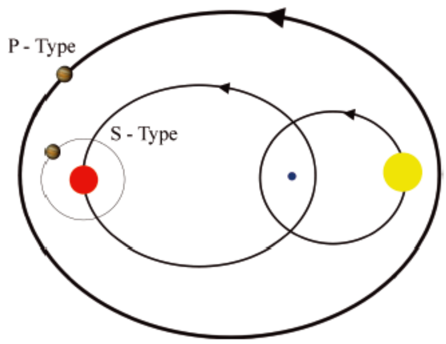

Figure 1.3: The stellar components of the binary system are shown by the red and yellow circles. The centre of mass of the system is denoted by the small blue circle. S-type planets are those which orbit one of the two stellar components, while P-type planets orbit both stellar components. Image reproduced from Schwarz et al. (2011)

.

With the high precision observations of eclipsing binary stars, we are able to accurately determine the mid-eclipse times for every eclipse observed within a system. These eclipse times can be used to determine a linear ephemeris and produce an O-C diagram to look for eclipse time variations.

A program called Transit Analysis Package or TAP (Gazak et al. 2012) is designed to detect the time of eclipses seen in binary stars. TAP automatically detects eclipses in a light curve. Automatic eclipse detections allow whole data sets to be processed at once rather than individually selected eclipses. TAP uses the functions found in Mandel and Agol (2002). The functions use the system parameters: orbital period, radius ratio of the two objects, scaled semi-major axis, orbital inclination, orbital eccentricity, argument of periastron, mid-time of the eclipse/transit and two parameters specifying quadratic limb-darkening, to describe a system at various points around an orbit for various size objects. These points include:

1. The star/s are unobstructed (i.e. no eclipse or transit is taking place)
2. An object lies on the limb of a star but doesn't cover the centre of the star
3. An object lies entirely within the stellar disc but doesn't cover the stellar centre
4. An object touches the centre of the stellar disc and entirely lies within the stellar disc
5. The object's diameter equals the radius of the star and touches both the stellar centre and the limb of the star
6. The edge of the object's disc touches the stellar centre, but the object is not entirely contained within the stellar disc
7. The object covers the centre and the limb of the stellar disc
8. The object's disc lies entirely within the stellar disc and the object covers the stellar centre
9. The object is concentric with the disc of the star
10. The object completely eclipses the star (likely another star)

Each parameter describing a system can be locked or unlocked. When unlocked the parameter will be adjusted to find the best-fit value. When locked, the input value will remain fixed. Markov Chain Monte Carlo (MCMC) techniques are used to fit light curves using the Mandel and Agol (2002) points above. With a model obtained, the mid-eclipse times for a system can be obtained.

There are a number of different features that can be seen within O-C diagrams (Borkovits et al. 2015; Borkovits et al. 2016). These include: 1) long term trends (both in and out of phase). It is possible that long term trends are actually periodic variations and the observation period was too short to observe a full variation period; 2) periodic variations. Periodic variations are variations that are shown to repeat with a regular and consistent period; 3) sudden/rapid changes in the variations. The variations seen in O-C diagrams may initially appear to be periodic or exhibit long term trends but then suddenly undergo a rapid change where eclipses go from occurring earlier than calculated to later than calculated (or vice versa) in a short period of time. Despite the wide ranging features that can be seen in O-C diagrams, additional bodies of varying masses and orbital characteristics can cause these O-C variations. For example, KIC 7821010 reportedly has a third body mass in the planetary range of 2.6 Jupiter masses while KIC 5952403 has a reported third body mass of 3 solar masses and would be a tertiary star (Borkovits et al. 2016).

There are a number of different techniques that can be used to detect additional bodies around stars in addition to transit/eclipse timing variations. These techniques include (but are not limited to) direct observation, radial velocity and transit photometry. Direct observations require the light of the additional body to be bright enough to be observed with a separation great enough to be resolved (Kalas et al. 2008). As an additional body moves around the parent stars the motion will have an effect on the radial velocity the parent star/s. As the additional body's orbit becomes more inclined, the effect on the radial velocity decreases and makes detection of the additional body more difficult. This also results in uncertainty in the mass estimates of the third body (Rodler, Lopez-Morales, and Ribas 2012). Transit photometry observes the drop in light from the parent star/s as the additional body passes in front of a star. This requires the additional bodies to have orbital inclinations specific enough to observe the body passing in front of a star.

However, while some of these techniques require certain orbital characteristics of the third body in order to be detected, for example to detect additional bodies via transits the additional bodies must have an orbital plane that aligns with Earth (Rodler, Lopez-Morales, and Ribas 2012), eclipse timing variations can detect additional bodies whether the additional bodies align with Earth or not. All bodies in a system have an effect on the host star/s as such the limiting factor in whether timing variations can be used to detect third bodies around an eclipsing system is the accuracy of the observed eclipse times. Without accurate eclipse times, variations may not be found or may lead to incorrect detections or characterisations of any additional bodies (Borkovits et al. 2015).

Modelling of a system with a third body present may be able to explain the observed eclipse time variations. However, more must be done to ensure the accuracy of the third bodies properties and orbital characteristics and therefore the actual existence of the third body itself. The dynamical stability of a proposed system should be tested to check the orbits are stable. Third bodies in unstable orbits are likely to be ejected from the system in relatively short timescales. Given the unlikeliness of planets forming and being observed within that time frame it is much more likely that planets with the given orbital characteristics don't exist. There have been a number of planetary mass bodies detected whose existence were questioned after dynamical stability studies of these systems were presented.

One example is the NN Serpentis system studied by Beuermann et al. (2010). Two scenarios were proposed for the existence of two planets in the system. The first had the planets in a 2:1 mean-motion resonance (MMR), while the second had the planets in a 5:2 MMR. In the analysis the eccentricity of the more massive planet was constrained to zero. A follow up stability study of the system by Horner et al. (2012b) found that the proposed orbits are dynamically feasible. However, re-analysing the system without the artificial constraint of a zero eccentricity for the more massive planet found a non-zero eccentricity provided a better fit to the observational data. A dynamical study of this new solution found the orbits for the less massive planet to be highly unstable. As such, while the proposed architecture of the system is dynamically stable, further observations of the system are required to identify the system's true nature as even the slightest change in the eccentricity of the outer, more massive, planet results in an unstable system.

A dynamical investigation into the HD 181433 planetary system by Horner et al. (2019) found the system to be dynamically unstable for a wide range of orbital eccentricities, semi-major axis and mutual inclinations. A dynamical stability study of an alternative proposed architecture provided greater stability while a re-fit with additional observations provided a new architecture for the system that was dynamically stable for a wide range of potential orbital parameter space. The dynamical stability across the orbital parameter space increases confidence in the system existing as described.

Dynamical studies can be used to rule out planetary/third body companions but can also be used to constrain the properties of any companions and as such is an important and necessary step in determining the existence of the companions.

1.4.1 Detection Limits

Ribas (2006) states that with timing accuracies of $\sim$10 seconds for select eclipsing binaries with sharp eclipses detecting large, $\sim 10M_J$, planets in long orbital periods of $\sim$10-20 years will be a “relatively easy task”.

Watson and Marsh (2010) state that for an exterior planet of mass M_p on an orbit with a semi-major axis a_{out}, the amplitude of the timing deviation is:

$$\delta t \approx \left(\frac{M_p}{M_J}\right)\left(\frac{a_{out}}{au}\right) \tag{1.2}$$

While the semi-major axis, a, of an object's orbit is related to the orbital period, p, of the object's orbit (Lissauer and Pater 2013) by:

$$p^2 \propto a^3 \tag{1.3}$$

One consequence of this is that for a detectable δt, small mass objects are only detectable with larger semimajor axis and, therefore, longer orbital period. Larger mass objects that are closer to the host stars are detectable.

As previously mentioned, the Kepler mission, providing high precision, quality observations of such a large number of stars provides the unique opportunity to perform eclipse timing studies. The detectability limits of the Kepler mission, and similar equipment is something that is required to know in order to determine the accuracy of detections. Very little has been done to determine the detectability limits of third bodies using eclipse timing variations with real observations and current equipment. From Sybilski, Konacki, and Kozłowski (2010), the relationship between a planet's mass (M_P) and period (P) from a timing amplitude (A) is given by

$$M_P = \left(\frac{4\pi^2 M_B^2}{P^2 G}\right)^{\frac{1}{3}} (Ac) \tag{1.4}$$

Where M_B is the binary mass, G is the gravitational constant and c is the speed of light. In order to detect giant circumbinary planets, timing precisions of 0.1-1s is required and can be provided by both the Kepler and the CoRoT missions (Sybilski, Konacki, and Kozłowski 2010) however challenges in detections arise from the pre-defined target pool of the missions. For the Kepler mission, Sybilski, Konacki, and Kozłowski (2010) also say that the target pool of the mission puts an upper limit of 40 potentially detectable circumbinary gas giants "in the best-case scenario".

Formation and migration of third bodies is another factor that must be considered when detecting third bodies. The truncation radius of a binary star is the radius at which the disk of material surrounding the binary star is truncated or cleared. The truncation radius is estimated to be between 1.8 and 2.6 times the separation of the binary star, a_b (Pierens and Nelson 2007). With equation 1.3, this results in a truncation radius between approximately 2.4 and 4.2 times the binary star period. As such, no third bodies are expected to form within this radius. It may still be possible to detect third bodies within this radius. However, the third body would likely form outside the radius and migrate inwards.

1.5 Research Questions

The questions this thesis aims to address are:

1.5.1 What Can We Expect To Find With Eclipse Timing Studies?

Chapter 2 addresses the limits of eclipse timing studies based on real-world observations. In Getley et al. (2021), idealised systems are simulated and Kepler derived jitter is introduced. The idealised system results are compared with previously reported simulated results in Sybilski, Konacki, and Kozłowski (2010). The systems with Kepler derived jitter introduced are used to probe the limits of mass and orbital period detectability. The effects of eccentricity on detectability are also explored.

1.5.2 What Can We Learn About Detected Planets and Other Third Bodies?

Chapter 3 studies the source of complex O-C variations and the stability of proposed third bodies that were detected from eclipse timing studies. The stability of third bodies is an important consideration in the existence of the third body as well as the accuracy of the detected characteristics. In Getley et al. (2020) previously reported third bodies are studied to determine if the systems are stable.

Chapter 4 focuses on the detection of a new planetary mass third body using eclipse timing variations. Getley et al. (2017) uses Kepler observations to determine the eclipse times for KIC 5095269. The eclipse time variations indicate a planetary mass third body. A dynamical analysis of the proposed system is also performed to determine the stability of the system.

Chapter 5 focuses on a discussion of how the results from Chapters 2, 3 and 4 are interrelated and provide evidence for using eclipse timing variations as a way to detect planetary and brown dwarf companions from binary star surveys.

CHAPTER 2

WHAT CAN BE FOUND?

An important component of any survey is understanding the limits of the methods used. Equally important is having reasonable expectations on what can be achieved from the survey. Sybilski, Konacki, and Kozłowski (2010) use simulated data and present an equation (Eq. 1.4) showing the mass-period relationship of a third body for a given timing amplitude. Two questions naturally arise from this work: 1) does the mass-period relationship accurately represent real-world data and 2) is the mass-period relationship accurate across the entire parameter space.

In Getley et al. (2021), three exemplar Kepler systems were selected as base systems. Third bodies were then injected into the exemplar systems and eclipse times simulated. In order to determine the limits of eclipse time variation studies, an ETV study was performed to try to detect the injected third bodies. Ideally more than three Kepler systems would have been selected, however due to the computing resources required and time constraints it was not possible to include more systems.

2.1 Getley et al. (2021) "The detectability of binary star planetary and brown dwarf companions from eclipse timing variations"

The published paper Getley et al. (2021), "The detectability of binary star planetary and brown dwarf companions from eclipse timing variations" is presented below.

Monthly Notices of the ROYAL ASTRONOMICAL SOCIETY
MNRAS **504,** 4291–4301 (2021) doi:10.1093/mnras/stab1207
Advance Access publication 2021 April 29

The detectability of binary star planetary and brown dwarf companions from eclipse timing variations

A. K. Getley [1]★ B. Carter [1] R. King[1] and S. O'Toole [2]
[1] University of Southern Queensland, Centre for Astrophysics, Toowoomba, Qld 4350, Australia
[2] Australian Astronomical Optics, Macquarie University, PO Box 915, North Ryde, NSW 1670, Australia

Accepted 2021 April 23. Received 2021 April 22; in original form 2021 February 28

ABSTRACT

In this paper, we determine the detectability of eclipsing binary star companions from eclipse timing variations using the Kepler mission data set. Extensive and precise stellar time-series photometry from space-based missions enable searches for binary star companions. However, due to the large data sets and computational resources involved, these searches would benefit from guidance from detection simulations. Our simulations start with and benefit from the use of empirical *Kepler* mission data, into which we inject third bodies to predict the resulting timing of binary star eclipses. We find that the orbital eccentricity of the third body and the orbital period of the host binary star are the key factors in detecting companions. Target brightness is also likely to be a factor in detecting companions. Detectable third body masses and periods can be efficiently bound using just two equations. Our results enable the setting of realistic expectations when planning searches for eclipsing binary star planetary and brown dwarf companions. Our results also suggest the brown dwarf desert is real rather than observational selection.

Key words: binaries: eclipsing.

1 INTRODUCTION

For binary stars, eclipse timing variations (ETVs) measured from time-series photometry enable searches for the gravitational effect of additional, planetary, or brown dwarf companions. Today the precise time-series observations needed come from space telescope missions such as *Kepler* (Prša et al. 2011; Slawson et al. 2011) and *TESS* (Ricker et al. 2014). However, due to the large data sets and computational resources involved, searches for binary star companions need detection simulations to improve their efficiency. Realistic detection expectations save resources by directing searches to those systems where companions and their characteristics are most likely to be reliably obtained from the available data set. A determination of the detectability of a companion reduces the rate of false positives and provides a check on the robustness of existing detections.

Over 2000 eclipsing binary stars are listed in the Kepler Eclipsing Binary Star Catalogue (Prša et al. 2011), which is the focus of this study as it alone provides such a large number of systems for ETV studies. Nevertheless, given that all observations will contain some level of random and systematic light-curve errors, an understanding of the inherent capacity of the data set to produce detections can assist with the identification of previously missed companions, and provide a check on known candidates. Thus it is important to understand the limitations on detections based on ETVs, and this can be done using simulations that introduce companions into a data set of eclipsing binary star systems.

★ E-mail: alan.getley@usq.edu.au

Planets with a large mass of ∼10 Jupiter Masses in long (∼10–20 yr) orbits can be detected with timing accuracies of ∼10 s (Ribas 2006). Giant circumbinary planets can be detected through eclipse timing studies with timing precisions of between 0.1 and 1 s (Sybilski, Konacki & Kozłowski 2010). Numerical simulations performed by Sybilski et al. (2010) indicate this required precision can be reached with the *Kepler* and the *CoRoT* missions. It is unlikely this precision can be achieved in practice. However, very little has been done to determine the practical limits of what has been observed and what third body masses may be too small to detect with these 'real-world' observations. By using a binary star system that has been observed by *Kepler* and modelling the system in JKTEBOP (Southworth, Maxted & Smalley 2004) we are able to estimate masses for the binary star components as well as orbital characteristics such as orbital period and inclination. By creating a model system based on these estimates we are then able to inject a third body with varying characteristics and run an eclipse time study on these simulated systems.

In past papers we have presented evidence for a planetary mass third body orbiting KIC 5095269 found via an ETV study (Getley et al. 2017) as well as the stability of third bodies found around *Kepler* systems via ETV studies (Getley et al. 2020). These papers naturally lead us to the question what the limits of ETV studies are when using 'real-world' data (or *Kepler* derived jitter) as a base.

In this paper, we report the results of an eclipse time study on simulated systems using three different systems observed by *Kepler* as a base that have then been injected with third bodies. Therefore, we are able to report on the limits of detection using eclipse time variations using actual limits of the *Kepler* observations and variability inherent to the system. We are also able to report on what characteristics of third bodies may be detected or not within these

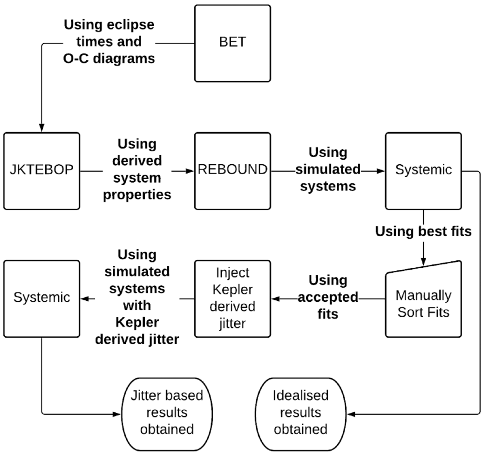

Figure 1. Summary of the major processes of the methodology. BET was used to determine eclipse times and produce O–C diagrams to identify systems for use in the study. System properties were obtained from JKTEBOP, followed by simulated systems being made in REBOUND. SYSTEMIC was then used to find the best fits (producing the idealized results). *Kepler* derived jitter was introduced into the simulated systems with visually comparable O–C fits and SYSTEMIC was again used to find the best fits (producing the jitter based results).

limits. We performed this investigation using a mostly automated technique that is more widely applicable, as a manual process for thousands of systems is impractical unless there is a specific reason to look at a system manually (for example, if another investigation into a specific system indicated a third body).

2 METHOD

The methodology has been summarized in the flow chart in Fig. 1.

The eclipse times of the eclipsing binary stars found in the 'Kepler Eclipsing Binary Star Catalog' (Prša et al. 2011) were determined using a custom program, BET, based on the software TRANSIT ANALYSIS PACKAGE or TAP (Gazak et al. 2012). Three case study example systems, KIC 3654950, KIC 6521542, and KIC 6593363, were chosen as the basis of this study as the eclipse time variations appear minimal and random or quasi-periodic at most. The O–C diagrams for these systems can be seen in Figs 2, 3, and 4. It can be seen that variations range from a fraction of a minute (KIC 6593363) up to two minutes (KIC 3654950). If the variations were periodic it's possible that a third body would already be present in the system (Beuermann et al. 2010) and interfere with the results of the third body detection methods. The eclipsing binaries found in the Kepler eclipsing binary catalogue have O–C diagram's with varying characteristics. KIC 3654950, KIC 6521542, and KIC 6593363 were selected as their O–C diagrams, with minimal, random, and/or quasi-periodic variations, are also representative of the other O–C diagram characteristics seen from *Kepler* eclipsing binaries.

JKTEBOP (Southworth et al. 2004) was used to determine estimates for the characteristics of the binary star (including the mass ratio of the binary stars, orbital period, inclination). The temperature of the systems were estimated as in Getley et al. (2017, 2020). The temperatures were then used to estimate individual star masses in the binary system. These systems were also chosen for their different binary star

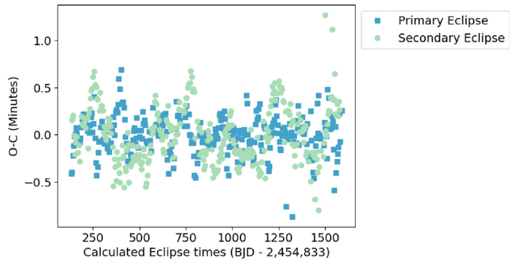

Figure 2. O–C diagram for KIC 6521542. KIC 6521542 was chosen as one of the base systems for this ETV study due to the quasi-periodic variations with typical amplitude between ± 1 min.

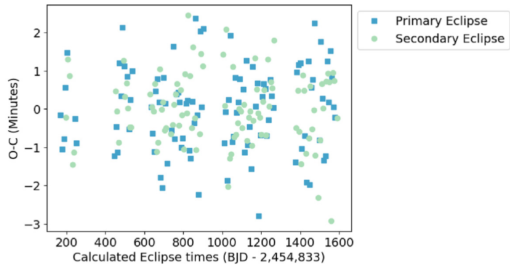

Figure 3. O–C diagram for KIC 3654950. KIC 3654950 was chosen as one of the base systems for this ETV study due to the random variations with typical amplitude between ± 2.5 min.

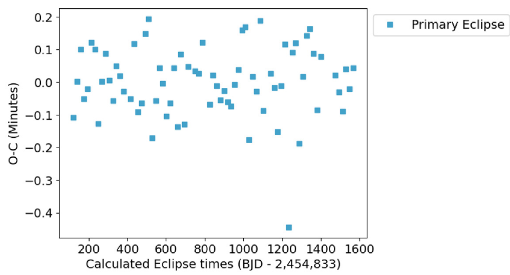

Figure 4. O–C diagram for KIC 6593363. KIC 6593363 was chosen as one of the base systems for this ETV study due to the random variations with typical amplitude between ± 0.2 min.

orbital periods. The orbital periods for KIC 6521542, 3654950, and 6593363 are 4.42575, 8.13475, and 18.52783 d, respectively. These complementary systems are thus used to determine how differing binary configurations alter the detectability of a third body.

REBOUND is an *N*-body integrator with Python and C implementations (Rein & Spiegel 2015). Systems of bodies are able to be set up and integrated over time to determine eclipse timing variations for the characteristics of the objects entered. With the characteristics of the *Kepler* systems determined from JKTEBOP (Table 1), these values were used to set up base binary star systems in REBOUND. A series of third bodies was then added to each of the systems. The characteristics of the injected third body had masses ranging

Table 1. Properties for the three case study example systems used as the base of this eclipse timing study. Binary stars with varying orbital periods were selected in order to determine the effect binary orbital period has on the third body detection rate.

Property	KIC 6521542	KIC 3654950	KIC 6593363
Kepler $T_{\rm eff}$ (K)	5880	5233	5865
Kepler mag	14.280	15.858	12.893
Primary mass ($M_\odot$)	1.07	0.86	1.07
Secondary mass ($M_\odot$)	0.365	0.442	0.740
Period (d)	4.42575	8.13475	18.52783
Inclination (°)	88.99	89.25	89.93

between 0.5 Jupiter masses and 500 Jupiter masses.[1] The orbital period of the third body was set between 6 and 2000 d.[2] Eccentricities were also set to 0.0, 0.1, and 0.5 for each mass/period combination along with random mean anomalies, longitude of ascending node, and longitude of pericentre. The inclination of the third bodies was fixed to 70 deg. If the inclination is any closer to 90 deg, the third bodies will start to transit the parent stars and will be detectable via other methods (Charbonneau et al. 2006). Therefore, an inclination of 70 deg is more representative of an eclipse timing study system. These systems were then integrated with REBOUND and the eclipse times of the binary stars were recorded. These simulated eclipse times form the basis of an idealized scenario i.e. no jitter was introduced due to unwanted internal effects, such as star spots, or external effects such as observational errors. O–C variations, or *Kepler* derived jitter, from the case study example systems can then be added to the simulated eclipse times. These eclipse times with *Kepler* derived jitter added then form the basis for a 'real-world' scenario based on actual observation data.

The binary star systems were set up in SYSTEMIC (Meschiari et al. 2009; Meschiari & Laughlin 2010) using the characteristics of the system found from JKTEBOP and the simulated eclipse times from REBOUND. We followed an iterative process to determine the best possible fit. A third body was then inserted into SYSTEMIC with the mass set in the range 5, 10, 25, 50, 100, 250, 500, and 1000 Jupiter masses as initial values. The system properties were then optimized to search for the best-fitting values for the third body characteristics. The best two masses were selected as upper and lower limits and the systems were re-run to find the best fit. This was repeated until the minimum and maximum masses differ by less than a Jupiter mass. The best fit at the end of the calculations were then saved. O–C diagrams for the best fits from SYSTEMIC were then saved and sorted into three categories: good fit, bad fit, uncertain fit. Manual intervention in finding a model with SYSTEMIC may be able to provide better fits, however given the extremely large number of systems that there are to work with and that one of the purposes of this investigation is to find the limits of a largely automated calculation, manual intervention is not practical.

After the systems were processed in SYSTEMIC, the next step was to determine if the fitted third body characteristics matched the injected third body characteristics. The O–C diagram of the simulated system versus the best fit was inspected, if the O–C diagrams were a visually poor fit the system was rejected as not a detection. From here, the third body masses were checked to see if they fell within ±25 per cent, ±50 per cent, or ±100 per cent of the injected third body's characteristics. Successful detections can then be used to determine what third body characteristics are detectable under ideal conditions as well as 'real-world' conditions.

Given the large number of simulated systems, the long processing time, and limited computing resources available some compromises had to be made. As the period of a third body can be estimated from the period of variability in the O–C diagram, the period of the third body in SYSTEMIC was fixed to the known simulated/injected period of the third body. This significantly reduced computing time required for fitting. After the entire set of idealized simulations were run, only systems that had visually acceptable O–C fits were then used for the simulated systems with *Kepler* derived jitter added. This is because adding noise makes a detection less likely, therefore if a detection is unsuccessful under idealized conditions, it will be unsuccessful under less than idealized conditions.

3 RESULTS

While finding the precise mass of an object is the ideal outcome, uncertainty is unavoidable. As such, we analyse the results with varying uncertainty to describe a mass detection. We considered the cases where the found mass was within ±25 per cent, ±50 per cent, ±100 per cent of the injected third body's known mass. We also consider the effect of eccentricity and host binary star characteristics on detection rates.

Simulations that had best-fitting O–C variations that did not visually match the actual O–C variations were immediately regarded as a non-detection. For the purposes of this study any O–C fit that was considered visually uncertain (i.e. it was not an obvious rejection) were included with the visually good O–C diagram fits in consideration as a possible detection. By including the systems with O–C diagrams that were deemed uncertain, we aim to remove some of the 'human error' involved in sorting the O–C diagrams and letting the rest of the processes determine what was and was not a detection.

It is unsurprising that increasing the range of acceptable masses considered to be a detection results in increases in the detection rate (seen by comparing neighbouring columns in Figs 5 to 10). Adding *Kepler* derived jitter lowered the detection rate (for example by comparing Figs 6 and 9). However, it was also found that in all cases (with and without the introduced jitter), increasing the eccentricity of the third body lowered the successful detection rate of the third body.

The properties of the host binary star can have a noticeable effect on the detection rate of third bodies when the period of the third body is closer to the period of the host binary star. For example, comparing the detection rate of KIC6521542 (with a binary period of 4.42575 d) in Figs 5 and 8 with the detection rate of KIC6593363 (that has a binary period of 18.52783 d) in Figs 7 and 10. With a longer host binary period, the detections occur at longer periods while a shorter host binary period has detections at shorter periods.

Smaller period changes in the host binary period may not lead to an entire shift in the period of detections. Smaller period changes may result in new regions where the number of detections drop significantly or even completely (Figs 5 and 6).

By comparing the best-fitting mass with the actual mass of the injected third body (Table 2 and Table 3), we find that generally we are more likely to overestimate the injected third body's mass than underestimate the mass. This is particularly evident in the ±100 per cent accuracy for both the idealized results and simulations

[1]Masses used were: 0.5, 1, 2, 3, 4, 5, 6, 7, 8, 9, 10, 15, 20, 25, 30, 35, 40, 45, 50, 55, 60, 65, 70, 75, 80, 85, 90, 95, 100, 110, 120, 130, 140, 150, 200, 300, 400, and 500 Jupiter masses

[2]Periods used were: 6, 7, 8, 9, 10, 15, 20, 25, 30, 35, 40, 45, 50, 100, 200, 300, 400, 500, 1000, and 2000 d

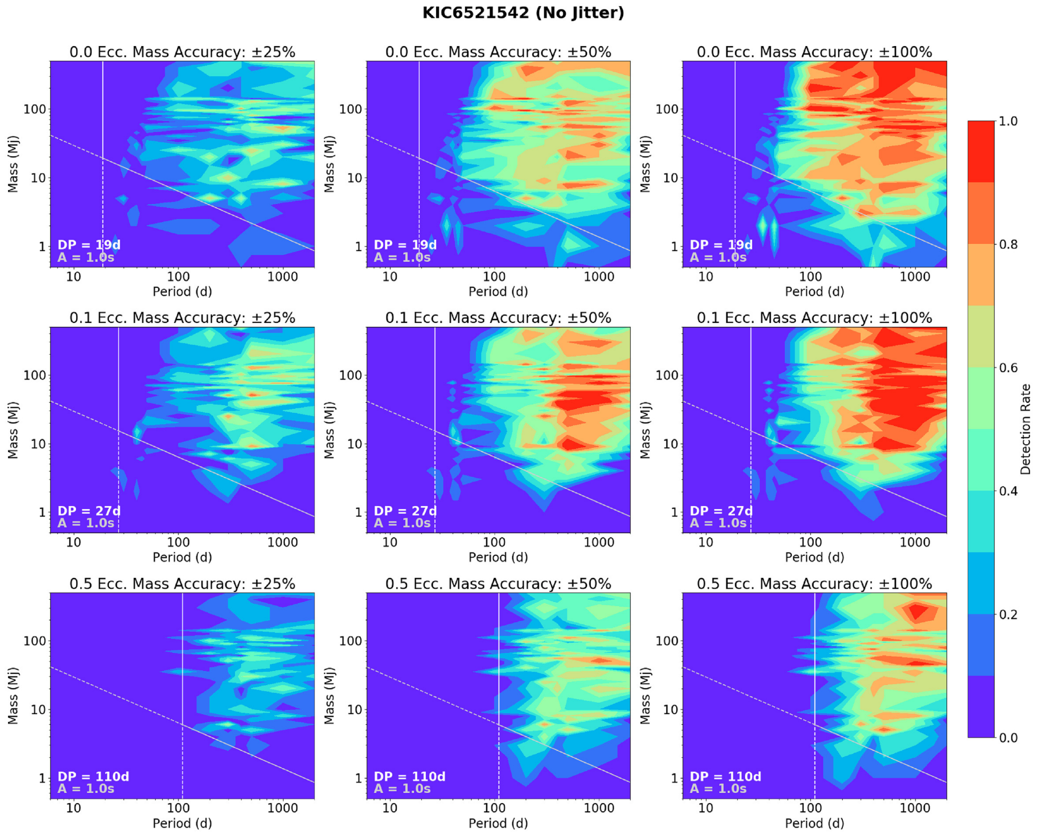

Figure 5. Detection rate of injected third bodies around KIC 6521542. Detections made under idealized conditions (i.e. with no *Kepler* derived jitter added). From top to bottom are third bodies injected with eccentricities (Ecc) of 0, 0.1, and 0.5, respectively. From left to right, mass accuracy used for a successful detection is ± 25 per cent, ± 50 per cent, and ± 100 per cent. The minimum detection period (from equation 1) is shown by the vertical line. The mass–period relationship (from equation 2) is shown by the diagonal line. The timing accuracy, A, was set to 1.0 s. The solid portion of the lines indicate masses and/or periods that fit both equations (1) and (2). The dashed portion indicate masses and/or periods that fit only one of the equations.

injected with *Kepler* derived jitter. When considering systems with *Kepler* derived jitter injected at ± 25 per cent there are a similar number of systems where the third body mass is underestimated as overestimated.

4 DISCUSSION

The truncation radius of a binary star is expected to range between 1.8 and 2.6 times the binary separation, a_b (Pierens & Nelson 2007). Using Kepler's third law ($P^2 \propto a^3$) this would be an approximate range of between 2.4 and 4.2 times the orbital period of the binary. For the three systems listed in Table 1 no third body detections would be expected with orbital periods less than approximately 34.1, 18.6, and 77.8 d for KIC 3654950, 6521542, and 6593363, respectively. As seen in Figs 5 to 10 no detections were made within these ranges in either the idealized case (i.e. the *Kepler* mission time sampling with no added jitter) or the case where *Kepler* derived jitter was introduced. The smallest detection, in either case at any mass, was at 70 d for KIC 3654950, 40 d for KIC 6521542, and 100 d for KIC 6593363. Detections increase significantly when a third body has an orbital period at or greater than 100 d both in the ideal scenario and with variations. This indicates that while it is possible in some cases for eclipse timing variation studies to detect third bodies close to the minimum formation period they are most sensitive to 100 d+ orbital periods.

Using the approximate upper limit of the truncation radius as a foundation, and comparing the start of detections in both the idealized case and the case with *Kepler* derived jitter added for all eccentricities, we empirically find that the minimum detection period can be approximately described with the equation

$$\mathrm{DP} = (59{e_p}^2 + 12.1e_p + 4.2)P_b, \qquad (1)$$

where DP is the minimum detection period, e_p is the eccentricity of third body, and P_b is the orbital period of the host binary. This detection period is indicated in Figs 5 to 10 by the solid and dashed vertical lines. As we simulated the third bodies with 20 discrete periods, the precise period where detections begin had to be estimated. However, the step sizes were 100 d or less for periods

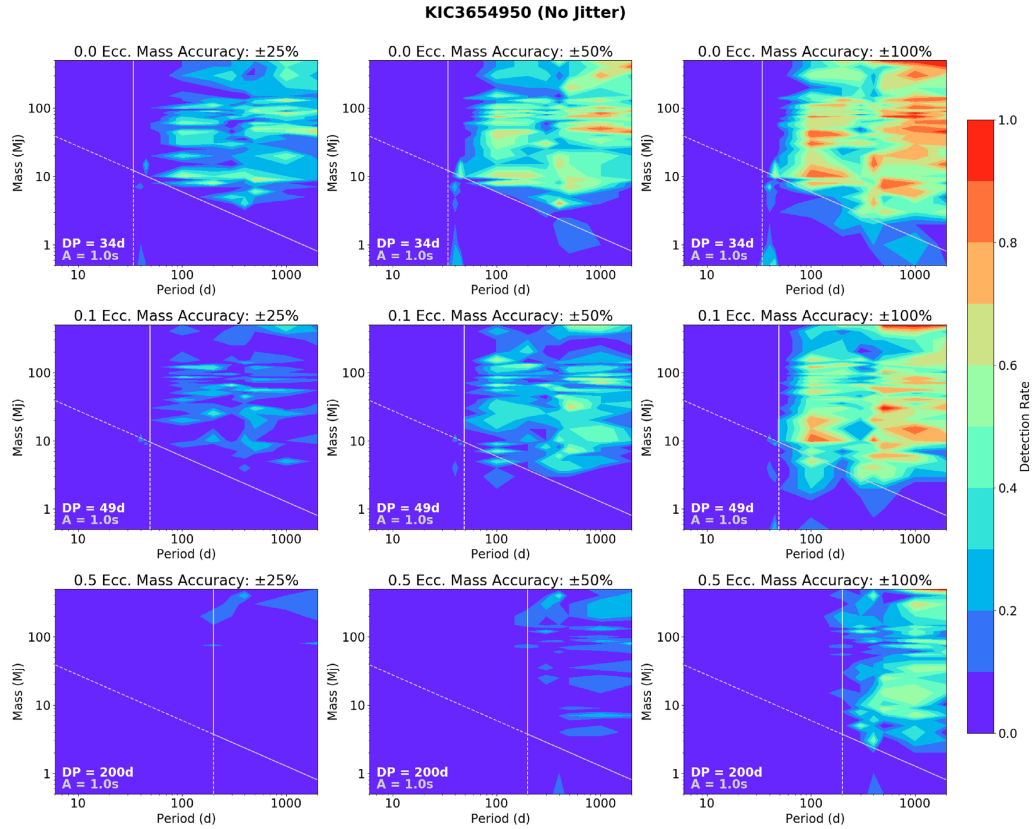

Figure 6. Detection rate of injected third bodies around KIC 3654950. Detections made under idealized conditions (i.e. with no *Kepler* derived jitter added). From top to bottom are third bodies injected with eccentricities (Ecc) of 0, 0.1, and 0.5, respectively. From left to right, mass accuracy used for a successful detection is ±25 per cent, ±50 per cent, and ±100 per cent. The minimum detection period (from equation 1) is shown by the vertical line. The mass–period relationship (from equation 2) is shown by the diagonal line. The timing accuracy, A, was set to 1.0 s. The solid portion of the lines indicate masses and/or periods that fit both equations (1) and (2). The dashed portion indicate masses and/or periods that fit only one of the equations.

up to 500 d. As the detections all appear to begin at or before a 500 d orbital period, equation (1) is expected to be a useful and accurate estimate. Should future studies use smaller step sizes, the equation may be able to be refined further.

From Sybilski et al. (2010), the equation to obtain a planet's mass from a period and timing amplitude is

$$M_P = \left(\frac{4\pi^2 {M_B}^2}{P^2 G}\right)^{\frac{1}{3}} (Ac), \tag{2}$$

where M_P and P is the mass and period of a planet/third body companion, M_B is the total mass of the binary star, G is the gravitational constant, A is the timing amplitude, and c is the speed of light. As such, with the total mass of the binary star and an estimate for the timing errors from a system, we can calculate the minimum detectable mass for a given orbital period of a third body companion. This is shown in Figs 5 to 10 by the solid and dashed vertical lines.

By using both equations (1) and (2), we can calculate an approximate minimum orbital period and an approximate minimum mass for detections of a third body companion at a specific orbital period. As such, reliable approximations on what type of companions may be detectable can be found from minimal binary star information. These realistic expectations can be used as a guide for future eclipse timing studies.

From Watson & Marsh (2010), the amplitude of the timing deviation, δt, is related to the mass of the exterior planet, M_p, and its semimajor axis, $a_{\rm out}$ by

$$\delta t \approx \left(\frac{M_p}{M_J}\right)\left(\frac{a_{\rm out}}{\rm au}\right). \tag{3}$$

As a result of equation (3), assuming the minimum detectable timing deviation, a detectable third body will have a decreasing mass as the orbital period increases. This can generally be seen to be the case, particularly in the ideal simulation scenario in Figs 5, 6, and 7. It can also be seen from Fig. 9 that introducing jitter affects this property of timing deviations. As such, while simulations are a great launching point and can be used to rule out detections based on mass/period properties, this does not guarantee a detected third body is accurate.

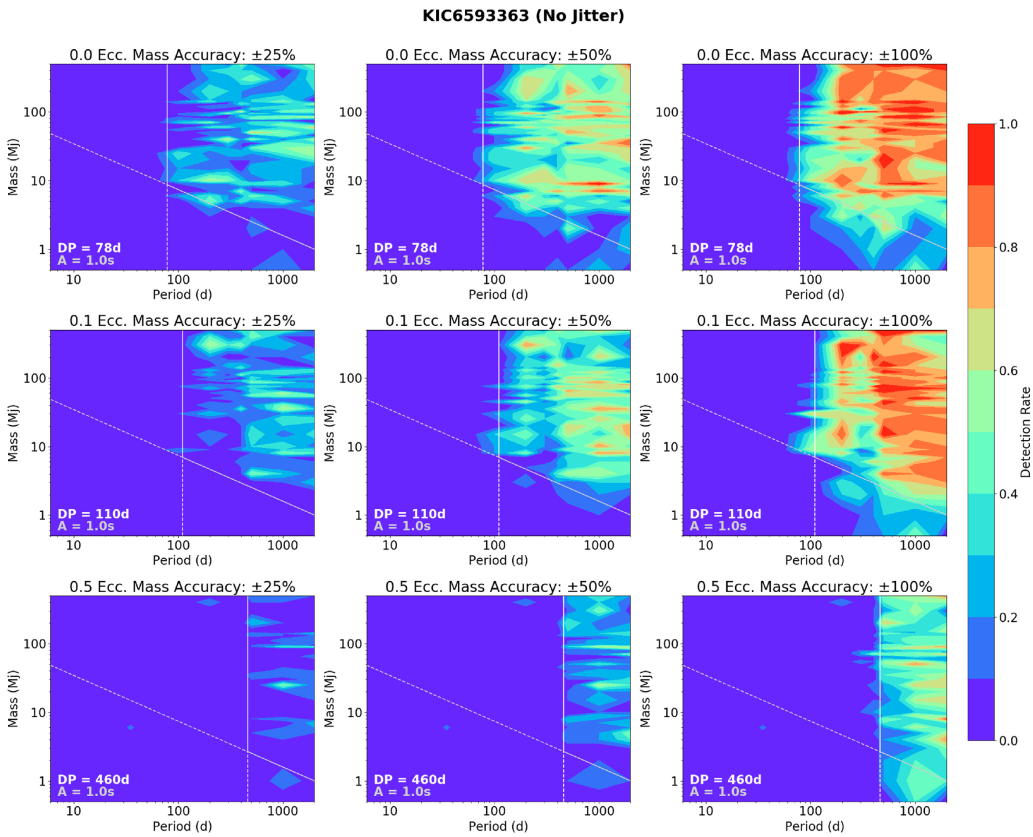

Figure 7. Detection rate of injected third bodies around KIC 6593363. Detections made under idealized conditions (i.e. with no *Kepler* derived jitter added). From top to bottom are third bodies injected with eccentricities (Ecc) of 0, 0.1, and 0.5, respectively. From left to right, mass accuracy used for a successful detection is ±25 per cent, ±50 per cent, and ±100 per cent. The minimum detection period (from equation 1) is shown by the vertical line. The mass–period relationship (from equation 2) is shown by the diagonal line. The timing accuracy, A, was set to 1.0 s. The solid portion of the lines indicate masses and/or periods that fit both equations (1) and (2). The dashed portion indicate masses and/or periods that fit only one of the equations.

The largest difference between the idealized systems and systems with *Kepler* derived jitter added can be seen between Figs 6 and 9 for KIC 3654950. There is a significant detection rate across a wide range of masses and periods when looking at idealized simulations alone. However, with the *Kepler* derived jitter added the detection rate is very low except for the larger brown dwarf and stellar masses at low eccentricity. Low detection rate occurs in the systems with shorter orbital periods, i.e. KIC 3654950 and 6521542. The estimated timing accuracy for KIC 3654950 at 33.5 s is significantly larger than the other systems and explains the significant difference between the idealized systems and the simulations with *Kepler* derived jitter added. There are a number of detections below the timing accuracy line but only at shorter orbital periods. The reason for these detections is unclear.

In Fig. 6, there appears to be an exception to the above. With 0.0 and 0.1 eccentricity, detections of 0.5–1 M_J third bodies occur between 35 d and 50 d orbital periods. This is particularly evident with ±100 per cent accuracy but can also be seen in ±25 per cent and ±50 per cent accuracy with 0.0 eccentricity. The extra group of detections are not seen in other systems and not seen when *Kepler* derived jitter was included in the simulations. It is possible that these detections are just coincidences and not real detections. However, this raises the question of why the detections are grouped together and not randomly spread around the various simulated values.

It is also possible for the magnitude of the binary star to have an effect on detectability. The brighter the observed target, the better signal-to-noise ratio (SNR) that is obtainable and therefore less variability within the observations. With a magnitude of 15.858, KIC 3654950 is the dimmest of the three case study example systems. It is therefore likely that the poorer timing accuracy, and lack of detections, is partially the result of the increased magnitude.

4.1 KIC 5095269

KIC 5095269 has a 7.7M_J planetary mass third body in a 237.70817 d orbital period with an eccentricity of 0.06 (Getley et al. 2017). The orbital period of the host binary is approximately 18.61 d which closely matches orbital period of the binary found in KIC 6593363. From Fig. 10, we can see the detection rate is very low (at 0.0

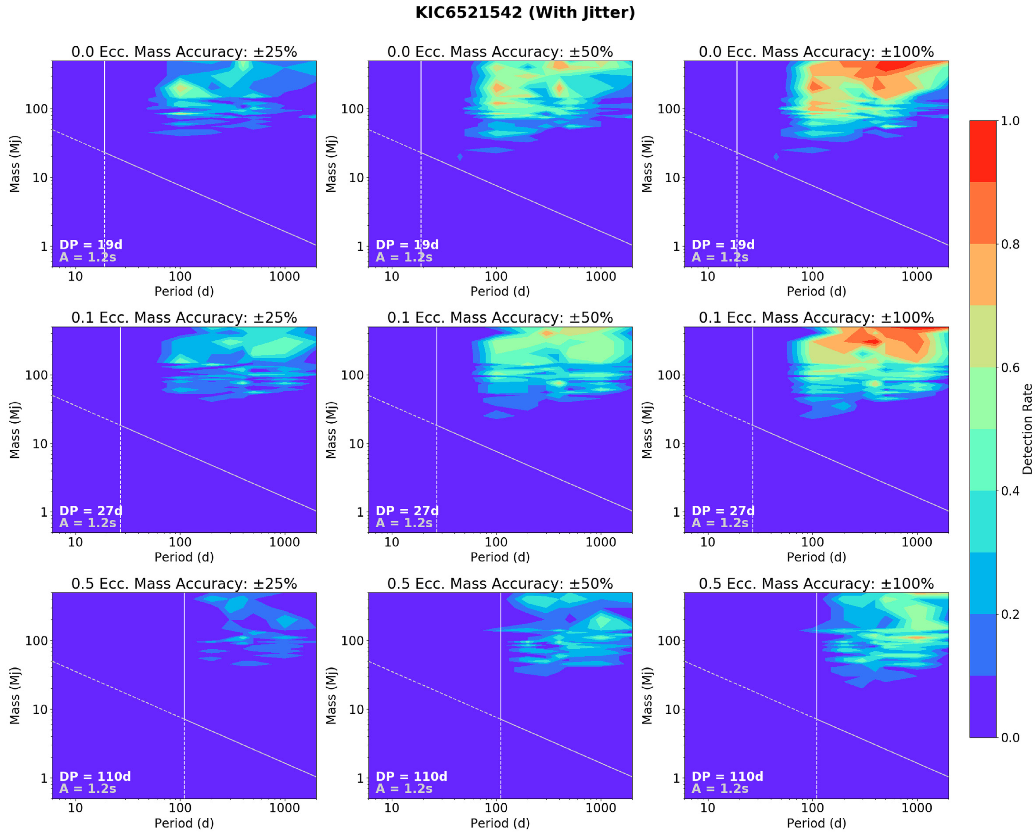

Figure 8. Detection rate of injected third bodies around KIC 6521542. Detections made under less than idealized conditions (i.e. with *Kepler* derived jitter added). From top to bottom are third bodies injected with eccentricities (Ecc) of 0, 0.1, and 0.5, respectively. From left to right, mass accuracy used for a successful detection is ±25 per cent, ±50 per cent, and ±100 per cent. The minimum detection period (from equation 1) is shown by the vertical line. The mass–period relationship (from equation 2) is shown by the diagonal line. The timing accuracy, A, was estimated to be 1.2 s. The solid portion of the lines indicate masses and/or periods that fit both equations (1) and (2). The dashed portion indicate masses and/or periods that fit only one of the equations.

eccentricity) or zero (at 0.1 eccentricity) at this mass/period when a ±25 per cent mass accuracy is used but significantly higher (at 0.0 eccentricity) with a ±50 per cent mass accuracy or ±100 per cent (at 0.1 eccentricity). We can also use equations (1) and (2) to estimate the mass and periods in a detectable range. The minimum detectable period is estimated to be 96 d. With an approximate median timing error of 2.4 s, the approximate minimum detectable mass of a third body with a 237.70817 d orbital period is $9.6M_J$. From Fig. 10 detections can be made with slightly lower masses than estimated from the timing error. As detection of a third body at this mass and period is possible, confidence of the third body's existence is increased. We can see from Table 3 that the mass is more likely to be an overestimate than an underestimate. It is therefore possible the $7.7M_J$ may be an upper estimate.

4.2 KIC 7821010

KIC 7821010 has a stable planetary third body with mass of $\sim 2.6M_J$ (Borkovits et al. 2016; Getley et al. 2020). The host binary has an orbital period of 24.238219 d while the third body has an orbital period of 991 d and an eccentricity of 0.372. The most comparable system with these properties is KIC 6593363 (Fig. 10). At 0.1 eccentricity a third body with these properties has a low detection rate, while at 0.5 eccentricity there are no detections. We have seen that detection rates increase as the host binary orbital period increases. Using equation (1), we find that third bodies around KIC 7821010 have a minimum detection period of 400 d. An approximate minimum detectable mass of a third body with an orbital period of 991 d and an approximate median timing error of 0.18 s is just $0.34M_J$. Not only is this planetary mass third body expected to be detectable with an eclipse timing study but Saturn mass third bodies could be detectable using eclipse timing studies around KIC 7821010 (or similar systems) with more observations.

4.3 Brown dwarf desert

Brown dwarfs are generally considered to be bodies with masses ranging from approximately $13M_J$ to $80M_J$ (Sahlmann et al. 2011;

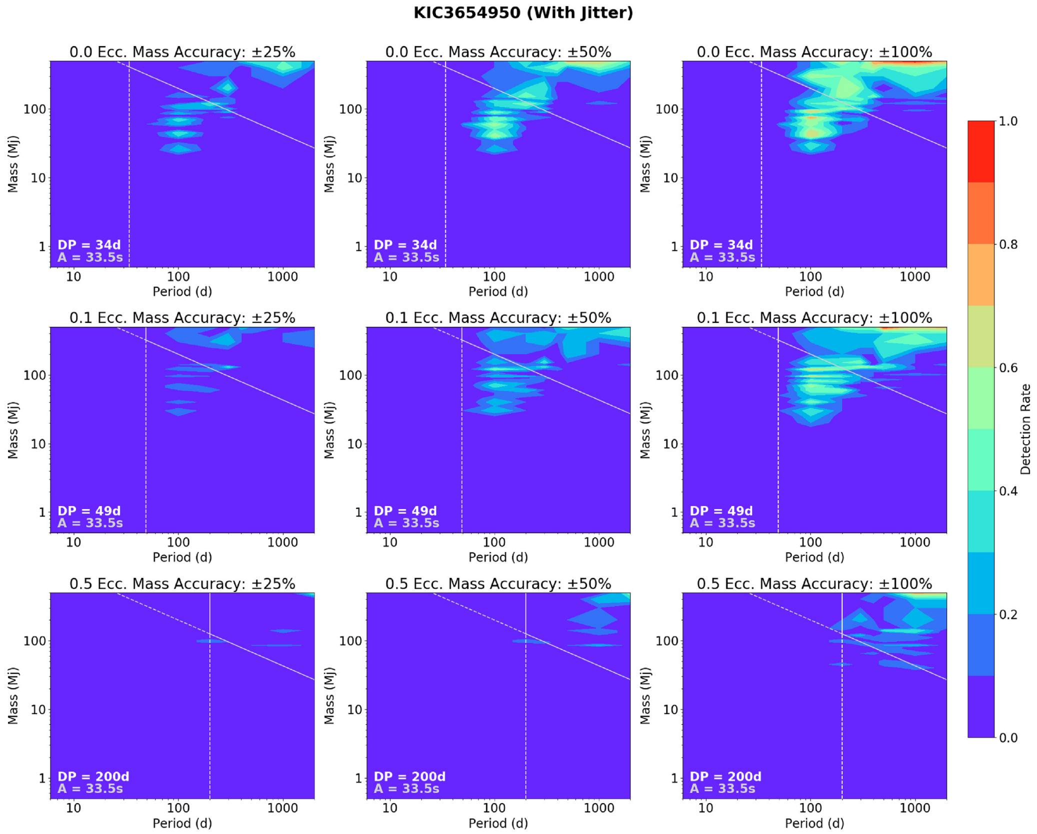

Figure 9. Detection rate of injected third bodies around KIC 3654950. Detections made under less than idealized conditions (i.e. with *Kepler* derived jitter added). From top to bottom are third bodies injected with eccentricities (Ecc) of 0, 0.1, and 0.5, respectively. From left to right, mass accuracy used for a successful detection is ±25 per cent, ±50 per cent, and ±100 per cent. The minimum detection period (from equation 1) is shown by the vertical line. The mass–period relationship (from equation 2) is shown by the diagonal line. The timing accuracy, A, was estimated to be 33.5 s. The solid portion of the lines indicate masses and/or periods that fit both equations (1) and (2). The dashed portion indicate masses and/or periods that fit only one of the equations.

Spiegel, Burrows & Milsom 2011). There exists a brown dwarf desert where brown dwarf bodies are sporadically found around single stars or multiple star systems for a range of orbital periods (Grether & Lineweaver 2006; Fontanive et al. 2019). An estimated 16 per cent of Sun-like stars have third bodies in close orbits of less than 5 yr. However, less than 1 per cent of these are brown dwarf masses.

Third bodies within the brown dwarf mass range with orbits less than ~5 yr are detectable around all systems listed in Table 1. This supports the idea that the brown dwarf desert is not due to detection issues. Therefore, the lack of brown dwarfs are more likely due to other factors such as formation or migration processes as stated in Grether & Lineweaver (2006).

4.4 Computing resources

Ideally, more systems, more eccentricities, and more data sets would have been included in this study. While it is clear the detection rate drops as the eccentricity of the third body increases, including more eccentricities would have allowed a clearer understanding of the detection rate. For example, is the drop relatively linear or is there a ‘detection rate cliff’ where eccentricity has minimal effect and then rapidly has a significant effect? More systems would have allowed for a clearer understanding of the effect of the host binary orbital period on the detection rate for orbital periods between the short, 8 d, systems and the longer, 18 d, systems. The simulations are resource intensive to run and due to the technical limitations, we chose to thoroughly cover a small number of representative systems rather than partially cover a larger number of systems. For example, 38 different masses, 20 different orbital periods, three different eccentricities each combination run with 10 random initial conditions for each of the three systems is a total of 68 400 simulations just for the ideal conditions. Each simulation required one CPU and had a wall-time of 24 h. An additional system or eccentricity would therefore add a minimum of 22 800 simulations each and significantly increases the amount of resources needed.

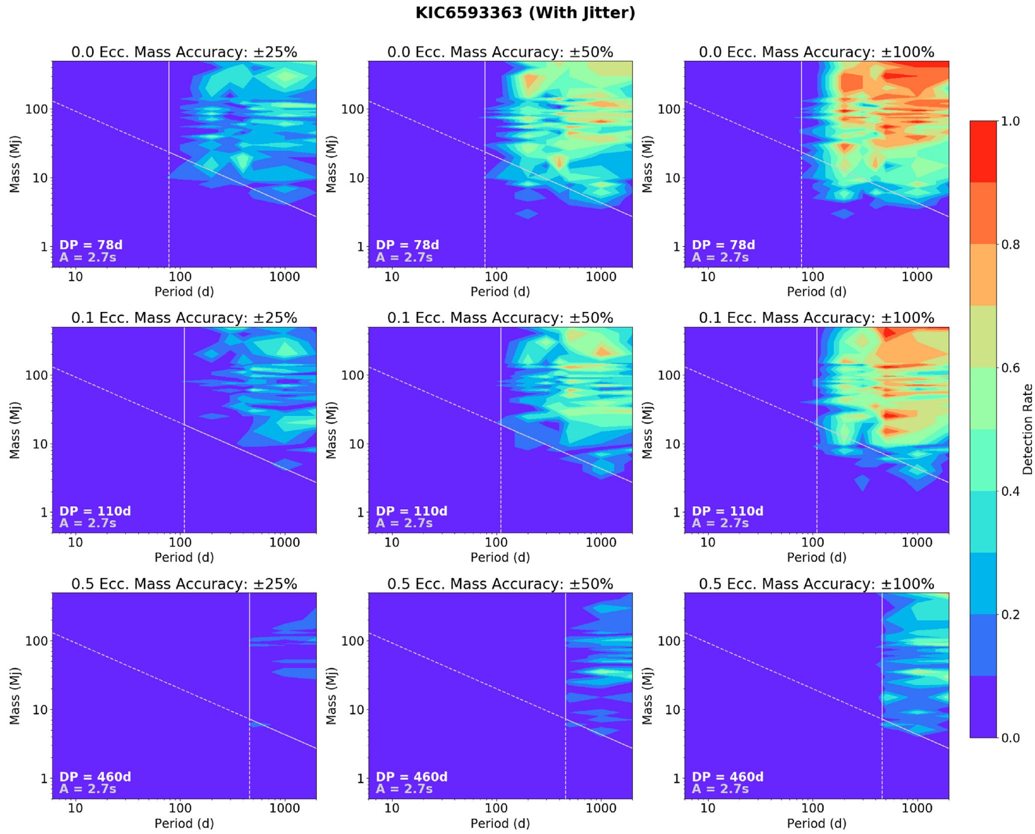

Figure 10. Detection rate of injected third bodies around KIC 6593363. Detections made under less than idealized conditions (i.e. with *Kepler* derived jitter added). From top to bottom are third bodies injected with eccentricities (Ecc) of 0, 0.1, and 0.5, respectively. From left to right, mass accuracy used for a successful detection is ±25 per cent, ±50 per cent, and ±100 per cent. The minimum detection period (from equation 1) is shown by the vertical line. The mass–period relationship (from equation 2) is shown by the diagonal line. The timing accuracy, A, was estimated to be 2.7 s. The solid portion of the lines indicate masses and/or periods that fit both equations (1) and (2). The dashed portion indicate masses and/or periods that fit only one of the equations.

4.5 Application to other space-based photometric data sets

The simulations results here, including equation (1), are specific to the *Kepler* data set. Nevertheless, the approach taken here can be applied to other space-based photometric data sets of similar precision, cadence, and extended time coverage. Thus, we briefly consider the application of our approach to *TESS* and *PLATO*.

TESS observes sectors of the sky for 27.4 d, before re-pointing the field of view, with the all-sky survey taking 2 yr (Ricker et al. 2014). While *TESS* provides high-precision observations of bright nearby stars, the duration of the observations of the objects is significantly shorter than *Kepler*'s. Therefore, detecting third bodies with orbital periods greater than the 27.4 d seems unlikely. So equations (1) and (2) can apply to missions such as *TESS*, although the maximum detectable period is then limited to the duration of the observations. In addition, as mentioned in Section 4.4, the computational resources required to perform the necessary simulations are substantial. Consequently, we leave the exploration of the *TESS* data set to the future when there is a more extended time coverage.

We also note the upcoming *PLATO* (PLAnetary Transits and Oscillations of stars) mission aims to observe bright stars (2 to 3 magnitudes brighter than Kepler observed stars) for a period of 4 yr. By observing brighter stars than *Kepler*, *PLATO* measurements should have a greater precision than *Kepler* over similar time periods. As such it is feasible that our approach can be applied to the *PLATO* data sets.

5 SUMMARY AND CONCLUSIONS

In this paper, we have simulated the *Kepler* eclipsing binary systems KIC 3654950, KIC 6521542, and KIC 6593363 with injected third bodies with varying characteristics in order to determine (1) the detectability of third bodies with specific masses and periods, (2) the effect of ‘real-world’ observations (or *Kepler* derived jitter with the *Kepler* mission time sampling) on the detectability of third bodies, and (3) the effectiveness of using eclipse timing variations to hunt for planetary mass third bodies.

Table 2. The total number of successful detections and the number of systems that underestimated and overestimated the third body mass at each eccentricity (Ecc), accuracy level, and system in the study for the simulations with no variations added.

System (KIC)	Ecc	Accuracy (per cent)	# under	# over	Total
6521542	0.0	±25	330	503	833
		±50	646	964	1610
		±100	770	1261	2031
	0.1	±25	248	630	878
		±50	374	1170	1544
		±100	416	1436	1852
	0.5	±25	104	368	472
		±50	168	794	962
		±100	189	1034	1223
3654950	0.0	±25	273	354	627
		±50	445	612	1057
		±100	470	1061	1531
	0.1	±25	117	187	304
		±50	191	442	633
		±100	203	1052	1255
	0.5	±25	18	49	67
		±50	33	158	191
		±100	35	490	525
6593363	0.0	±25	276	302	578
		±50	532	624	1156
		±100	618	1080	1698
	0.1	±25	124	303	427
		±50	192	686	878
		±100	213	1335	1548
	0.5	±25	44	74	118
		±50	57	200	257
		±100	63	470	533

Table 3. The total number of successful detections and the number of systems that underestimated and overestimated the third body mass at each eccentricity (Ecc), accuracy level, and system in the study for the simulations with Kepler variations added.

System (KIC)	Ecc	Accuracy (per cent)	# under	# over	Total
6521542	0.0	±25	126	134	260
		±50	253	223	476
		±100	296	353	649
	0.1	±25	109	156	265
		±50	175	282	457
		±100	195	429	624
	0.5	±25	38	101	139
		±50	69	213	282
		±100	84	332	416
3654950	0.0	±25	62	59	121
		±50	108	113	221
		±100	114	235	349
	0.1	±25	36	45	81
		±50	61	109	170
		±100	64	252	316
	0.5	±25	17	19	36
		±50	25	37	62
		±100	25	110	135
6593363	0.0	±25	211	247	458
		±50	380	493	873
		±100	436	827	1263
	0.1	±25	112	187	299
		±50	177	436	613
		±100	190	862	1052
	0.5	±25	27	32	59
		±50	42	99	141
		±100	48	208	256

Our study finds that, when using empirical data from the *Kepler* Eclipsing Binary Star Catalogue (Prša et al. 2011) as a starting point, in an idealized situation (i.e. with no *Kepler* derived jitter), small mass third bodies are able to be detected at long orbital periods while large mass third bodies are able to be detected in shorter orbital periods. This agrees with the results of the simulation analysis performed by Sybilski et al. (2010). We however find that in less than idealized situations, i.e. with the *Kepler* derived jitter added to the simulations, that this property only holds true with larger binary orbital periods. We also find that the eccentricity of a third body has a significant effect on the detection rate of third bodies, with a larger eccentricity making detection significantly more difficult in less than idealized circumstances. The brightness of the observed target is also likely to play a role in the detectability of third bodies.

The truncation radius of a binary star is expected to be between approximately 2.4 and 4.2 times the orbital period of the binary (Pierens & Nelson 2007). As such, no third bodies are expected to form within this radius and would only exist with planetary migration. We find that for binary stars with short orbital periods (~4 d and ~8 d) that third bodies are not detected until approximately twice the truncation radius. However, when the binary star has a longer orbital period such as KIC 6593363 with an 18.52783 d orbital period third bodies can be detected close to the truncation radius. With this information, we are able to see the detection rate of a *Kepler* observed system can be bound by equations (1) and (2).

It can be seen from KIC 6593363 that detection rates significantly increase with the longer host binary orbital period. We draw the conclusion that with the longer orbital period, and thus greater separation between the stellar components of the binary that the stars are not only significantly detached but also at a great enough distance that tidal distortions are less prominent. This results in smaller variations from within the system itself and allows the detection rate to increase.

Eclipse time variation studies can be, and have been, used to find planetary mass third bodies (Borkovits et al. 2016; Getley et al. 2020). However, ETV studies are more sensitive to brown dwarf and stellar mass companions. As such, while ETV studies are an important tool in finding third bodies (of a wide range of masses and periods) it's important to understand the potential limitations of such studies in order to guide expectations and maximize the use of resources. As more missions like *Kepler* are launched, existing binary systems will be observed for even longer periods of time. This will allow third bodies with longer orbital periods and smaller masses to be discovered through ETV studies.

The upcoming *PLATO* mission aims to obtain high precision observations of bright stars for similar time periods to *Kepler* (Catala 2009). By observing bright stars, photon noise sources can be kept to a minimum. As such, *PLATO* observed binary stars are good potential targets for an ETV study.

ACKNOWLEDGEMENTS

This research has been supported by an Australian Government Research Training Program Scholarship. This research was undertaken with the assistance of resources from the National Computational Infrastructure (NCI Australia), an NCRIS enabled capability supported by the Australian Government.

We would like to thank the referee and editor for their helpful comments.

DATA AVAILABILITY

The data underlying this article will be shared on reasonable request to the corresponding author.

REFERENCES

Beuermann K. et al., 2010, A&A, 521, L60
Borkovits T., Hajdu T., Sztakovics J., Rappaport S., Levine A., Bíró I. B., Klagyivik P., 2016, MNRAS, 455, 4136
Catala C., 2009, Exp. Astron., 23, 329
Charbonneau D., Brown T. M., Burrows A., Laughlin G., 2006, in Reipurth B., Jewitt D., Keil K., eds, Protostars and Planets V. University of Arizona Press, Tucson, p. 701
Fontanive C., Rice K., Bonavita M., Lopez E., Mužić K., Biller B., 2019, MNRAS, 485, 4967
Gazak J. Z., Johnson J. A., Tonry J., Dragomir D., Eastman J., Mann A. W., Agol E., 2012, Adv. Astron., 2012, 697967
Getley A. K., Carter B., King R., O'Toole S., 2017, MNRAS, 468, 2932
Getley A. K., Carter B., King R., O'Toole S., 2020, MNRAS, 498, 4356
Grether D., Lineweaver C. H., 2006, ApJ, 640, 1051
Meschiari S., Laughlin G. P., 2010, ApJ, 718, 543
Meschiari S., Wolf A. S., Rivera E., Laughlin G., Vogt S., Butler P., 2009, PASP, 121, 1016
Pierens A., Nelson R. P., 2007, A&A, 472, 993
Prša A. et al., 2011, AJ, 141, 83
Rein H., Spiegel D. S., 2015, MNRAS, 446, 1424
Ribas I., 2006, in Aerts C., Sterken C., eds, ASP Soc. Pac. Conf. Ser. Vol. 349, Astrophysics of Variable Stars. Astron. Soc. Pac., San Francisco, p. 55
Ricker G. R. et al., 2014, J. Astron. Telesc. Instrum. Syst., 1, 1
Sahlmann J. et al., 2011, A&A, 525, A95
Slawson R. W. et al., 2011, AJ, 142, 160
Southworth J., Maxted P. F. L., Smalley B., 2004, MNRAS, 351, 1277
Spiegel D. S., Burrows A., Milsom J. A., 2011, ApJ, 727, 57
Sybilski P., Konacki M., Kozłowski S., 2010, MNRAS, 405, 657
Watson C. A., Marsh T. R., 2010, MNRAS, 405, 2037

This paper has been typeset from a TEX/LATEX file prepared by the author.

2.2 Summary of Results

The results from the 68,400 idealised simulations and an estimated 12,196 real-world simulations performed in Getley et al. (2021) show that real-world Kepler observations largely match simulated data and agree with equation 1.4. However, it was also found that there is more to the real-world processes than equation 1.4 suggests.

Detections were considered successful if the best-fit O-C matched the actual O-C of the system and the mass fell within a defined range of the injected third body. Anything else was considered a non-detection. While every simulation had a planet injected, not every injected planet was detectable. The most likely reason a detection didn't match the injected signal and was therefore unable to identify the injected planet is that the eclipse time variations were small. For example, noise within the system (such as slight variations in the stellar object's brightness) may "hide" the injected ETVs and as such the best-fit model fails to accurately determine the inject planets properties.

The results show that the eccentricity of a third body has a significant effect on the detection rate. The larger the eccentricity the more difficult it becomes to detect third bodies at shorter orbital periods. The orbital period of the host binary also has an effect on detectability. Detection rates increase significantly with a longer host binary orbital period.

It is not immediately clear why the eccentricity of a third body has such a significant effect on the detectability. It is possible that the magnitude of eclipse timing variations decreases as eccentricity increases making detections more difficult. Future research would be required to confirm if this is the case and if the effect can be calculated.

The truncation radius of a binary star also appears to play an important role in detectability of third bodies. Equation 2.1 was based on the truncation radius of a binary star and empirically derived from the detectability of third bodies by noting the orbital period when successful detections begin to occur and finding a best-fit quadratic equation. The minimum detection period, DP, is dependent on the period of the host binary star, P_b, and the eccentricity of the third body, e_p.

$$DP = (59{e_p}^2 + 12.1e_p + 4.2)P_b \tag{2.1}$$

Initial values that vary significantly from the true values may take a long time to converge in an interative fit process. As such it is possible solutions (and thus more successful detections) could have occurred had the computing wall time been been able to increase beyond 24 hours. However, as highlighted in section 4.4 of Getley et al. (2021) practical and computational limits restrict what was able to be run. The detection rates therefore should be considered a minimum detection rate.

The detectability of third bodies can be estimated with equations 1.4 and 2.1. As a result, the limits of ETV studies are more accurately known and realistic expectations on detectability can be set before undertaking a study.

CHAPTER 3

WILL THESE BODIES BE STABLE?

While finding system characteristics capable of reproducing the eclipse timing variations is a crucial step in detecting third bodies, equally important is performing a dynamical stability analysis on the proposed system. If bodies are in unstable orbits they may be ejected from the system within a short time period. The longer a body remains within a system, the more likely it is to exist as described (Horner et al. 2012b; Horner et al. 2012a).

In Getley et al. (2020), a dynamical stability analysis was performed on previously reported Kepler binaries with third bodies detected from an Eclipse Timing Variation study. The O-C diagrams of the systems all contained complex variations in the form of a flip-flop effect where the values of the eclipse time variations begin to decrease, or increase, and then suddenly and rapidly reverse direction and change sign. The third bodies range from stellar to planetary mass companions.

The aim of Getley et al. (2020) was to determine what the systems with unusual, flip-flop, characteristics in the O-C diagram have in common and if these proposed systems were stable. If the systems were determined to be stable, it would show that it's not just simple sinusoidal variations that indicate third bodies.

3.1 Getley et al. (2020) "Stability of planetary, single M dwarf, and binary star companions to Kepler detached eclipsing binaries and a possible five-body system"

The published paper Getley et al. (2020), "Stability of planetary, single M dwarf, and binary star companions to Kepler detached eclipsing binaries and a possible five-body system" is presented below.

Monthly Notices of the ROYAL ASTRONOMICAL SOCIETY
MNRAS **498,** 4356–4364 (2020) doi:10.1093/mnras/staa2532
Advance Access publication 2020 August 21

Stability of planetary, single M dwarf, and binary star companions to *Kepler* detached eclipsing binaries and a possible five-body system

A. K. Getley,[1★] B. Carter,[1] R. King[1] and S. O'Toole[2]
[1]*Centre for Astrophysics, University of Southern Queensland, Toowoomba, QLD 4350, Australia*
[2]*Australian Astronomical Optics, Macquarie University, PO Box 915, North Ryde, NSW 1670, Australia*

Accepted 2020 August 17. Received 2020 August 16; in original form 2020 March 3

ABSTRACT

In this study, we identify 11 *Kepler* systems (KIC 5255552, 5653126, 5731312, 7670617, 7821010, 8023317, 10268809, 10296163, 11519226, 11558882, and 12356914) with a flip-flop effect in the eclipse timing variations O − C diagrams of the systems, report on what these systems have in common and whether these systems are dynamically stable. These systems have previously reported high eccentric binary stars with highly eccentric third bodies/outer companions. We find that all of the additional bodies in the system are dynamically stable for the configurations previously reported and are therefore likely to exist as described. We also provide additional evidence of KIC 5255552 being a quadruple star system composed of an eclipsing binary pair and non-eclipsing binary pair with the possibility of a fifth body in the system. With the advent of the NASA's *Transiting Exoplanet Survey Satellite* (*TESS*) exoplanet survey, its precision photometric monitoring offers an opportunity to help confirm more local eclipsing binary star companions, including planets.

Key words: binaries: eclipsing.

1 INTRODUCTION

The *Kepler* Eclipsing Binary Catalog contains more than 2000 eclipsing binary stars that have been observed during the *Kepler* mission (Prša et al. 2011; Slawson et al. 2011). The high precision observations from *Kepler* enable eclipse time studies to be performed where variations in the eclipse times of binary stars can be used to detect third bodies (e.g. Borkovits et al. 2016; Getley et al. 2017). Binary stars that have orbits aligned with the Earth will eclipse each other, and detached and isolated binary stars should have eclipses that occur at predictable intervals. Plots of observed eclipse times (O) minus the calculated eclipse times (C), or O − C plots, may show variations from these predicted intervals. If these variations are also periodic, it may be the result of a third body orbiting the binary stars (Beuermann et al. 2010).

When performing an eclipse timing study on the eclipsing binaries contained in the *Kepler* catalogue, several O − C diagrams were found where the values begin to decrease, or increase, and then suddenly and rapidly reverse direction and change sign, i.e. eclipses that occur earlier than expected change to later than expected, or vice versa. The O − C curves for these systems then rapidly reverse sign again, or flip-flop (see Fig. 1 for a visual example). The secondary eclipse O − C curve is out of phase with the primary eclipse O − C curve by a half orbital period. Examples of these flip-flop systems can be seen in Borkovits et al. (2016). Most of these systems also appear to have eclipse depth variations with differing magnitudes for each system. These systems all have similar reported eccentricities of the eclipsing binary and the highly eccentric orbit of the reported third body/outer companion. For the purposes of this paper, eclipsing binary is defined as the primary and secondary stars that eclipse each other, i.e. producing the eclipses seen in the system O − C diagrams while third body/outer companion refers to one (or more) additional bodies orbiting the eclipsing binary.

The flip-flop features of the O − C diagrams and the high eccentricities raise the question of the dynamical stability of the systems and whether the systems with the reported configurations are stable. The dynamical stability of systems is important as outer companions in unstable orbits may result in the outer companion being ejected from the system within a short time period. However, stable orbits suggest the outer companion will remain within the system and are, therefore, more likely to exist as described and be observed (Horner et al. 2012a,b). If an outer companion is stable for a range of configurations, then the outer companion is more likely to exist as any detection errors will not have a dramatic effect on the determination of the stability of the system.

The aims of this study are to perform a dynamical stability analysis on the systems found with highly eccentric binary star orbits and extremely high eccentric outer companion orbits; report on the source of the flip-flop effect and the stability of the systems KIC 5255552, KIC 5653126, KIC 5731312, KIC 7670617, KIC 7821010, KIC 8023317, KIC 10268809, KIC 10296163, KIC 11519226, KIC 11558882, and KIC 12356914 with the proposed third bodies; comment on the likelihood of these proposed third bodies existing; and comment on the likelihood of more of these flip-flop systems existing that continue to go undetected.

2 METHOD

The *Kepler* data were used to produce O − C diagrams for detached eclipsing binaries to study eclipse timing variations. We created a C++ program, called Binary Eclipse Timings (BET), to determine the

★ E-mail: alan.getley@usq.edu.au

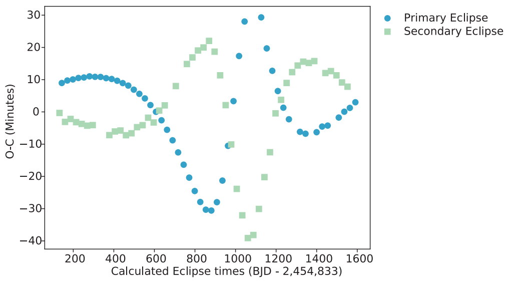

Figure 1. Observed minus calculated (O − C) diagram of KIC 12356914 showing the sudden and rapid period flip in the primary (blue circles) and secondary (green squares) eclipses. For example, at ∼900 d the primary eclipses go from occurring ∼30 min earlier than calculated to ∼30 min later than calculated in the space of ∼200 d.

mid-eclipse times of as many primary and secondary eclipses in the *Kepler* detached binary systems as possible (see Getley et al. 2017). BET is based on the software Transit Analysis Package (TAP; Gazak et al. 2012) that uses the analytic formulae from Mandel & Agol (2002). The analytic formulae describe a system of two objects, using parameters including orbital period, radius ratio of the two objects, mid-eclipse time, orbital inclination, and eccentricity, during various points throughout an orbit. The O − C diagrams of the *Kepler* systems shown in this paper were created using BET and found to contain rapid variations with the primary and secondary eclipse O − C curves out of phase.

REBOUND is an *N*-body integrator with PYTHON and C implementations (Rein & Spiegel 2015). Systems of bodies are able to be set up and integrated over time to estimate the orbital characteristics, such as semimajor axis and eccentricity, at various intervals. By simulating the positions and the evolution of the estimated orbital characteristics of a system over a long time period, we can determine if the proposed system is in a stable orbit (allowing it to have been observed) or if it is in an unstable orbit and likely to eject one or more of the bodies. Eclipse times were obtained from the simulation and an O − C diagram produced to make sure that the distinctive characteristics of the actual O − C diagrams were present. The systems with these orbital characteristics were also integrated for 10^6 yr. These same systems were then integrated again 40 times for 10^4 yr with random values for the mean longitude, argument of pericentre and longitude of ascending node of the orbit of the outer companion, and the eclipsing binary. The purpose of the random values was to see if the third bodies were stable in this very specific configuration or if third bodies were stable for a range of configurations.

For the REBOUND models used, the value for the longitude of the ascending node for the eclipsing binary (i.e. $\Omega_{\rm binary}$) was fixed to 90°. We found when it was fixed to 0°, although the flip-flop features of the O − C diagrams still occurred, the primary and secondary eclipse O − C curves were in phase rather than out of phase as seen within the real O − C diagrams. The value for the longitude of the ascending node for the outer companion (i.e. $\Omega_{\rm companion}$) was set such that $\Omega_{\rm companion} = \Omega_{\rm binary} + \Delta\Omega$.

The individual masses for the primary and secondary star were calculated using the sum of the masses in Borkovits et al. (2016) and the temperature of the systems. Making the assumption that the primary star significantly dominates the temperature of the system, we can search for the corresponding mass of a star at that temperature from Pecaut & Mamajek (2013).[1] This becomes the estimate for the mass of the primary star. Using either a calculated mass ratio or a sum of masses of the primary and secondary star with the estimated primary star mass, calculating the estimated mass of the secondary star becomes trivial. Finally, we compare the $J - H$ colour/magnitude difference of the system with the estimate for the primary star in order to perform a check on the assumption that the primary star significantly dominates the system. We tested this process for estimating masses against *Kepler* systems with known masses for the primary and secondary stars, Kepler-16 (Doyle et al. 2011), Kepler-34 and Kepler-35 (Welsh et al. 2012), Kepler-38 (Orosz et al. 2012b), and Kepler-47 (Orosz et al. 2012a), all with at least one confirmed planet. Our estimates for the primary and secondary masses agree with the reported masses within ∼10 per cent or less. We also tested against systems with no confirmed outer companions, KIC 9851142 (Çakırlı 2015) and KIC 1571511 (Ofir et al. 2012), and found our mass estimates agreed with the reported masses within ∼20 per cent or less.

The first systems to be selected for the dynamical stability study were KIC 5255552, KIC 5731312, KIC 7670617, KIC 10268809, and KIC 12356914 as these systems were identified as part of our own eclipse time study of the *Kepler* eclipsing binaries that had matching entries in Borkovits et al. (2016). These systems all contained a unique flip-flop feature or sudden period change in their O − C diagrams as seen in Fig. 1. The inferred properties of these systems were compared to see what all the systems had in common. The systems were found to have binary eccentricities ranging between ∼0.25 and ∼0.42 and third bodies with eccentricities of at least 0.385. The rest of the systems in Borkovits et al. (2016) were checked to see if there were any other systems that matched these criteria. Finally, the O − C diagrams of the systems were visually compared to find other possible candidates. The complete list of systems and their orbital properties can be found in Tables 1 and 2. Two systems, KIC 4055092 and KIC 9715925, were found to match the selection criteria, however these systems were not a part of the dynamical stability study as both of these systems have mass estimates for the primary star that exceed the mass estimates for the total system. Another two systems, KIC 6794131 and KIC 7177553, were also possible candidates for the dynamical stability study, however accurate values for $m_{\rm a+b}$ were not obtainable from Borkovits et al. (2016). As such, reliable models in REBOUND were unable to be made for these four systems and they were not included in the study.

The systems in Table 2 are listed separately due to the long-period nature of the outer companions. These third bodies all have periods longer than the window of *Kepler*'s observations, and so, while models and fits can give us an indication of the properties and type of third bodies located within the systems, the margin of error in the values is likely too great to make firm conclusions. We can expect any estimate of the orbital period to be a lower limit due to the uncertainty involved in observing a system for less than one complete orbital period. The outer companion mass is likely to be an upper limit as lower masses are more detectable at longer periods (Watson & Marsh 2010). For those systems with orbital periods less than the period of *Kepler*'s observations, the values listed in Table 1 are likely to be accurate with a smaller margin of error.

The primary and secondary masses for the systems listed in Tables 1 and 2 were calculated as described and are listed in Table 3.

[1]With additional details from http://www.pas.rochester.edu/~emamajek/EEM_dwarf_UBVIJHK_colors_Teff.txt

Table 1. A list of orbital properties for the systems used in the dynamical stability studies. Values from Borkovits et al. (2016). With orbital periods for the third bodies less than, or approximately equal to, the *Kepler* viewing window the orbital periods of the third bodies and their properties will be likely to reflect the true nature of the systems.

KIC no.	P_1 (d)	P_2 (d)	m_{a+b} ($M_\odot$)	m_c	e_1	e_2	i_1 (°)	i_2 (°)	ω_1 (°)	ω_2 (°)	$\Delta\Omega$ (°)
5255552	32.465339	862.1	1.7	0.7 $M_\odot$	0.30668	0.4342	83.8	89.5	105.27	37.3	−2.8
5653126	38.49233	968	1.8	1.1 $M_\odot$	0.247	0.189	87	78	313	326	−5
5731312	7.9464246	911	1.1	0.13 $M_\odot$	0.4196	0.584	88.5	77.3	183.9	25.9	36.4
7821010	24.2382191	991	2.3	2.6 M_{Jup}	0.6791	0.372	88	105	239.234	126	−19
8023317	16.57907	610.6	1.3	0.15 $M_\odot$	0.2511	0.249	88	93	177.7	164	−49.3
11519226	22.161767	1437	1.44	1.25 $M_\odot$	0.18718	0.332	88	89	358.4	321.7	17.0

Table 2. A list of orbital properties for the systems used in the dynamical stability studies. With orbital periods for the third bodies larger than the *Kepler* viewing window the ability to accurately resolve these properties is difficult, however they still give an indication of the possible configuration of these systems. Values from Borkovits et al. (2016).

KIC no.	P_1 (d)	P_2 (d)	m_{a+b} ($M_\odot$)	m_c ($M_\odot$)	e_1	e_2	i_1 (°)	i_2 (°)	ω_1 (°)	ω_2 (°)	$\Delta\Omega$ (°)
7670617	27.70317	3304	0.9	0.55	0.249	0.707	86	89	135	86.4	−147.8
10268809	24.70843	7000	1.5	1.4	0.314	0.737	84	94	143.1	292.6	21.6
10296163	9.296847	15271	1.4	0.5	0.354	0.73	86	127	45.7	355	−40
11558882	73.9135	4050	1.9	0.4	0.365	0.30	88	84	169	105	−43
12356914	27.3083183	1804	1.8	0.41	0.325	0.385	88	60	113.2	36.5	−30.4

Table 3. Additional information about the systems found in Tables 1 and 2. The temperature of the system comes from the *Kepler* Eclipsing Binary Catalog. Pecaut & Mamajek (2013) and the temperature are used to estimate the primary star mass and, with the values of m_{a+b} from Tables 1 and 2, the secondary star mass.

KIC no.	Temperature (K)	m_a ($M_\odot$)	m_b ($M_\odot$)
5255552	4775	0.96[a]	0.74
5653126	5766	1.02	0.78
5731312	4658	0.73	0.37
7821010	6298	1.23	1.07
8023317	5625	0.98	0.32
11519226	5646	0.98	0.46
7670617	4876	0.75	0.15
10268809	5787	1.07	0.43
10296163	6229	1.21	0.19
11558882	6066	1.14	0.76
12356914	5368	0.90	0.90

[a]Mass of the primary star is larger than would be expected from the temperature of the system, though the total mass of the binary star system matches and is expected to be useful to determine the stability of the outer companion.

A number of the systems in Tables 1 and 2 have outer companion masses that are almost as large, or even larger, than one or both of the stars in the binary system. If these third bodies significantly contribute to the flux of the system, then the individual mass for the primary star would be larger than estimated and the mass for the secondary star would be lower (although the total mass of the binary system would be unaffected).

With the systems set-up in REBOUND and integrated, plots are produced showing eccentricity versus time and semimajor axis versus time. By considering these plots, we are able to view the evolution of the system over the defined period and determine whether any object is likely to be ejected from the system. For example, by considering the change in semimajor axis we can tell if an outer companion stays within the system or is moving further away from the binary stars and being ejected out of the system.

The light curves for the systems with inclinations of close to 90° were also visually inspected to look for any additional eclipsing events. Additional eclipsing events are a direct way of confirming the existence of additional bodies and may provide additional information about the characteristics and orbital properties of any additional bodies.

3 RESULTS

The *Kepler* flip-flop systems appear visually unique upon the first consideration of their O − C diagram (Fig. 1). The primary and secondary eclipses O − C variations are out of phase with each other, and there are sharp and rapid flip-flops indicating eclipses rapidly transitioning from earlier than expected to later than expected (or vice versa). An example of a simulated model's O − C diagram can be seen in Fig. 2. The simulated O − C diagram shows the same out of phase and rapid variations that can be seen in the actual O − C diagrams from observed data.

The models from REBOUND allowed us to produce visual representations of the bodies and their orbits within the systems found in Tables 1 and 2. By producing visual representations of the binary star orbits (Fig. 3), animating the binary star and outer companion orbits and the inclination evolution of the systems (Fig. 4), we were able to determine that all systems with the flip-flop O − C variations exhibit similar behaviour/orbital configurations as described in Section 2. The binary stars are locally bound together and both orbit and exhibit apsidal precession around the centre of mass of the entire system. The period of the eclipsing binary apsidal precession around the centre of mass appears to be the same as the orbital period of the outer companion, likely due to the dynamical interactions between the outer body and primary and secondary stars. The third bodies orbit the centre of mass opposite the binary stars. The orbits of the binary stars and the system as a whole are provided as animations available as additional supplementary material online. The models

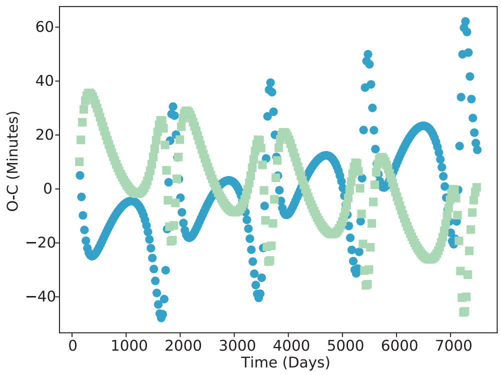

Figure 2. Simulated observed minus calculated (O − C) diagram of KIC 12356914 showing the sudden and rapid period flip in the primary (blue circles) and secondary (green squares) eclipses like the sudden flip-flops seen in Fig. 1.

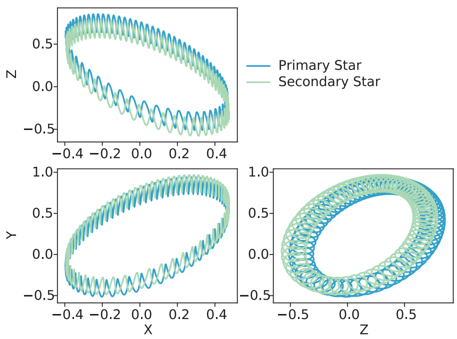

Figure 3. Plot of the *XYZ* coordinates of the two stars in the eclipsing binary of KIC 12356914 showing a wobble around the centre of mass of the systems and the apsidal precession (particularly noticeable in the *YZ* plot) throughout a single orbit of the outer companion. Note: animations of the binary star and outer body orbits will be available online as supplementary material. The observer is in the positive *X* direction with the *Y*-axis running horizontal and the *Z*-axis vertical.

provide clarity on the orbits of the bodies within the system and explain the features seen in the O − C diagrams.

The results of integrating the systems for 10^6 yr can be seen in Figs 5(a)–(f). All of these systems were found to be stable over 10^6 yr. The eccentricities of the eclipsing binary combined with the high eccentricities of the outer companion do not appear to compromise the long-term stability of the systems. While the eccentricities of the objects in the systems varied over differing time-scales and by differing amounts, the semimajor axis remained relatively constant and, therefore, the outer companions remained within each system. As illustrated by Figs 5(d) and (f), while the eccentricity of the binary stars can vary significantly, this did not necessarily translate to a major change in eccentricity of the outer companion or the semimajor axis of the system. The systems were also found to be stable for 10^4 yr when random values were used for the mean longitude, argument of pericentre and longitude of pericentre of the outer companion, and the eclipsing binary. This increases the likelihood of

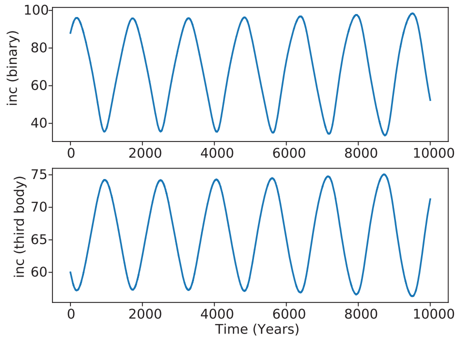

Figure 4. The change in inclination of the eclipsing binary (top) and third body (bottom) for the system KIC 12356914 over 10^4 yr. The eclipsing binary inclination changes between ∼40° and ∼100°. As a result, there are likely to be extended intervals of time when no eclipses of the eclipsing binary will be seen from the Earth.

the outer companions existing as slight changes or deviations from the proposed orbital properties still produced stable orbits.

4 DISCUSSION

The out of phase variations in the O − C diagrams for primary and secondary eclipses are likely the result of apsidal motion (Zasche et al. 2015). The apsidal motion and rapid eclipse time transitions are features that appear in all of the O − C diagrams of the models when an outer companion as described in Tables 1 or 2 is present. The light curves of some of these systems also show significant eclipse depth variations. The eclipse depth variations are likely due to the dynamics of the system at play due to apsidal and nodal precession (Kane, Horner & von Braun 2012), and the evolution of the inclination in the system over time. Apsidal motion and nodal precession are illustrated in the simulated orbits in Fig. 3, while inclination evolution over time for a system can be seen in Fig. 4. Inclination evolution does not necessarily only change the depth of the eclipses seen but also whether we see the eclipses at all. For example, secondary eclipses for KIC 11558882 are not initially seen in the light curve but begin to appear around 800 d (BJD – 245 4833) and remain for the rest of the observing window (Fig. 6).

The *Kepler* mission viewed these systems for approximately 1400 d (Conroy et al. 2014), and it is fortunate that the observation period of *Kepler* coincided with the point in the outer companion's orbit that results in the sudden flip-flop nature of the period changes. For third bodies that have orbital periods greater than 1400 d, part of the orbit will be unobserved and the flip-flop effect potentially missed. The greater the orbital period of the outer companion, the greater the chance of missing this dynamical effect in the observations. The sudden period changes are so rapid, some occurring over approximately 100 d, that even an orbital period of ∼1700 d could result in this system characteristic going undetected in the *Kepler* data.

The set of orbital properties within a system jointly influences the potential for transits or eclipses to be seen in the light curve. The probability of a transit occurring decreases as the orbital period increases (Kane & von Braun 2009) so while KIC 10268809, for example, has inclinations that may indicate the possibility of transits (84° and 94° for the binary stars and outer companion, respectively), the very long orbital period of the outer companion results in transits being unlikely to occur. Extra events can be seen in the light curve

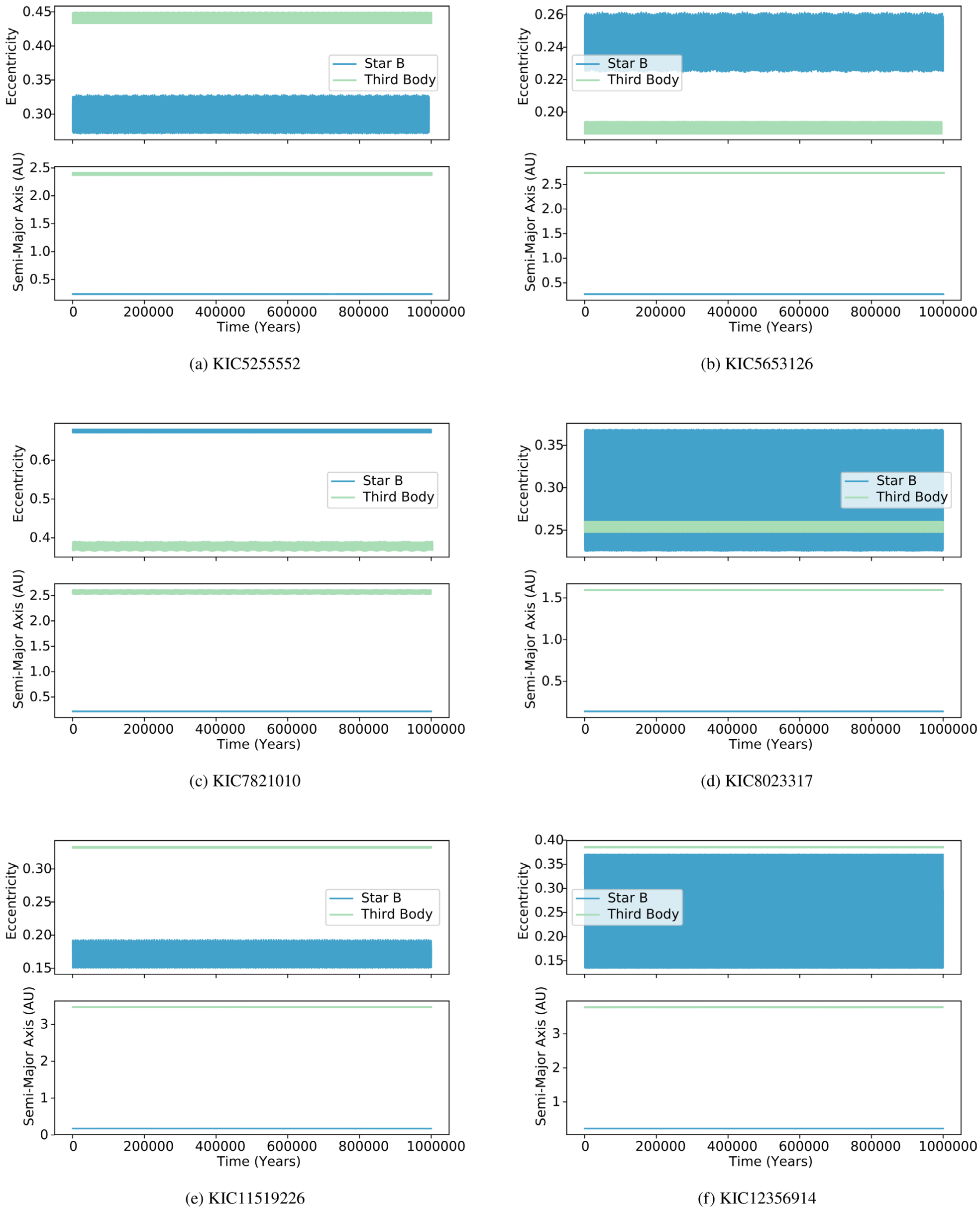

Figure 5. Eccentricity and semimajor axis of the secondary star and third body/outer companion after integration in REBOUND for a period of 10^6 yr for the systems listed in Tables 1 and 2. Note: figures for additional systems will be available online as supplementary material.

of KIC 5255552, indicating that transits occur, and there are also additional eclipses that a third body may not account for, thus indicating the possibility of a quadruple system (Zhang et al. 2018). None of the other systems considered in this study have definite or clear additional events occurring within the light curve, however it is possible KIC 11519226 contains an additional eclipse (described in Section 4.4). The equation for the probability of a third body transit/eclipse being seen from the Earth is

$$P_{\rm tr} = 0.0045 \left(\frac{1\,\rm au}{a}\right) \left(\frac{R_\star + R}{\rm R_\odot}\right) \left[\frac{1 + e\cos(\frac{\pi}{2} - \omega)}{1 - e^2}\right], \qquad (1)$$

where a is the semimajor axis, e is the eccentricity, and ω is the longitude of periastron of the third body and the orientation of the

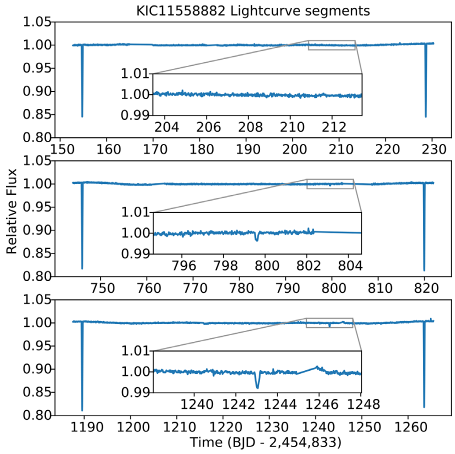

Figure 6. Secondary eclipses for KIC 11558882 are not initially viewable. However, as time progresses and the inclination/binary star orientation changes secondary eclipses come in to view.

orbit of the third body is assumed to be random (Charbonneau et al. 2006). Using equation (1) and the mean radius of stars from Pecaut & Mamajek (2013) with the masses and other orbital characteristics in Table 1, we can calculate the probabilities of seeing transits from the systems with third bodies. We find that the probability of extra events occurring in KIC 5255552, KIC 8023317, and KIC 11519226 to be less than 1 per cent and that the extra events seen in KIC 5255552 must be due to an extremely fortuitous occurrence.

In some systems, the sudden period flip in the O − C diagram may be the only indication of the presence of an outer companion. It is likely, given the large number of eclipsing binary stars observed with *Kepler*, that there are a number of systems that have been observed and classified as not containing an outer companion when in actuality the observations of *Kepler* have not been long enough to observe the effects of an outer companion. With only 11 systems displaying the flip-flop behaviour out of the more than 2000 *Kepler* eclipsing binary systems and almost half of the systems having an outer companion reported with greater than a ∼1400 d orbital period, it is likely that there are many more systems that have outer companions that remain undetected due to orbital configurations that did not result in notable O − C diagrams within the *Kepler* viewing window. The approximately 1400 d viewing window of *Kepler* will necessarily bias the detection results to systems that have outer companions with orbital periods of less than 1400 d. As Tables 1 and 2 contain a similar number of systems, it is possible, if not likely, that the flip-flop characteristic seen in the O − C diagrams will exist in a wide range of systems that have already been observed but not during this flip-flop window.

All of the systems in Tables 1 and 2 were integrated 40 times each for 10^4 yr with random initial values for the mean longitude, argument of pericentre and longitude of pericentre of the third body orbit, and the eclipsing binary. While the random values can produce systems with O − C diagrams that vary significantly from the previously calculated values, the systems are still found to be stable. This exercise shows that even for a wide range of (though not necessarily all) orbital configurations systems with these mass and eccentricity values are likely to be stable.

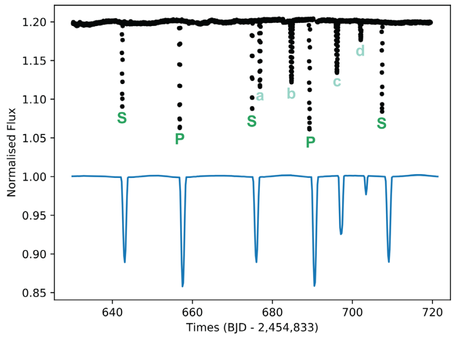

Figure 7. Top (black): a vertically shifted segment of the KIC 5255552 light curve showing the regular primary (P) and secondary (S) eclipses and the additional eclipsing events (a, b, c, and d). Bottom (blue): a segment of the modelled light curve of KIC 5255552 eclipsing binary system with a single companion as described. While there are extra eclipsing events (corresponding to events c and d in the actual light curve), a single companion does not account for the a and b eclipsing events.

4.1 KIC 5255552

The KIC 5255552 reported outer companion mass of 0.7 $M_\odot$ (Borkovits et al. 2016) closely matches the estimated mass of the secondary star at 0.74 $M_\odot$. If this system were to contain a similar tertiary star to the secondary star, we would expect this to have an effect on the system, for example, in the reported colours of the system and therefore affect mass estimates. KIC 5255552 has a Two Micron All Sky Survey (2MASS) $J - H$ magnitude difference of 0.507 that approximately matches a K3V star (Pecaut & Mamajek 2013). Larger mass dwarf stars will have a smaller $J - H$ magnitude difference, while smaller mass stars have a larger $J - H$ value. If the mass of the outer companion was as large as or larger than that of the secondary star, we would expect a smaller $J - H$ magnitude difference, and therefore earlier spectral type. The estimated primary star mass was higher than expected from the temperature of the system and it is possible the $J - H$ magnitude difference indicating a K3V star with a mass of 0.75 $M_\odot$ more accurately reflects the primary star mass.

KIC 5255552 is unique amongst all of the systems considered in this study as it showed clear eclipsing events that cannot be attributed to the binary star alone. The light curve of KIC 5255552 has a number of groups of extra eclipsing events, one group is shown in the top plot of Fig. 7. Four extra observed eclipses (a, b, c, and d) can be seen in this group. This system was then modelled using the PhysicsofEclipsingBinaries (PHOEBE; Horvat et al. 2018) with the binary stars and a third body as described in Table 1. However, only two additional eclipsing events can be seen in the modelled light curve in the bottom section of Fig. 7, corresponding to eclipses c and d seen in the actual light curve. The number of observed eclipsing events indicates that KIC 5255552 contains a fourth body, while the grouping of eclipsing events suggests that the third and fourth body are themselves in a binary star configuration. As no eclipses from the companion binary star are seen in the light curve, we interpret this system as a non-eclipsing binary that itself eclipses an eclipsing binary.

There are clear additional groups of eclipsing events located around approximately 690 and 1542 d, representing the eclipsing binary passing in front of the companion binary, and 948 d, representing the eclipsing binary passing behind the companion binary (Zhang et al. 2018). A particularly large eclipsing event occurs at approximately 1548 d and is expected to be the primary star of the eclipsing binary blocking the light from both stars of the companion binary. Zhang et al. (2018) note a possible additional eclipsing event occurs at approximately 1278 d; however, it is a very shallow and isolated event. It is possible other events occurred slightly earlier than this event. However, they correspond to a time when no observations were taken. Given the probable binary nature of the companion if this is an independent, physical, eclipsing event, it may indicate the presence of a fifth body in the system rather than a fourth body suggested by Zhang et al. (2018).

4.2 KIC 5653126

The mass of the outer companion around KIC 5653126 is reported to be 1.1 $M_\odot$ (Borkovits et al. 2016). Using the method described in Section 2, we estimate the masses of the eclipsing binary primary and secondary stars to be 1.02 and 0.78 $M_\odot$, respectively.

The 2MASS $J-H$ magnitude difference of KIC 5653126 is 0.247 that approximately matches an F9.5V star that is consistent with the mass of the reported outer companion. This may be because the outer companion is a single star that dominates the $J-H$ colour of the system. The presence of significant third light can result in unreliable mass ratio determinations (Hambálek & Pribulla 2013). As a result the mass estimates for the primary and secondary stars of the eclipsing binary would not be accurately determined. Alternatively, the primary star of the eclipsing binary may dominate the temperature of the system with the outer companion contributing only slightly to the $J-H$ colour of the system. However, assuming relatively accurate combined mass estimates, in either case the outcome of the stability check performed would remain the same.

In the second case, if the outer companion contributes slightly to the $J-H$ colour of the system, it is possible that the outer companion is itself an additional binary rather than a single star companion. As there are no additional eclipsing events seen in the light curve of KIC 5653126, this potential additional binary is unlikely to be eclipsing, nor is it likely that a star in either the eclipsing binary or this potential companion binary eclipses a star in the other binary. This is the expected result with the inclination of the outer companion being 78°.

4.3 KIC 7821010

Another system of note is KIC 7821010 that has a third body mass of just ~2.6 Jupiter masses (Borkovits et al. 2016). The evidence for this third body mass (i.e. the eclipse timing fit, the models reproducing the O − C effects, and the stability of the system) all strongly point to the existence and viability of this as a planetary candidate. The third body in this system is in an orbit with an inclination of 105° and with a configuration similar to that of the planetary mass third body found orbiting KIC 5095269 (Getley et al. 2017). It is also further evidence that low-mass objects can have a significant effect on the orbital properties of the host stars and also that, for at least some orbital configurations, eclipse timing variations are a valid way of detecting planetary mass bodies. Eclipse timing variations are particularly useful for detecting planetary mass bodies in orbital configurations that would go undetected with other methods such as searching for transits that require specific orbital characteristics (such as a compatible inclination) to be viewed from the Earth. The $J-H$ magnitude difference of KIC 7821010 from 2MASS is 0.195 and approximately matches the $J-H$ magnitude difference of a 1.25 $M_\odot$ F6V star that is consistent with the mass estimated for the primary star of the system. A planetary mass third body would contribute essentially nothing to the colours of the system and therefore allows for more accurate estimates of the masses of the primary and secondary stars.

4.4 KIC 11519226

KIC 11519226 comprises an outer companion with a mass of 1.25 $M_\odot$ (Borkovits et al. 2016), and eclipsing binary primary and secondary star mass of 0.98 and 0.46 $M_\odot$, respectively. Like KIC 5653126 in Section 4.2, a third body with such a large mass relative to the binary stars would dominate the light from the system.

The inclination of 89° for an additional body around KIC 11519226 indicates the possibility of additional eclipse events taking place within the light curve; however, there is a lot of variability within the light curve of KIC 11519226 that could hide such events. The long-period nature of the additional bodies would also limit the number of eclipses that could be observed. Period04 (Lenz & Breger 2005) was used to attempt to clean the periodicity from the light curve of KIC 11519226 in an attempt to locate additional eclipsing events without success. Despite this, there is a possible additional eclipse event located within the light curve as seen in Fig. 8, however, more observations would be required to confirm if this is an additional eclipse or some other kind of variability.

The 2MASS $J-H$ magnitude difference of KIC 11519226 is 0.321 that is approximately equivalent to a G6V star and closely matches the estimate for the primary star. This $J-H$ colour, coupled with the possibility of an additional shallow eclipsing event despite the 89° inclination, suggests that similar to KIC 5653126 the reported third body may contribute nothing to the colours of the system. An outer companion with a larger mass than the primary and secondary star that does not contribute to the colour of the system suggests the outer companion may be an additional binary, comprised of two smaller stars, or a white dwarf.

A periodogram of the variability was produced using the Lomb–Scargle approach in GATSPY (VanderPlas & Ivezić 2015) and is shown in Fig. 9. Two large peaks can be seen, the first at 5.3023 d and the second at 13.3276 d, while a smaller peak can be seen at 2.7084 d. The variability periods of 2.7084, 5.3023, and 13.3276 d are in an approximately 1:2:5 ratio.

δ Scuti variable stars exhibit pulsations in the orders of hours (Rodríguez & Breger 2001), while γ Doradus variable stars are typically early F- to late A-type stars (Van Reeth Tkachenko & Aerts 2016) as opposed to the G6 primary star estimated in this system. The vast majority of γ Doradus candidates listed in Handler (1999) have variability periods of less than 2 d. One system, HD 109838, stands out as an exception to the typical periods of a γ Doradus star with possible periods of 14 and 2.9 d, however the periods are listed as uncertain. The variability periods for HD 109838 are comparable to the variability periods seen in KIC 11519226.

5 SUMMARY AND CONCLUSIONS

In this study, we used custom software BET based on TAP to perform an eclipse timing study on *Kepler* eclipsing binary stars. During the eclipse timing study we found systems that had O − C diagrams that displayed flip-flop or out of phase variations between the primary and secondary eclipse O − C curves and rapid period change variations. REBOUND was used to simulate these systems. The systems in Tables 1 and 2 were chosen as they all exhibited a unique flip-flop effect within their O − C diagrams. Outer companions with

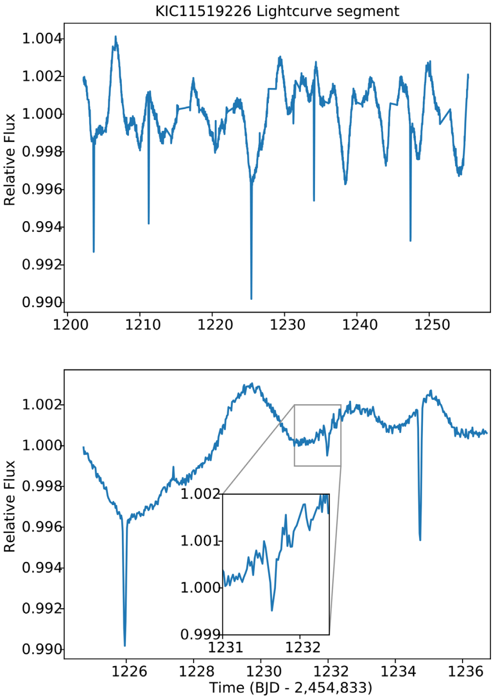

Figure 8. Top panel: a segment of the light curve of KIC 11519226 showing a number of primary and secondary eclipses, the variability in the light curve, and a possible extra eclipsing event. Bottom panel: a possible extra eclipsing event in the light curve of KIC 11519226. The primary eclipse can be seen on the left, the secondary eclipse on the right, and the possible extra eclipsing event is shown in the rectangle. Given the long period of the outer companion, no additional eclipses would be seen and secondary eclipses are likely lost in the variability of the light curve itself.

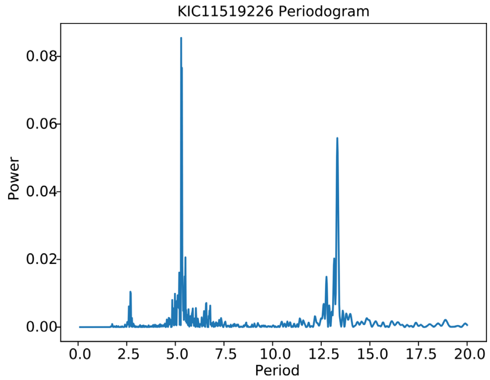

Figure 9. A periodogram of the variability in the out of eclipse light curve of KIC 11519226. Two large peaks can be seen, first at 5.3023 d and second at 13.3276 d, and one smaller peak can be seen at 2.7084 d.

the characteristics described all account for the features seen in the O − C diagrams such as the out of phase eclipse time variations and the flip-flop effect. With the systems simulated in REBOUND we then integrated the systems as described for 10^6 yr. We found that all systems were dynamically stable for at least 10^6 yr and, therefore, bodies in these orbital configurations are likely to be stable and observable. We also integrated these systems with random values for the mean longitude, argument of pericentre and longitude of pericentre of the third body, and the binary star for 10^4 yr and found that the systems were stable for a wide range of orbital configurations. The evidence suggests the outer companions for the systems listed in Table 1 are an additional pair of stars in a binary configuration (KIC 5255552, KIC 5653126, and KIC 11519226), a single M dwarf star (KIC 5731312 and KIC 8023317), and a planet (KIC 7821010).

We also suspect that a larger number of systems that have been observed would also show similar flip-flop characteristics if observed over longer or much longer time spans. However, due to the limits of the *Kepler* viewing window and large orbital periods estimated for the third bodies/outer companions the flip-flop effect continues to go undetected. As more and more systems are found with multiple bodies, the dynamical stability of the system as a whole is an important consideration when determining the likelihood of their existence. Of particular note is KIC 7821010 that has a third body mass of ∼2.6 Jupiter masses. At ∼2.6 Jupiter masses it is well within planetary mass range and shows that even a relatively small mass can have large effects on the motion of its parent stars.

Other stand-out systems from this study include KIC 5255552, where there are additional eclipses in the light curve (Zhang et al. 2018) that may indicate the presence of a fourth star bound in a binary with the third star. A fifth body in the KIC 5255552 system is a possibility and further observations of the system are crucial in determining the true nature of this system. While a triple star explanation cannot be ruled out for the systems KIC 5653126 and KIC 11519226, the photometric and dynamical analysis performed for this study suggests these systems are detached eclipsing binary stars with binary star companions.

Some of the systems presented, for example KIC 11558882, cannot be reliably studied with ground-based observations. The orbital period of the binary stars can be so great that observing eclipses to get meaningful data were only made possible with *Kepler*. Without space-based observations these systems, and their O − C variations, may have continued to go undetected.

Transiting Exoplanet Survey Satellite (*TESS*; Ricker et al. 2015) is an all-sky survey of bright local stars with the ability of detecting planets with orbital periods of a few hours to a year or more. The launch of *TESS* provides more opportunities to locate comparable systems that are more local to the Solar system and capable of follow-up studies. With the launch of *TESS* and future projects, we expect the number of systems that have similar characteristics to increase significantly.

ACKNOWLEDGEMENTS

This research has been supported by an Australian Government Research Training Program Scholarship. We would like to thank the referee and editor for their helpful feedback.

DATA AVAILABILITY

The data underlying this paper will be shared on reasonable request to the corresponding author.

REFERENCES

Beuermann K. et al., 2010, A&A, 521, L60
Borkovits T., Hajdu T., Sztakovics J., Rappaport S., Levine A., Bíró I. B., Klagyivik P., 2016, MNRAS, 455, 4136
Çakırlı Ö., 2015, New Astron., 38, 55
Charbonneau D., Brown T. M., Burrows A., Laughlin G., 2006, in Reipurth B., Jewitt D., Keil K., eds, Protostars and Planets V. Univ. Arizona Press, Tucson, AZ, p. 701
Conroy K. E., Prša A., Stassun K. G., Orosz J. A., Fabrycky D. C., Welsh W. F., 2014, AJ, 147, 45
Doyle L. R. et al., 2011, Science, 333, 1602
Gazak J. Z., Johnson J. A., Tonry J., Dragomir D., Eastman J., Mann A. W., Agol E., 2012, Adv. Astron., 2012, 697967
Getley A. K., Carter B., King R., O'Toole S., 2017, MNRAS, 468, 2932
Hambálek Ľ., Pribulla T., 2013, Contr. Astron. Obser. Skalnate Pleso, 43, 27
Handler G., 1999, MNRAS, 309, L19
Horner J., Wittenmyer R. A., Hinse T. C., Tinney C. G., 2012a, MNRAS, 425, 749
Horner J., Hinse T. C., Wittenmyer R. A., Marshall J. P., Tinney C. G., 2012b, MNRAS, 427, 2812
Horvat M., Conroy K. E., Pablo H., Hambleton K. M., Kochoska A., Giammarco J., Prša A., 2018, ApJS, 237, 26
Kane S. R., von Braun K., 2009, in Pont F., Sasselov D., Holman M. J., eds, Proc. IAU Symp. Vol. 253, Transiting Planets. Cambridge Univ. Press, Cambridge, p. 358
Kane S. R., Horner J., von Braun K., 2012, ApJ, 757, 105
Lenz P., Breger M., 2005, Commun. Asteroseismol., 146, 53
Mandel K., Agol E., 2002, ApJ, 580, L171
Ofir A., Gandolfi D., Buchhave L., Lacy C. H. S., Hatzes A. P., Fridlund M., 2012, MNRAS, 423, L1
Orosz J. A. et al., 2012a, Science, 337, 1511
Orosz J. A. et al., 2012b, ApJ, 758, 87
Pecaut M. J., Mamajek E. E., 2013, ApJS, 208, 9
Prša A. et al., 2011, AJ, 141, 83
Rein H., Spiegel D. S., 2015, MNRAS, 446, 1424
Ricker G. R. et al., 2015, J. Astron. Telesc. Instrum. Syst., 1, 014003
Rodríguez E., Breger M., 2001, A&A, 366, 178
Slawson R. W. et al., 2011, AJ, 142, 160
VanderPlas J. T., Ivezić Ž., 2015, ApJ, 812, 18
Van Reeth T., Tkachenko A., Aerts C., 2016, A&A, 593, A120
Watson C. A., Marsh T. R., 2010, MNRAS, 405, 2037
Welsh W. F. et al., 2012, Nature, 481, 475
Zasche P., Wolf M., Vraštil J., Pilarčík L., 2015, AJ, 150, 183
Zhang J., Qian S. B., Wang S. M., Sun L. L., Wu Y., Jiang L. Q., 2018, A&A, 610, A72

SUPPORTING INFORMATION

Supplementary data are available at *MNRAS* online.

Please note: Oxford University Press is not responsible for the content or functionality of any supporting materials supplied by the authors. Any queries (other than missing material) should be directed to the corresponding author for the article.

This paper has been typeset from a TEX/LATEX file prepared by the author.

3.2 Summary of Results

It was found in Getley et al. (2020) that eccentric binary stars with highly eccentric third bodies are capable of producing the flip-flop effect seen in the O-C diagrams of some Kepler systems. It was also found that these third body companions were dynamically stable over at least 10^6 years and are therefore likely to be stable and observable.

The method for estimating primary and secondary star masses was tested against known systems to check for accuracy. The mass estimates were found to be within ~10 per cent or less of the reported values for systems with a confirmed tertiary companion. For systems without a third body the masses were found to be within ~20 per cent or less. While the masses of the individual stellar components may not be precise, the total mass of the binary stars is expected to be accurate. As such the stability of the third body would be expected to remain the same even if there were variations in the stellar masses from predicted. However, future work may be needed to confirm this.

Due to the rapid nature of the flip-flop effect, some occurring over just 100 days, it is likely that a larger number of these systems exist. However, due to the Kepler viewing window, and long orbital periods estimated for the third bodies, the flip-flop feature continues to go undetected.

KIC 7821010 has a reported third body of ~2.6 Jupiter Masses in a 991 day orbital period. This aligns with expectations using equations 1.4 and 2.1 and shows that even relatively small mass third bodies can have a large effect on the motion of the parent stars.

During the analysis of the systems, additional eclipses in the KIC 5255552 suggested the presence of a fourth body. The system is likely comprised of an non-eclipsing binary pair which itself eclipses the eclipsing binary pair. It is possible a fifth body is present in this system, however further analysis is required to confirm. The evidence also suggested additional stars in KIC 5653126 and KIC 11519226.

PHOEBE was used in Getley et al. (2020) to help illustrate that three bodies were unable to produce the additional eclipsing events seen in KIC 5255552. It should be noted that while the PHOEBE code technically allows for tertiary bodies, this functionality of the code has not been rigorously tested and released. The grouping of extra eclipsing events and particularly the extremely deep eclipsing event overwhelmingly suggests a second binary and the results from PHOEBE provides a simple visualisation of the system and supplementary evidence.

CHAPTER 4

AN OUT OF THIS WORLD DISCOVERY

One of the primary purposes of the thesis was to search for planetary mass third bodies by timing binary star eclipses. In Getley et al. (2017) an eclipse time variation study was performed on detached eclipsing binary stars using custom software Binary Eclipse Timings or BET (appendix B). The detached eclipsing binary stars were selected from the Kepler Eclipsing Binary Catalog. Detached eclipsing binary stars were selected as variations in eclipse times should be due to factors external to the binary star (such as from a third body), rather than internal to the system (such as tidal forces distorting the stars).

With O-C diagrams produced for the eclipsing binaries, systems with periodic variations in the O-C diagram were selected to be analysed in order to locate potential third bodies. KIC 5095269 was manually identified as a system potentially hosting a third body.

Getley et al. (2017) presents the results of an eclipse time study on KIC 5095269 and the evidence for a planetary mass third body.

4.1 Getley et al. (2017) "Evidence for a planetary mass third body orbiting the binary star KIC 5095269"

The published paper Getley et al. (2017) "Evidence for a planetary mass third body orbiting the binary star KIC 5095269" is presented below.

Monthly Notices of the ROYAL ASTRONOMICAL SOCIETY
MNRAS **468,** 2932–2937 (2017)
Advance Access publication 2017 March 14
doi:10.1093/mnras/stx604

Evidence for a planetary mass third body orbiting the binary star KIC 5095269

A. K. Getley,[1★] B. Carter,[1] R. King[1] and S. O'Toole[2]

[1]*Computational Engineering and Science Research Centre, University of Southern Queensland, Toowoomba, QLD 4350, Australia*
[2]*Australian Astronomical Observatory, PO Box 915, North Ryde, NSW 1670, Australia*

Accepted 2017 March 9. Received 2017 March 8; in original form 2016 September 11

ABSTRACT

In this paper, we report the evidence for a planetary mass body orbiting the close binary star KIC 5095269. This detection arose from a search for eclipse timing variations amongst the more than 2000 eclipsing binaries observed by *Kepler*. Light curve and periodic eclipse time variations have been analysed using SYSTEMIC and a custom BINARY ECLIPSE TIMINGS code based on the TRANSIT ANALYSIS PACKAGE which indicates a $7.70 \pm 0.08 M_{\mathrm{Jup}}$ object orbiting every 237.7 ± 0.1 d around a $1.2\,\mathrm{M}_\odot$ primary and a $0.51\,\mathrm{M}_\odot$ secondary in an 18.6 d orbit. A dynamical integration over 10^7 yr suggests a stable orbital configuration. Radial velocity observations are recommended to confirm the properties of the binary star components and the planetary mass of the companion.

Key words: binaries: eclipsing.

1 INTRODUCTION

Planet formation is widely considered to be dominated by core accretion, but an alterative disc instability mechanism has been proposed to explain gas giant planets and brown dwarfs (Boss 2012; Chabrier et al. 2014). In addition, while it is convenient to set a mass divide (at around 13 Jupiter masses) between planets and deuterium burning brown dwarfs (Burgasser 2008), it has been argued that a separation of planets and brown dwarfs based on the formation mechanism is more physically meaningful (Nordlund 2011). A key way to constrain planet formation models is to test their predictions as to the frequency, masses, orbits and stability of planets orbiting eclipsing binary stars, whose mutual eclipses can also provide accurate host star properties. The problem to be solved however is to find such planets, as to date very few such circumbinary planets have been found (Sigurdsson et al. 2003; Correia et al. 2005; Lee et al. 2009; Doyle et al. 2011; Kostov et al. 2016). In particular, the discovery of the long-period transiting circumbinary planet Kepler-1647b may represent an example of a large population of distantly orbiting massive planets orbiting close binary stars (Kostov et al. 2016). Our research therefore represents the initial results of a search for eclipsing binary planets that use eclipse timings to enable planets orbiting above or below the stellar orbital plane to be detected.

Contained in the 'Kepler Eclipsing Binary Catalog' are more than 2000 eclipsing binaries that have been observed over the life of the *Kepler* mission (Prša et al. 2011; Slawson et al. 2011). Predominately detached binaries stars, i.e. binary stars with a morphology classification of less than 0.5, account for almost half of the systems in the eclipsing binary catalog. The high precision observations that were performed allows an eclipse time study to be performed. Eclipsing binary stars that are detached and isolated should have eclipses that occur at a constant and predictable time apart. Plotting the observed eclipse time (O) minus the calculated eclipse time (C) against a best-fitting linear ephemeris, variations from this constant time may be able to be seen. Periodic variations may be the result of a third body orbiting the binary (Beuermann et al. 2010).

In systems that show periodic variations, the properties of the binary stars need to be estimated in order to fit and determine the characteristics of any additional bodies. Estimates for the masses of the binary stars are calculated from the colour data given in the Kepler data and modelling the light curve in JKTEBOP (Southworth, Maxted & Smalley 2004). Colours and masses for spectral types are given in Pecaut & Mamajek (2013). With a mass ratio and mass estimate from the system colours, individual masses can be worked out. By using SYSTEMIC (Meschiari et al. 2009; Meschiari & Laughlin 2010), a system can be set up with the masses and characteristics of the binary stars. From here additional bodies can be added and fit to determine if characteristics can account for eclipse time variations.

In this paper, we report on the results of an eclipse time study of a specific Kepler system, KIC 5095269, and the follow-up SYSTEMIC study in order to determine the characteristics of a third body. We propose the existence of a third body around KIC 5095269 with a mass of 7.70 ± 0.08 Jupiter masses.

2 O − C PRODUCTION AND IDENTIFICATION

We used the Kepler data to produce O − C diagrams to study eclipse timing variations. Detached eclipsing binaries were selected in order to minimize variations from within the system itself. A

★ E-mail: alan.getley@usq.edu.au

primary eclipse occurs when the larger star passes in front of the smaller star, while a secondary eclipse occurs when the smaller star passes in front of the larger star. The time of as many primary eclipses and secondary eclipses as possible must be determined in order to perform an eclipse time variation study. We created a program, called BET or BINARY ECLIPSE TIMINGS, to determine eclipse times. BET is based on the software TRANSIT ANALYSIS PACKAGE or TAP (Gazak et al. 2012) and uses the analytic formulae for the transit or eclipse of a star which are found in Mandel & Agol (2002). The analytic formulae in Mandel & Agol (2002) describe a system of two objects during various points in its orbit. The objects can be a star and a planet (i.e. describing transits) or two stars (i.e. describing eclipses). The systems are described using the parameters: orbital period, the radius ratio of the two objects, scaled semimajor axis, orbital inclination, orbital eccentricity, argument of periastron, mid-time of eclipse/transit and two parameters specifying quadratic limb darkening. BET detects eclipses from the Kepler data and uses the analytic formulae to accurately determine the mid-eclipse times of a system.

With the observed eclipse times of a system determined, calculated eclipse times are needed in order to produce an O − C diagram. Since the time between eclipses should be constant, a calculated eclipse time can be found with the equation

$$T_n = P \times n + T_0, \tag{1}$$

where P is the period of the system, n is the cycle number and T_0 is the initial eclipse time.

Equation (1) can be modified to account for primary and secondary eclipses and take the form seen in (2):

$$\begin{aligned} T_{np} &= P \times n + T_{0\mathrm{p}}, \\ T_{ns} &= P \times n + T_{0\mathrm{s}}, \end{aligned} \tag{2}$$

where $T_{0\mathrm{p}}$ is the initial primary eclipse, $T_{0\mathrm{s}}$ is the initial secondary eclipse, n is the cycle number and P is the period of the system which is common to both primary and secondary eclipses.

By performing a least-squares best fit to the observed eclipse times with (2) the best-fitting period and initial eclipse times will be found. Expected eclipse times can then be calculated. By plotting the observed eclipse time minus the calculated eclipse time against the predicted eclipse time, variations from the expected may be observed. These variations have been separated into five different, custom defined, categories based on their O − C diagrams: no or irregular variations, periodic variations, sudden period flips, long-term trends and out of phase long-term trends. Variations may be caused by star spots (Orosz et al. 2012), apsidal motion (Beuermann et al. 2010) or dynamical interactions (Borkovits et al. 2003). It is also possible that periodic variations are caused by the effects of a third body (Beuermann et al. 2010).

The times of observations in the Kepler data is in Barycentric Julian Date (BJD) which is the Julian Date that has been corrected for the effects of the Earth's orbit. This correction will prevent Earth's orbit from appearing in the O − C diagrams. During the eclipse timing study, systems with no or irregular variations could be seen. These O − C variations would range from 0 to approximately 30 s and appear with no recurring pattern. Systems that have O − C variations larger than 30 s and particularly those that exhibit periodic O − C variations that are suspected to be caused by the addition of a third body should be prioritised for further investigation. However, as apsidal motion may also be the cause of periodic variation (Beuermann et al. 2010), it cannot be assumed that third bodies are the cause of the O − C variations. In the hunt for planets, small amplitude variations (i.e. a few minutes) are also prioritised over larger variations as larger objects (i.e. stars) will have more of an effect on binary stars than smaller objects (i.e. dwarf stars or planets).

Table 1. Table of eclipse times for KIC 5095269. The eclipse time is in BJD − 2454833. The eclipse times are used to produce an O − C diagram to look for eclipse timing variations. A sample of the table is shown here, the full table is available online.

Eclipse time (BJD − 2454833)	Error (d)
133.865203	2.78×10^{-5}
152.478622	2.76×10^{-5}
171.091481	2.72×10^{-5}
189.702749	2.71×10^{-5}
208.313380	2.67×10^{-5}
226.924859	2.71×10^{-5}
245.537254	2.63×10^{-5}
264.150062	3.12×10^{-5}

3 FOLLOWING UP ON IDENTIFIED O − C DIAGRAMS

With an O − C diagram showing periodic variability, the next task is to try to determine the cause of the variability. In this study, the software SYSTEMIC (Meschiari et al. 2009; Meschiari & Laughlin 2010) has been used to model the system and estimate the characteristics of a third based on its effect on the binary stars. SYSTEMIC can be used to model eclipse and transit timing variations. In order to accurately determine the properties of any potential third bodies the mass for the primary and secondary stars must be estimated. Radial velocity data are needed to determine the mass of binary stars; however, these data can be difficult to obtain for Kepler stars without the use of a large telescope. As a result, mass estimates for the binary stars were calculated based on the data in the Kepler data base and the light curve of the system.

JKTEBOP (Southworth et al. 2004) was used to find the best fit to model the light curve in order to determine/estimate the parameters of the system such as the orbital period, mass ratio of the binary stars and inclination of the system. Other data for the binary star systems such as the $V - K$ colour can be used to help validate and guide the mass estimates of the binary star. By using the colours of the system and the mass ratio and other property estimates from JKTEBOP, a system can be set up in SYSTEMIC to determine the properties of a potential third body. If the colours fall between two star types, the larger masses can be used and as a result the mass of any third body present should be an upper estimation of the mass. JKTEBOP was selected as it is capable of fitting the parameters of a system, including limb darkening and mass ratio.

4 RESULTS

Having processed the detached eclipsing binary stars from the Kepler 'Eclipsing Binary Catalog', the O − C diagrams were then classified. One of the systems identified from the O − C diagrams as a potential host to a third body was KIC 5095269. The primary eclipse times and the errors reported by the fitting function from BET can be seen in Table 1 and an example eclipse fit from BET is shown in Fig. 1. Secondary eclipses were too shallow and unable to be fit and have accurate times determined.

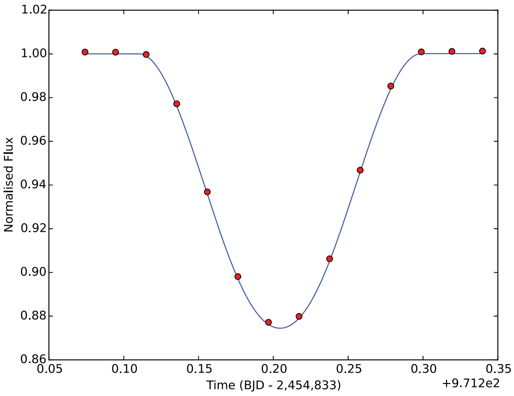

Figure 1. Example of a primary eclipse fit by BET (blue solid line) to the data obtained from *Kepler* (red circles).

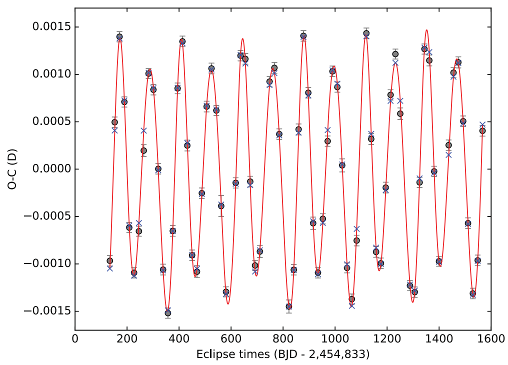

Figure 2. The O − C points and best-fitting model to explain the eclipse timing variations. The grey circles are the O − C points for KIC 5095269 while the red line is the modelled eclipse time variations. A blue X marks the best-fitting O − C points. SYSTEMIC takes the entered eclipse times, integrates the system to find the eclipse time closest to the entered time and plots the O − C value. Non-Keplerian dynamics and the orbital characteristics of the third body (visualized in Fig. 5) are thought to be the source of the variation in the maxima and minima in this O − C diagram.

Using the data found in Table 1 and fitting using the functions found in (2), the period of the system, P, was found to be 18.611 957 d and the initial primary eclipse, T_{0p}, occurred at 133.866 170 (BJD − 2454833). The secondary eclipses were found to be too shallow to accurately fit and as such no secondary eclipse times were obtained. The O − C diagram and data for the primary eclipses in KIC 5095269 are shown by the circles in Fig. 2. The O − C diagram shows periodic variability that has a period of approximately 120 d with variations in the eclipse times of up to approximately 2 min.

In addition to the orbital period of 18.611 957 d and an initial eclipse occurring at 133.866170 (BJD − 2454833), modelling the light curve in JKTEBOP (Southworth et al. 2004) found a mass ratio of approximately 0.421 and an inclination of 80.02 deg. An eclipse from the Kepler data with the modelled light curve from JKTEBOP can be seen in Fig. 3. With a Kepler magnitude of 13.528 and a 2MASS K magnitude of 12.215, this system has a $V - K$ value

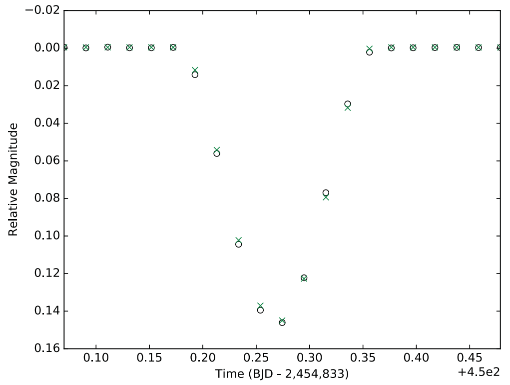

Figure 3. A small section of the light curve from *Kepler* and the model from JKTEBOP showing an eclipse. The light-curve data from *Kepler* is shown by the circles, while the model data obtained from JKTEBOP is shown by ×.

of 1.313. This $V - K$ value approximately matches an F7 star (Bessell & Brett 1988). If the secondary star were much hotter than an M star it would have an impact on the K magnitude of the system, and therefore the $V - K$ value. This is not consistent with observations. With an F7V primary star with a mass of 1.21 $M_{\odot}$ (Pecaut & Mamajek 2013) and a mass ratio of 0.421, the secondary star would have a mass of 0.51 $M_{\odot}$. This is consistent with the mass of an M star as the $V - K$ colour suggests.

SYSTEMIC (Meschiari et al. 2009; Meschiari & Laughlin 2010) was then used to set up a representative system with the main (larger) star being set to a mass of 1.21 solar masses. 'Planet 1' was set up with the characteristics of the secondary star and the system, i.e. a mass of 0.51 solar masses, an orbital period of 18.611 957 d and an inclination of 80.0235 deg. The masses as well as the orbital period and inclination of the binary stars were fixed while all the other parameters were free to be fit by the program. An additional planet (Planet 2) was added to the system with the period of the O − C variability set as the period of the planet. All parameters for the additional body were also free to be fit. The eclipse times were loaded into SYSTEMIC and the uncertainties in the eclipse times were doubled in SYSTEMIC in order to estimate the true uncertainty in the eclipse times. A best fitting was then performed by SYSTEMIC to find the values for the system that best explains the O − C variability.

The results of the SYSTEMIC best fitting can be seen in Fig. 2, the residuals of the fit are shown in Fig. 4 and the data for the binary system are shown in Table 2 while the data for the third body are shown in Table 3. The properties of the binary system were entered into PHysics Of Eclipsing BinariEs or PHOEBE (Prša & Zwitter 2005; Degroote et al. 2013) to view a synthetic light curve. PHOEBE suggested an inclination of approximately 86.5 deg was required to view a primary eclipse but no/minimal secondary eclipse as can be seen in the light curve. The inclination of the system was kept at 80.02 deg suggested by JKTEBOP as this was found by fitting the light curve; however, the larger inclination from PHEOBE was noted.

5 DISCUSSION

The results of the SYSTEMIC fit indicate that a third body with an orbital period of 237.708 17 ± 0.122 13 d and a mass of 7.70 ± 0.08

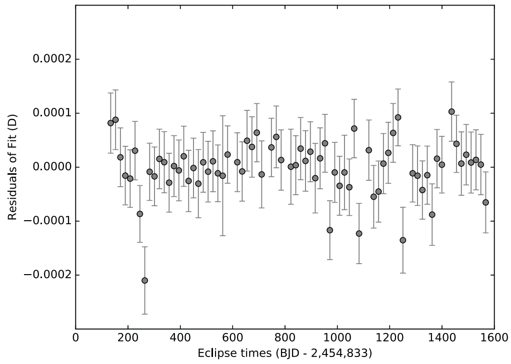

Figure 4. Residuals of the SYSTEMIC fit showing the difference between the observed eclipse times and the modelled eclipse times. The smaller the values of the residuals, the closer the modelled eclipse times are to the observed eclipse times.

Table 2. Table of data provided by the SYSTEMIC fit for the binary system. The mass of the primary and secondary stars, the orbital period of the binary stars and the inclination were fixed at pre-calculated values while the rest of the parameters were free to be fit. The median and median absolute deviation (MAD) values were also determined by SYSTEMIC.

Property	Best-fitting value	Median value	MAD value
Primary star mass ($M_{\odot}$)	1.21	N/A	N/A
Secondary star mass ($M_{\odot}$)	0.51	0.51	1.24×10^{-3}
Orbital period (d)	18.611 96	18.611 96	1.55×10^{-7}
Mean anomaly (deg)	7.44	7.44	1.31×10^{-4}
Eccentricity	0.246	0.246	9.3×10^{-6}
Long. peri (deg)	22.82	22.82	2.23×10^{-4}
Inclination (deg)	80.0	80.0	0.02
Node (deg)	305.54	305.54	2.3×10^{-4}

Table 3. Table of data provided by the SYSTEMIC fit for the third body. All of the parameters were free to be fit. The Median and MAD values were also determined by SYSTEMIC.

Property	Best-fitting value	Median value	MAD value
Mass (M_j)	7.698	7.693	0.054
Orbital period (d)	237.70817	237.68977	0.08237
Mean anomaly (deg)	290.92	289.44	2.34
Eccentricity	0.0604	0.0603	0.0021
Long. peri (deg)	27.67	29.03	2.07
Inclination (deg)	105.92	105.83	0.98
Node (deg)	64.19	64.10	0.28

Jupiter masses could account for the eclipse timing variations seen (all errors are quoted to a single standard deviation unless otherwise noted). The mass of this third body is expected to be an upper limit and suggests the third body is actually a planet orbiting the binary stars. The best-fitting orbit of the binary stars is 18.611 96 d. The eccentricity of the binary stars and planet as determined by SYSTEMIC was found to be 0.246 and 0.060 ± 0.003, respectively. The data produced from SYSTEMIC found that the best fit to match the eclipse timing variations occurs when there is a third body with a mass of 7.70 ± 0.08 Jupiter masses. This mass is below the proposed planet/brown dwarf boundary of roughly 13 Jupiter masses (Burgasser 2008) and as such the third body is regarded

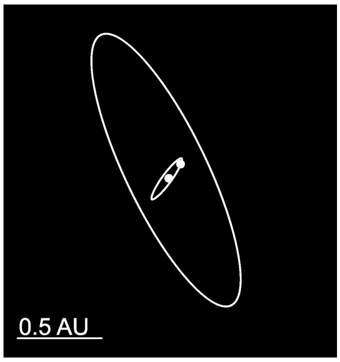

Figure 5. A visualization of the system as determined by the program SYSTEMIC. The primary and secondary stars are at the centre and the third body is found to be orbiting both stars.

as a planet rather than a brown dwarf. Though how this object formed may determine whether it is a large planet or a small brown dwarf (Nordlund 2011). If this third body is confirmed to be a circumbinary planet it would join a small number of previously confirmed circumbinary planets (Sigurdsson et al. 2003; Correia et al. 2005; Lee et al. 2009; Doyle et al. 2011; Kostov et al. 2016), and this body would have one of the largest masses of these circumbinary planets.

With the period of the O − C variability being approximately 120 d, it was expected that the orbital period of the third body would be approximately the same. However, the SYSTEMIC fit was significantly better (both visually and by reduced χ^2 value) with a period of 237.7 d and therefore this fit was chosen as the optimal fit. SYSTEMIC incorporates non-Keplerian dynamics found in Fabrycky (2010) and it is thought that the orbital characteristics of the planet (as visualized in Fig. 5) coupled with non-Keplerian dynamics are the reason the orbital period of the planet varies from what was expected and also accounts for the variation seen in the maxima and minima of the O − C diagram in Fig. 2. The orbital period of the planet approximately matches the period of the variation in the maxima and minima of the O − C diagram.

The found system was tested in order to check the robustness of the fit. By testing the binary star system in PHOEBE, we can confirm that the values for the binary star system are reasonable. The inclination of the system was changed in SYSTEMIC to 86.5 deg as found by PHOEBE. The results of the third body remain consistent with the mass of the third body changing to 7.72 Jupiter masses. The next test involved changing the mass of the primary and secondary stars to determine if the best-fitting system correspondingly changed the mass of the third body. The mass ratio between the stars and the planet was found to remain the same regardless of the actual masses used. During the robustness test, the mass ratio of the stars and planet was also changed. In all cases, a third body with significantly less mass than the binary stars was able to account for the eclipse timing variations seen. With a mass ratio between the binary stars of 0.7889 (i.e. the primary remains at our estimated value and the secondary star mass set to the largest value allowed by SYSTEMIC for additional bodies of 1000 Jupiter masses), the best-fitting mass for the third body was found to be 10.35 Jupiter masses which is still below the putative planet/brown dwarf boundary of 13 Jupiter masses. With a mass ratio 0.01 (i.e the secondary star has a mass that is 0.01 times the mass of the primary star), the best-fitting mass for

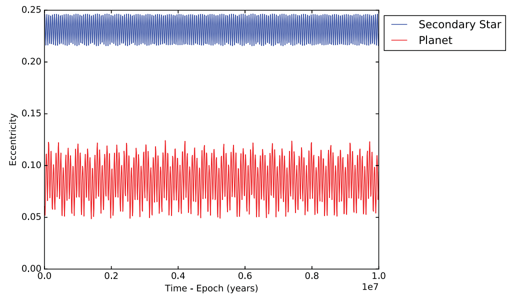

Figure 6. Eccentricity of the secondary star and planet after integration of the SYSTEMIC system over a period of 10^7 yr. The secondary star has very little variation in eccentricity. The planet has some variation in the eccentricity.

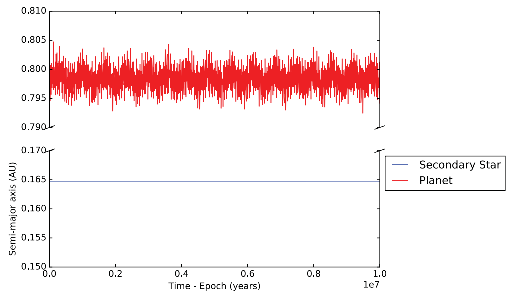

Figure 7. Semimajor axis of the secondary star and planet after integration of the SYSTEMIC system over a period of 10^7 yr. The secondary star has an almost constant semimajor axis while the planet has some variation in the semimajor axis.

the third body is 5.04 Jupiter masses. In all of the tests performed, with varying properties of the binary system, a planetary mass third body is capable of producing the eclipse timing variations seen. The effect of limb darkening on the mass ratio of the binary stars was also analysed with JKTEBOP. It was found that as the amount of limb darkening of both stars increased, the mass ratio decreased. It was also found that increasing the amount of limb darkening on the primary star only resulted in a lower mass ratio, while increasing the amount of limb darkening on the secondary star only had a very minor effect and slightly increased the mass ratio.

The stability of the proposed orbits are important in determining whether the proposed orbits are the correct interpretation of the eclipse timing variations (Hinse, Horner & Wittenmyer 2014). The system was integrated over a period of 10^7 yr to determine the long-term stability of the system. SYSTEMIC (Meschiari et al. 2009; Meschiari & Laughlin 2010) was used to perform the integration on the best-fitting system found. The eccentricity results of the integration can be found in Fig. 6 while the semimajor axis results of the integration can be found in Fig. 7. The semimajor axis of the planet was found to vary between 0.795 and 0.805 au while the eccentricity was found to fluctuate between 0.05 and 0.13 and indicates the planet orbits the binary stars in an almost circular orbit. As the orbits were found to be stable over large time periods, a planet in the proposed configuration is unlikely to be ejected from the system and is therefore the likely source of the eclipse timing variations seen (Hinse et al. 2014).

With a proposed inclination of $105\overset{\circ}{.}92 \pm 1\overset{\circ}{.}45$, the probability of transits occurring needs to be considered. Kane & von Braun (2008) presented an analysis of the effect of orbital parameters, specifically eccentricity and argument of periastron, on the probability of a transit as a function of the orbital period. The probability of a transit occurring for a planet in a circular orbit drops dramatically as the orbital period of the planet increases. As the planet found in this system has a proposed orbit of approximately 237 d and a nearly circular orbit, the expected transit probability is less than approximately 0.01. By viewing the light curve, no transits can be seen to occur which can be expected with such a low probability of a planet in this orbit transiting the parent stars.

6 CONCLUSIONS

In this paper, we presented the evidence for a third body with a mass below the proposed planet/brown dwarf boundary (Burgasser 2008) around KIC 5095269. An eclipse timing variation study was performed on the Kepler detached binaries where KIC 5095269 was found to exhibit periodic eclipse time variations. As eclipse time variations may be the result of a third body (Beuermann et al. 2010), estimates for the mass of the binary stars were calculated and a model was produced with SYSTEMIC (Meschiari et al. 2009; Meschiari & Laughlin 2010).

The model produced by SYSTEMIC suggests the cause of the eclipse timing variations is a third body with a mass of 7.70 ± 0.08 Jupiter masses. Based on the proposed planet/brown dwarf mass boundary (Burgasser 2008), we propose that this third body is a planetary candidate; however, how this object formed may determine whether it is a planet or a brown dwarf (Nordlund 2011). The system was also found by SYSTEMIC to be stable over a period of 10^7 yr with an eccentricity of the third body that varies between 0.05 and 0.13. No transits could be seen to occur within the light curve although a planet with an orbital period of approximately 237 d has a probability of transit of less than 0.01.

In the future, we will be attempting to obtain radial velocity data for the system in order to further constrain the properties of the system. This planetary candidate has provided us with a template, both the features of $O - C$ variations and the method for analysis, to use for future systems with periodic variations. Systems with low-mass secondary stars, combined with small $O - C$ variations, are the best chance for detecting planetary sized bodies via the eclipse time variation method.

ACKNOWLEDGEMENTS

We would like to thank the referee and editor for their feedback and for helping us to fine tune the details of the paper. We would also like to thank Stefano Meschiari for his assistance with SYSTEMIC.

NOTE ADDED IN PRESS

The triple nature of this system was first reported in Borkovits et al., 2016, MNRAS, 455, 4136.

REFERENCES

Bessell M. S., Brett J. M., 1988, PASP, 100, 1134
Beuermann K. et al., 2010, A&A, 521, L60
Borkovits T., Érdi B., Forgács-Dajka E., Kovács T., 2003, A&A, 398, 1091
Boss A. P., 2012, MNRAS, 419, 1930
Burgasser A. J., 2008, Phys. Today, 61, 70

Chabrier G., Johansen A., Janson M., Rafikov R., 2014, Protostars and Planets VI, 914, 619
Correia A. C. M., Udry S., Mayor M., Laskar J., Naef D., Pepe F., Queloz D., Santos, N. C., 2005, A&A, 440, 751
Degroote P., Conroy K., Hambleton K., Bloemen S., Pablo H., Giammarco J., Prša A., 2013, in Pavlovski K., Tkachenko A., Torres G., eds, EAS Publ. Ser. Vol. 64, Setting a New Standard in the Analysis of Binary Stars. EDP Sciences, Les Ulis, France, p. 277
Doyle L. R. et al., 2011, Science, 333, 1602
Fabrycky D. C., 2010, in Seager S., ed., Non-Keplerian Dynamics of Exoplanets. The Univ. Arizona Press, Exoplanets. Arizona, p. 217
Gazak J. Z., Johnson J. A., Tonry J., Dragomir D., Eastman J., Mann A. W., Agol E., 2012, Adv. Astron., 2012. 697967
Hinse T. C., Horner J., Wittenmyer R. A., 2014, J. Astron. Space Sci., 31, 187
Kane S. R., von Braun K., 2008, in Mamajek E. E., Soderblom D. R., Wyse R. F. G., eds, Proc. IAU Symp. 4, The Age of Stars. Cambridge Univ. Press. Cambridge, p. 358
Kostov V. B. et al., 2016, ApJ, 827, 86
Lee J. W., Kim S.-L., Kim C.-H., Koch R. H., Lee C.-U., Kim H.-I., Park J.-H., 2009, AJ, 137, 3181
Mandel K., Agol E., 2002, ApJ, 580, L171
Meschiari S., Laughlin G. P., 2010, ApJ, 718, 543
Meschiari S., Wolf A. S., Rivera E., Laughlin G., Vogt S., Butler P., 2009, PASP, 121, 1016
Nordlund Å., 2011, in Sozzetti A., Lattanzi M. G., Boss A. P., eds, Proc. IAU Symp. 276, The Astrophysics of Planetary Systems: Formation, Structure, and Dynamical Evolution. Cambridge Univ. Press. Cambridge, p. 105
Orosz J. A. et al., 2012, Science, 337, 1511
Pecaut M. J., Mamajek E. E., 2013, ApJS, 208, 9
Prša A., Zwitter T., 2005, ApJ, 628, 426
Prša A. et al., 2011, AJ, 141, 83
Sigurdsson S., Richer H. B., Hansen B. M., Stairs I. H., Thorsett S. E., 2003, Science, 301, 193
Slawson R. W. et al., 2011, AJ, 142, 160
Southworth J., Maxted P. F. L., Smalley B., 2004, MNRAS, 351, 1277

SUPPORTING INFORMATION

Supplementary data are available at *MNRAS* online.

Table 1. Table of eclipse times for KIC 5095269. The eclipse time is in BJD − 2454833.

Please note: Oxford University Press is not responsible for the content or functionality of any supporting materials supplied by the authors. Any queries (other than missing material) should be directed to the corresponding author for the article.

This paper has been typeset from a TEX/LATEX file prepared by the author.

4.2 Summary of Results

Graczyk (2003) state that a light curve is almost insensitive to the mass ratio of the stellar components unless the system has a very low mass ratio. As the secondary eclipses were very shallow, an inclination favourable to eclipses and a low mass and radius ratio was assumed. JKTEBOP was used to model the binary and produced a mass ratio estimate. The colours of the system were then compared to make sure the mass ratio was a reasonable approximation.

By using custom software, the eclipse times of KIC 5095269 were able to be accurately determined. Using the software SYSTEMIC, orbital characteristics of a third body were found to be able to reproduce the O-C variations seen. The primary star was estimated to be a $1.21 M_{\odot}$ F7 star while the secondary star was estimated to be a $0.51 M_{\odot}$. Getley et al. (2017) presented evidence for a 7.70 ± 0.08 Jupiter mass third body (to the expected, correct, significant figures) orbiting KIC 5095269 as the result of an eclipse time variation study.

The properties of the host binary star and proposed third body as output by the software are summarised in Tables 4.1 and 4.2. As the mass of the third body is below the proposed planet/brown dwarf boundary (Burgasser 2008) the third body is thought to be a planetary candidate. However, how the third body formed may determine if it is actually a planet or brown dwarf (Nordlund 2011).

Table 4.1: Raw properties of the host binary star KIC 5095269. Reproduced from Getley et al. (2017).

Property	Best-Fit Value	Median Value	MAD Value
Primary Star Mass ($M_{\odot}$)	1.21	N/A	N/A
Secondary Star Mass ($M_{\odot}$)	0.51	0.51	1.24×10^{-3}
Orbital Period (d)	18.61196	18.61196	1.55×10^{-7}
Mean anomaly (deg)	7.44	7.44	1.31×10^{-4}
Eccentricity	0.246	0.246	9.3×10^{-6}
Long. Peri (deg)	22.82	22.82	2.23×10^{-4}
Inclination (deg)	80.0	80.0	0.02
Node (deg)	305.54	305.54	2.3×10^{-4}

Table 4.2: Raw properties of the proposed third body orbiting KIC 5095269. Reproduced from Getley et al. (2017).

Property	Best-Fit Value	Median Value	MAD Value
Mass (M_j)	7.698	7.693	0.054
Orbital Period (d)	237.70817	237.68977	0.08237
Mean anomaly (deg)	290.92	289.44	2.34
Eccentricity	0.0604	0.0603	0.0021
Long. Peri (deg)	27.67	29.03	2.07
Inclination (deg)	105.92	105.83	0.98
Node (deg)	64.19	64.10	0.28

A dynamical stability analysis of KIC 5095269 with the proposed planetary mass third body found the system to be stable over a period of 10^7 years. This increases the likelihood of the system existing as proposed (Horner et al. 2012a; Horner et al. 2012b).

An artist's impression of the KIC 5095269 system appears in appendix C. The ETV study performed for this paper was a manual process. Using the results from Getley et al. (2021) and more automated ETV study could be performed which may be able to identify more third bodies, including planetary mass third bodies.

4.3 Further analysis

With the Gaia Data Release 2 (Evans, D. W. et al. 2018), additional information about the KIC 5095269 system has become available. With a parallax value of 0.813 ± 0.015mas and mean photometric magnitude of 13.44 (in the G band), the absolute magnitude of the system was found to be 2.99. Assuming the primary star dominates the flux (and therefore magnitude) of the system and the mass ratio calculated in Getley et al. (2017), this results in a binary system comprising a primary and secondary star with an upper mass estimate of $1.44M_{\odot}$ and $0.606M_{\odot}$ respectively. Assuming the primary star is an F star, the minimum mass for the primary star is $\sim$$1.08M_{\odot}$ with a $0.455M_{\odot}$ secondary star.

Using these new values for the primary and secondary star, the best fit for the third body's mass ranges from $9.17M_J$ (for a $1.44M_{\odot}$ primary star) to $6.87M_J$

(for a $1.08 M_{\odot}$ primary star). As such, a better estimate for the mass of the third body is 7.70 ± 1.47 M_J. In all cases, the third body remains within planetary mass range.

CHAPTER 5

DISCUSSION AND CONCLUSIONS

The number of exoplanets detected has been rapidly increasing since the first detected exoplanet in 1989 (Latham et al. 1989; Stassun, Collins, and Gaudi 2017). However, it is only with the relatively recent launch of missions designed to view large sections of the sky with high precision that eclipse time variation studies have become a feasible option for detecting planets and other third bodies. During the Kepler mission, thousands of eclipsing binary stars were observed providing a “treasure trove” of data that will continue to be analysed for decades to come.

One of the most important aspects of any study is to have realistic expectations on the possible outcomes. Simulated data is useful when there are no alternatives, however real-world data should always be prioritised when available. As was found in Chapter 2, real-world data doesn’t always match the results of simulated data. Importantly detectability of third bodies wasn’t able to be constrained by simulated work, and equation 1.4 alone. With real-world data, it was found that the eccentricity of a third body and the orbital period of the host binary apply additional constraints on the detectability of third bodies. As such equation 2.1 provides an additional, and significant, constraint on the detectability of third bodies around eclipsing binary stars that can be incorporated into simulations. It can also provide an additional check on the robustness of existing detections.

By knowing minimal information about a binary star system, i.e. the orbital period of the binary star and the eclipse timing accuracy, the minimum detectable mass and period for a third body with an eccentricity can be determined. This can be used as an additional check on previously detected third bodies as well as future detections from eclipse time variation studies.

When performing an eclipse time variation study a wide range of features can be seen within the variations of O-C diagrams. Periodic/sinusoidal variations may indicate the presence of a third body but it has also been found that variations can differ significantly from a sinusoidal wave. While performing an eclipse time variation study on the Kepler eclipsing binaries, systems were found where the O-C variations would begin to increase, or decrease, and then rapidly reverse direction and change sign. The O-C variations indicate that eclipses would occur earlier than expected and then suddenly and rapidly change to later than expected, or vice versa. These flip-flop systems were the focus of Chapter 3. The cause of the flip-flop effect was found to be due to highly eccentric binary star orbits with an extremely high eccentricity third body present in the system.

A dynamical stability analysis of these systems was performed and in each case the systems, as proposed, were all found to be stable for at least 10^6 years. The systems were also integrated for 10^4 years a number of times with random values for the mean longitude, argument or pericentre and longitude of pericentre of the third body and the host binary star. The systems were found to be stable over this time period for a wide range of orbital configurations. This indicates that should the precise orbital characteristics be incorrect, stable third bodies of those masses and orbital periods can still exist.

5.1 Detections

The successful detection and/or identification of additional bodies around some Kepler binary stars were found during the analysis for Chapter 3. The evidence for the detection of a planetary mass third body was also the focus of Chapter 4.

5.1.1 KIC 5255552

KIC 5255552 is an eclipsing binary star with a primary and secondary star mass estimated to be $0.96M_{\odot}$ and $0.74M_{\odot}$ respectively. During the stability analysis for KIC 5255552, additional eclipsing events were found in the light curve. Previously reported results indicated a third body. However, based on the analysis in Chapter 3, it was found that a third body was unable to account for all the extra eclipsing events. The grouping of the extra eclipsing events indicate that not only is a fourth body present in the system, but the third and fourth body form their own binary pair. No eclipses from this companion binary can be seen. As such KIC 5255552 is likely to be a system where a non-eclipsing binary itself eclipses an eclipsing binary.

A possible, single, shallow additional eclipsing event was previously reported by Zhang, J. et al. (2018). If this is a physical event that is independent of the existing bodies and eclipses it would indicate the presence of a fifth body within the system.

5.1.2 KIC 5653126

KIC 5653126 was found to contain a $1.02M_{\odot}$ primary star and a $0.78M_{\odot}$ secondary star. The outer companion was reported by Borkovits et al. (2016) to have a mass of $1.1M_{\odot}$. As with all the Kepler systems featured in Chapter 3, the color/2MASS J - H magnitude difference was considered. It is possible that the light from the outer companion dominates the system and as such the primary and secondary mass estimates would be unreliable. A cool, but massive, white dwarf companion would not be expected to contribute to the J-H colours of the system. However, if the light from the outer companion does not dominate the system and only contributes slightly to the J - H colour of the system, it is possible the outer companion is an additional binary. Unlike KIC 5255552, no additional eclipsing events can be seen to help determine the nature of the system. The outer companion has an inclination of 78° and as such no additional eclipsing events were expected.

5.1.3 KIC 7821010

A $1.23M_{\odot}$ primary star and $1.07M_{\odot}$ secondary star make up the eclipsing binary KIC 7821010. The system was reported by Borkovits et al. (2016) to contain an $\sim$2.6 Jupiter mass third body in a 991 day orbit. The eclipse timing fit, models reproducing the O-C effects performed by Borkovits et al. (2016) and the stability analysis performed in Chapter 3 all strongly indicate this planetary candidate exists and is viable.

KIC 7821010 is also further evidence that low-mass (planetary) objects are capable of having a significant effect on the orbits of the host stars. With an inclination of 105° no transits of this planet would be expected. As such, without eclipse timing studies, this planetary mass third body may have continued to go undetected.

5.1.4 KIC 11519226

KIC 11519226 is a system that contains a $0.98M_{\odot}$ primary star and a $0.46M_{\odot}$ secondary star. This system is similar to KIC 5653129 in that the reported companion (with a mass of $1.25M_{\odot}$) would dominate the light of the system. The J - H colour of the system suggests that the third body may not contribute to the colours of the system. An outer companion that is more massive than the the primary and secondary star but does not contribute to the J-H colours of the system may be a massive white dwarf or an additional binary comprising smaller components with a total mass of $1.25M_{\odot}$.

With an inclination of 89°, transiting events might be possible. However, the outer companion has a long, 1437 day, orbital period thus lowering the probability of viewing any transiting events. There is also a large amount of variability in the light curve of KIC 11519226 which adds to the complexity of looking for transits of the outer companion. Despite the difficulties, a possible extra eclipsing event was identified in the light curve. More observations of this system will be required to determine if this event is actually an additional eclipsing event/transit or part of the natural variability of the system. Additional observations of the system would also help to constrain the exact nature of KIC 11519226.

5.1.5 KIC 5095269

With the eclipse times of the Kepler systems determined, O-C diagrams were created. Periodic variations within the O-C diagrams were sought in an attempt to locate systems that potentially held additional bodies within the system. As a result of the eclipse time variation study in Getley et al. (2017) (presented in Chapter 4), KIC 5095269 was identified as a system hosting a potential companion.

A third body with a best fit mass of 7.70 $\pm$ 1.47 Jupiter masses in a 237.7 $\pm$ 0.1 day orbital period with an inclination and eccentricity of 105.92° $\pm$ 1.45° and 0.060 $\pm$ 0.003 (respectively) was found to reproduce the O-C variations found. The system, containing the proposed companion, was found to be stable for at least 10^7 years. The evidence presented in Getley et al. (2017), indicates that a third body is likely to exist around KIC 5095269.

It has been suggested that how a body forms is a more physically meaningful way to determine the classification of a companion than relying on the mass alone. However, based on the $\sim$13 Jupiter mass brown dwarf boundary, this third body is a possible planetary candidate.

5.2 Conclusions

In this thesis, empirical data from the Kepler Eclipsing Binary Star Catalog was used as a starting point to determine the detectability of third bodies using eclipse time variations. It was found that, in general, planetary mass companions are detectable with eclipse time variations. However, there are a large number of factors that play a role in the detectability of a companion. The orbital period of the host binary and the eccentricity of a potential companion affects the minimum detectable period of a third body. As the host binary orbital period or eccentricity of a potential companion increases, the minimum orbital period of a detectable third body increases according to equation 2.1. Given a timing accuracy of the eclipse times, the mass and orbital period of a potential companion also affects the detectability of that body. The detectable mass of a third body decreases as the orbital period increases.

Third bodies can have masses that range from planetary and brown dwarf masses to stellar masses. Depending on the characteristics of the system, a wide range of features can be seen in a system's O-C diagram (examples of O-C variations can be seen in appendix A). It was found that in addition to simple (sinusoidal like) variations, third bodies in stable orbits are capable of producing more complex O-C variations. Complex "flip-flop" O-C variations, where eclipses rapidly change from occurring later than predicted to earlier than predicted (or vice-versa) over a short period of time. The primary and secondary eclipses may also occur out of phase with each other i.e. primary eclipses occurring earlier (or later) than predicted while the secondary eclipses occur later (or earlier) than predicted. Third bodies, including a planetary mass third body, in highly eccentric orbits were found to be able to cause these complex O-C variations. The systems used in the study were all found to be in stable orbits for at least 10^6 years.

Finally, an eclipse time variation study was performed on the detached eclipsing binaries found in the Kepler Eclipsing Binary Star Catalog. KIC 5095269 was identified as potentially hosting a third body. As the result of the eclipse time variation study and further analysis on KIC 5095269, a $7.70 \pm 1.47 M_J$ companion was detected in a 237.7 ± 0.1d orbit. Importantly, this planetary mass companion was found to be stable for at least 10^7 years. An artist's impression of the KIC 5095269 system appears in appendix C.

5.3 The Future

The Kepler mission has provided high quality observations for thousands of eclipsing binary star systems. Current and future missions, such as TESS (The Transiting Exoplanet Survey Satellite) (Ricker et al. 2014), will provide additional high quality observations and be able to identify more eclipsing binary systems.

Further eclipse time variations studies, particularly on eclipsing binaries identified by the K2 or TESS mission, should be performed to identify further systems consisting of additional bodies. Follow up analysis on systems identified by previous eclipse time variation studies may also be useful in constraining the properties of the systems and provide additional confirmation on the third bodies. Systems (such as KIC 5255552) that have been identified as potentially hosting more bodies should be further analysed to confirm or rule out the presence of any additional bodies in the system.

As a result of this work, particularly Chapter 2 and equations 1.4 and 2.1, by knowing just the timing accuracy of eclipses and the orbital period of an eclipsing binary, a parameter space can be generated and used to determine the most likely masses of third bodies that are able to be detected. As such, targets can be more efficiently selected when searching for planetary mass companions.

With the development of artificial intelligence and the emergence of machine learning and artificial neural networks, it may be possible to develop a system that can be trained with the Kepler data to improve the accuracy of the estimated eclipse times. This would allow lower mass objects in shorter orbital periods to be detected from the existing Kepler observations. Given that complex O-C variations can be caused by stable planetary mass companions (Chapter 3; high eccentric third bodies create a flip-flop feature in O-C diagrams), future eclipse time studies should include all systems with simple and complex O-C variations where possible.

As this thesis demonstrates, it is only recently that eclipse time variation studies have begun to provide a feasible new planetary detection method. Nevertheless, as more analyses are performed on available eclipsing binary star light curves, and current and future space telescope missions observe more systems for longer times, it is reasonable to expect significantly more and lower mass eclipsing binary star planets to be discovered. Future studies of the type described in this thesis can thus contribute to our understanding of how binary star planets form and evolve.

REFERENCES

Note that the following references are for Chapters 1 and 5, the appendices and the introductory and summary sections of the remaining chapters. References for the papers located in Chapters 2 - 4 are included in the references sections of the papers.

Andrews, Jeff J., Katelyn Breivik, and Sourav Chatterjee (2019). "Weighing the Darkness: Astrometric Mass Measurement of Hidden Stellar Companions Using Gaia". *The Astrophysical Journal* 886.1, p. 68.

Beuermann, K., Hessman, F. V., Dreizler, S., Marsh, T. R., Parsons, S. G., Winget, D. E., Miller, G. F., Schreiber, M. R., Kley, W., Dhillon, V. S., Littlefair, S. P., Copperwheat, C. M., and Hermes, J. J. (2010). "Two planets orbiting the recently formed post-common envelope binary NN Serpentis*". *A&A* 521, p. L60.

Borkovits, T., Érdi, B., Forgács-Dajka, E., and Kovács, T. (2003). "On the detectability of long period perturbations in close hierarchical triple stellar systems". *A&A* 398.3, pp. 1091–1102.

Borkovits, T., T. Hajdu, J. Sztakovics, S. Rappaport, A. Levine, I. B. Bíró, and P. Klagyivik (2016). "A comprehensive study of the Kepler triples via eclipse timing". *Monthly Notices of the Royal Astronomical Society* 455.4, pp. 4136–4165.

Borkovits, T., S. Rappaport, T. Hajdu, and J. Sztakovics (2015). "Eclipse timing variation analyses of eccentric binaries with close tertiaries in the Kepler field". *Monthly Notices of the Royal Astronomical Society* 448.1, pp. 946–993.

Borucki, William J., David Koch, Gibor Basri, Natalie Batalha, Timothy Brown, Douglas Caldwell, John Caldwell, Jørgen Christensen-Dalsgaard, William D. Cochran, Edna DeVore, Edward W. Dunham, Andrea K. Dupree, Thomas

N. Gautier, John C. Geary, Ronald Gilliland, Alan Gould, Steve B. Howell, Jon M. Jenkins, Yoji Kondo, David W. Latham, Geoffrey W. Marcy, Søren Meibom, Hans Kjeldsen, Jack J. Lissauer, David G. Monet, David Morrison, Dimitar Sasselov, Jill Tarter, Alan Boss, Don Brownlee, Toby Owen, Derek Buzasi, David Charbonneau, Laurance Doyle, Jonathan Fortney, Eric B. Ford, Matthew J. Holman, Sara Seager, Jason H. Steffen, William F. Welsh, Jason Rowe, Howard Anderson, Lars Buchhave, David Ciardi, Lucianne Walkowicz, William Sherry, Elliott Horch, Howard Isaacson, Mark E. Everett, Debra Fischer, Guillermo Torres, John Asher Johnson, Michael Endl, Phillip MacQueen, Stephen T. Bryson, Jessie Dotson, Michael Haas, Jeffrey Kolodziejczak, Jeffrey Van Cleve, Hema Chandrasekaran, Joseph D. Twicken, Elisa V. Quintana, Bruce D. Clarke, Christopher Allen, Jie Li, Haley Wu, Peter Tenenbaum, Ekaterina Verner, Frederick Bruhweiler, Jason Barnes, and Andrej Prsa (2010). "Kepler Planet-Detection Mission: Introduction and First Results". *Science* 327.5968, pp. 977–980.

Boss, A. P. (2012). "Giant planet formation by disc instability: flux-limited radiative diffusion and protostellar wobbles". *Monthly Notices of the Royal Astronomical Society* 419.3, pp. 1930–1936.

Bozkurt, Z. and Ö. L. Değirmenci (2007). "Triple systems showing apsidal motion". *Monthly Notices of the Royal Astronomical Society* 379.1, pp. 370–378.

Burgasser, A. J. (2008). "Brown dwarfs: Failed stars, super Jupiters". *Phys. Today* 61.6, p. 70.

Carroll, Bradley W. and Dale A. Ostlie (2007). *An Introduction to Modern Astrophysics.* 2nd ed. San Francisco, CA: Addison-Wesley. ISBN: 0-8053-0402-9.

Chabrier, G., A. Johansen, M. Janson, and R. Rafikov (2014). "Giant Planet and Brown Dwarf Formation". *Protostars and Planets VI*, pp. 619–642.

Descamps, Pascal (2005). "Orbit of an Astrometric Binary System". *Celestial Mechanics and Dynamical Astronomy* 92.4, pp. 381–402.

Doyle, Laurance R. (2019). "The discovery of "Tatooine": Kepler-16b". *New Astronomy Reviews* 84, p. 101515.

Evans, D. W., Riello, M., De Angeli, F., Carrasco, J. M., Montegriffo, P., Fabricius, C., Jordi, C., Palaversa, L., Diener, C., Busso, G., Cacciari, C., van

Leeuwen, F., Burgess, P. W., Davidson, M., Harrison, D. L., Hodgkin, S. T., Pancino, E., Richards, P. J., Altavilla, G., Balaguer-Núñez, L., Barstow, M. A., Bellazzini, M., Brown, A. G. A., Castellani, M., Cocozza, G., De Luise, F., Delgado, A., Ducourant, C., Galleti, S., Gilmore, G., Giuffrida, G., Holl, B., Kewley, A., Koposov, S. E., Marinoni, S., Marrese, P. M., Osborne, P. J., Piersimoni, A., Portell, J., Pulone, L., Ragaini, S., Sanna, N., Terrett, D., Walton, N. A., Wevers, T., and Wyrzykowski, L. (2018). "Gaia Data Release 2 - Photometric content and validation". *A&A* 616, A4.

Gazak, J. Zachary, John A. Johnson, John Tonry, Diana Dragomir, Jason Eastman, Andrew W. Mann, and Eric Agol (2012). "Transit Analysis Package: An IDL Graphical User Interface for Exoplanet Transit Photometry". *Advances in Astron.* 2012.

Graczyk, Dariusz (2003). "Light-curve solutions for bright detached eclipsing binaries in the Small Magellanic Cloud: absolute dimensions and distance indicators". *Monthly Notices of the Royal Astronomical Society* 342.4, pp. 1334–1348.

Hilditch, R. W. (2001). *An Introduction to Close Binary Stars*. Cambridge University Press.

Horner, J., T. C. Hinse, R. A. Wittenmyer, J. P. Marshall, and C. G. Tinney (2012a). "A dynamical analysis of the proposed circumbinary HW Virginis planetary system". *Monthly Notices of the Royal Astronomical Society* 427.4, pp. 2812–2823.

Horner, J., R. A. Wittenmyer, T. C. Hinse, and C. G. Tinney (2012b). "A detailed investigation of the proposed NN Serpentis planetary system". *Monthly Notices of the Royal Astronomical Society* 425.1, pp. 749–756.

Horner, Jonathan, Robert A Wittenmyer, Duncan J Wright, Tobias C Hinse, Jonathan P Marshall, Stephen R Kane, Jake T Clark, Matthew Mengel, Matthew T Agnew, and Daniel Johns (2019). "The HD 181433 Planetary System: Dynamics and a New Orbital Solution". *The Astronomical Journal* 158.3, p. 100.

Howell, Steve B., Charlie Sobeck, Michael Haas, Martin Still, Thomas Barclay, Fergal Mullally, John Troeltzsch, Suzanne Aigrain, Stephen T. Bryson, Doug

Caldwell, William J. Chaplin, William D. Cochran, Daniel Huber, Geoffrey W. Marcy, Andrea Miglio, Joan R. Najita, Marcie Smith, J. D. Twicken, and Jonathan J. Fortney (2014). "The K2 Mission: Characterization and Early Results". *Publications of the Astronomical Society of the Pacific* 126.938, pp. 398–408.

Jain, Pankaj (2015). *An Introduction to Astronomy and Astrophysics*. 1st ed. Boca Raton, FL: CRC Press. ISBN: 9781439885918.

Kalas, Paul, James R. Graham, Eugene Chiang, Michael P. Fitzgerald, Mark Clampin, Edwin S. Kite, Karl Stapelfeldt, Christian Marois, and John Krist (2008). "Optical Images of an Exosolar Planet 25 Light-Years from Earth". *Science* 322.5906, pp. 1345–1348.

Kirk, Brian, Kyle Conroy, Andrej Prša, Michael Abdul-Masih, Angela Kochoska, Gal Matijevič, Kelly Hambleton, Thomas Barclay, Steven Bloemen, Tabetha Boyajian, Laurance R. Doyle, B. J. Fulton, Abe Johannes Hoekstra, Kian Jek, Stephen R. Kane, Veselin Kostov, David Latham, Tsevi Mazeh, Jerome A. Orosz, Joshua Pepper, Billy Quarles, Darin Ragozzine, Avi Shporer, John Southworth, Keivan Stassun, Susan E. Thompson, William F. Welsh, Eric Agol, Aliz Derekas, Jonathan Devor, Debra Fischer, Gregory Green, Jeff Gropp, Tom Jacobs, Cole Johnston, Daryll Matthew LaCourse, Kristian Saetre, Hans Schwengeler, Jacek Toczyski, Griffin Werner, Matthew Garrett, Joanna Gore, Arturo O. Martinez, Isaac Spitzer, Justin Stevick, Pantelis C. Thomadis, Eliot Halley Vrijmoet, Mitchell Yenawine, Natalie Batalha, and William Borucki (2016). "KEPLERECLIPSING BINARY STARS. VII. THE CATALOG OF ECLIPSING BINARIES FOUND IN THE ENTIREKEPLERDATA SET". *The Astronomical Journal* 151.3, p. 68.

Konacki, Maciej, Matthew W. Muterspaugh, Shrinivas R. Kulkarni, and Krzysztof G. Hełminiak (2010). "HIGH-PRECISION ORBITAL AND PHYSICAL PARAMETERS OF DOUBLE-LINED SPECTROSCOPIC BINARY STARS—HD78418, HD123999, HD160922, HD200077, AND HD210027". *The Astrophysical Journal* 719.2, pp. 1293–1314.

Kopal, Zdenek (1979). *Language of the Stars*. 1st ed. Dordrecht, Holland: Springer Netherlands. ISBN: 9789027710444.

Kovaleva, D., O. Malkov, L. Yungelson, and D. Chulkov (2016). "Visual Binary Stars: Data to Investigate Formation of Binaries". *Open Astronomy* 25.4, pp. 419–426.

Latham, David W., Tsevi Mazeh, Robert P. Stefanik, Michel Mayor, and Gilbert Burki (1989). "The unseen companion of HD114762: a probable brown dwarf". *Nature* 339.6219, pp. 38–40.

Libralato, M., D. Nardiello, L. R. Bedin, L. Borsato, V. Granata, L. Malavolta, G. Piotto, P. Ochner, A. Cunial, and V. Nascimbeni (2016). "A PSF-based approach to Kepler/K2 data – II. Exoplanet candidates in Praesepe (M 44)". *Monthly Notices of the Royal Astronomical Society* 463.2, pp. 1780–1796.

Lissauer, Jack J. and Imke de Pater (2013). *Fundamental Planetary Science : Physics, Chemistry and Habitability.* Cambridge, United Kingdom: Cambridge University Press. ISBN: 9780521618557.

Liu, Chunjian, Qing Ai, Zhen Yao, Hualian Tian, Jiayun Shen, and Haosen Wang (2018). "The formation of a gas giant planet in a viscously evolved protoplanetary disk within the core accretion model". *Astrophysics and Space Science* 363.9, p. 185.

Mandel, Kaisey and Eric Agol (2002). "Analytic Light Curves for Planetary Transit Searches". *ApJ* 580.2, p. L171.

Markwardt, Craig B. (2009). "Non-linear Least Squares Fitting in IDL with MPFIT". *Astronomical Data Analysis Software and Systems XVIII* (Quebec City, Canada). Ed. by David A. Bohlender, Daniel Durand, and Patrick Dowler. ASP Conf. Ser., p. 251. ISBN: 978-1-58381-702-5.

Nordlund, Ake (2011). "Formation of brown dwarfs and planets". *Proc. IAU* 6.S276, pp. 105–112.

Orosz, Jerome A. (2015). "Triple Stars Observed by Kepler". *Living Together: Planets, host stars and binaries* (Litomysl, Czech Republic). Ed. by S. M. Rucinski, G. Torres, and M. Zejda. ASP Conf. Ser., p. 55. ISBN: 978-1-58381-876-3.

Orosz, Jerome A., William F. Welsh, Joshua A. Carter, Daniel C. Fabrycky, William D. Cochran, Michael Endl, Eric B. Ford, Nader Haghighipour, Phillip J. MacQueen, Tsevi Mazeh, Roberto Sanchis-Ojeda, Donald R. Short, Guillermo

Torres, Eric Agol, Lars A. Buchhave, Laurance R. Doyle, Howard Isaacson, Jack J. Lissauer, Geoffrey W. Marcy, Avi Shporer, Gur Windmiller, Thomas Barclay, Alan P. Boss, Bruce D. Clarke, Jonathan Fortney, John C. Geary, Matthew J. Holman, Daniel Huber, Jon M. Jenkins, Karen Kinemuchi, Ethan Kruse, Darin Ragozzine, Dimitar Sasselov, Martin Still, Peter Tenenbaum, Kamal Uddin, Joshua N. Winn, David G. Koch, and William J. Borucki (2012). "Kepler-47: A Transiting Circumbinary Multiplanet System". *Science* 337.6101, pp. 1511–1514.

Petrova, A. V. and V. V. Orlov (2002). "Apsidal Motion in Detached Binary Stars: Comparison of Theory and Observations". *Astrophysics* 45.3, pp. 334–341.

Pierens, A. and R. P. Nelson (2007). "On the migration of protoplanets embedded in circumbinary disks". *A&A* 472.3, pp. 993–1001.

Ribas, I. (2006). "Binaries as Astrophysical Laboratories: Open Questions". *Astrophysics of Variable Stars*. Ed. by Conny Aerts and C. Sterken. Vol. 349. Astronomical Society of the Pacific Conference Series, p. 55.

Ricker, George R., Joshua N. Winn, Roland Vanderspek, David W. Latham, Gáspár Á. Bakos, Jacob L. Bean, Zachory K. Berta-Thompson, Timothy M. Brown, Lars Buchhave, Nathaniel R. Butler, R. Paul Butler, William J. Chaplin, David B. Charbonneau, Jørgen Christensen-Dalsgaard, Mark Clampin, Drake Deming, John P. Doty, Nathan De Lee, Courtney Dressing, Edward W. Dunham, Michael Endl, François Fressin, Jian Ge, Thomas Henning, Matthew J. Holman, Andrew W. Howard, Shigeru Ida, Jon M. Jenkins, Garrett Jernigan, John Asher Johnson, Lisa Kaltenegger, Nobuyuki Kawai, Hans Kjeldsen, Gregory Laughlin, Alan M. Levine, Douglas Lin, Jack J. Lissauer, Phillip MacQueen, Geoffrey Marcy, Peter R. McCullough, Timothy D. Morton, Norio Narita, Martin Paegert, Enric Palle, Francesco Pepe, Joshua Pepper, Andreas Quirrenbach, Stephen A. Rinehart, Dimitar Sasselov, Bun'ei Sato, Sara Seager, Alessandro Sozzetti, Keivan G. Stassun, Peter Sullivan, Andrew Szentgyorgyi, Guillermo Torres, Stephane Udry, and Joel Villasenor (2014). "Transiting Exoplanet Survey Satellite". *Journal of Astronomical Telescopes, Instruments, and Systems* 1, pp. 1 - 1 –10.

Rodler, Florian, Mercedes Lopez-Morales, and Ignasi Ribas (2012). “Weighing the non-transiting hot JUPITER τ Boo b”. *The Astrophysical Journal Letters* 753.

Schwarz, R., N. Haghighipour, S. Eggl, E. Pilat-Lohinger, and B. Funk (2011). “Prospects of the detection of circumbinary planets with Kepler and CoRoT using the variations of eclipse timing”. *Monthly Notices of the Royal Astronomical Society* 414.3, pp. 2763–2770.

Southworth, J. (2012). “Eclipsing Binary Stars: the Royal Road to Stellar Astrophysics”. *Orbital Couples: Pas de Deux in the Solar System and the Milky Way.* Ed. by F. Arenou and D. Hestroffer, pp. 51–58.

Stassun, Keivan G., Karen A. Collins, and B. Scott Gaudi (2017). “Accurate Empirical Radii and Masses of Planets and Their Host Stars with Gaia Parallaxes”. *The Astronomical Journal* 153.3, p. 136.

Sybilski, P., M. Konacki, and S. Kozłowski (2010). “Detecting circumbinary planets using eclipse timing of binary stars – numerical simulations”. *Monthly Notices of the Royal Astronomical Society* 405.1, pp. 657–665.

Watson, C. A. and T. R. Marsh (2010). “Orbital period variations of hot Jupiters caused by the Applegate effect”. *Monthly Notices of the Royal Astronomical Society* 405.3, pp. 2037–2043.

Welsh, William F., Jerome A. Orosz, Joshua A. Carter, Daniel C. Fabrycky, Eric B. Ford, Jack J. Lissauer, Andrej Prša, Samuel N. Quinn, Darin Ragozzine, Donald R. Short, Guillermo Torres, Joshua N. Winn, Laurance R. Doyle, Thomas Barclay, Natalie Batalha, Steven Bloemen, Erik Brugamyer, Lars A. Buchhave, Caroline Caldwell, Douglas A. Caldwell, Jessie L. Christiansen, David R. Ciardi, William D. Cochran, Michael Endl, Jonathan J. Fortney, Thomas N. Gautier III, Ronald L. Gilliland, Michael R. Haas, Jennifer R. Hall, Matthew J. Holman, Andrew W. Howard, Steve B. Howell, Howard Isaacson, Jon M. Jenkins, Todd C. Klaus, David W. Latham, Jie Li, Geoffrey W. Marcy, Tsevi Mazeh, Elisa V. Quintana, Paul Robertson, Avi Shporer, Jason H. Steffen, Gur Windmiller, David G. Koch, and William J. Borucki (2012). “Transiting circumbinary planets Kepler-34 b and Kepler-35 b”. *Nature* 481.7382, pp. 475–479.

Zhang, J., Qian, S. B., Wang, S. M., Sun, L. L., Wu, Y., and Jiang, L. Q. (2018). "The extraneous eclipses on binary light curves: KIC 5255552, KIC 10091110, and KIC 11495766". *A&A* 610, A72.

APPENDIX A

EXAMPLES OF O-C VARIABILITY

When viewing the O-C Diagrams produced for the Kepler sample, a number of different types of variability were seen and examples are presented below.

A.1 No or Irregular Variations

Most systems have no variations while some have irregular variations such as the O-C diagram for KIC 4908495 shown in Fig. A.1. Variability is present within Fig. A.1 however the period and amplitude of this variability is not regular or consistent throughout the diagram or between primary eclipses (blue circles) and secondary eclipses (green triangles). With no eclipse time variations no third bodies will be able to be located using this method. Star spots may be the source of variability seen within an O-C diagram and may be the source of irregular variations such as those seen in Fig. A.1. Star spots that are being eclipsed or are rotating into or out of view can lead to variations in an O-C diagram that are separate from any variations in actual eclipse times (Orosz et al. 2012). Star spots can cause a change in eclipse depth and shape. The difference between the actual eclipse depth and shape can lead to errors in determining the properties of bodies that are in the system.

Variations due to star spots may hide the presence of third bodies in a system. However, it is possible for O-C variations to be from a combination of star spots and the presence of a third body. As a result O-C variations may still be able to identify the presence of a third body even with the presence of star spots.

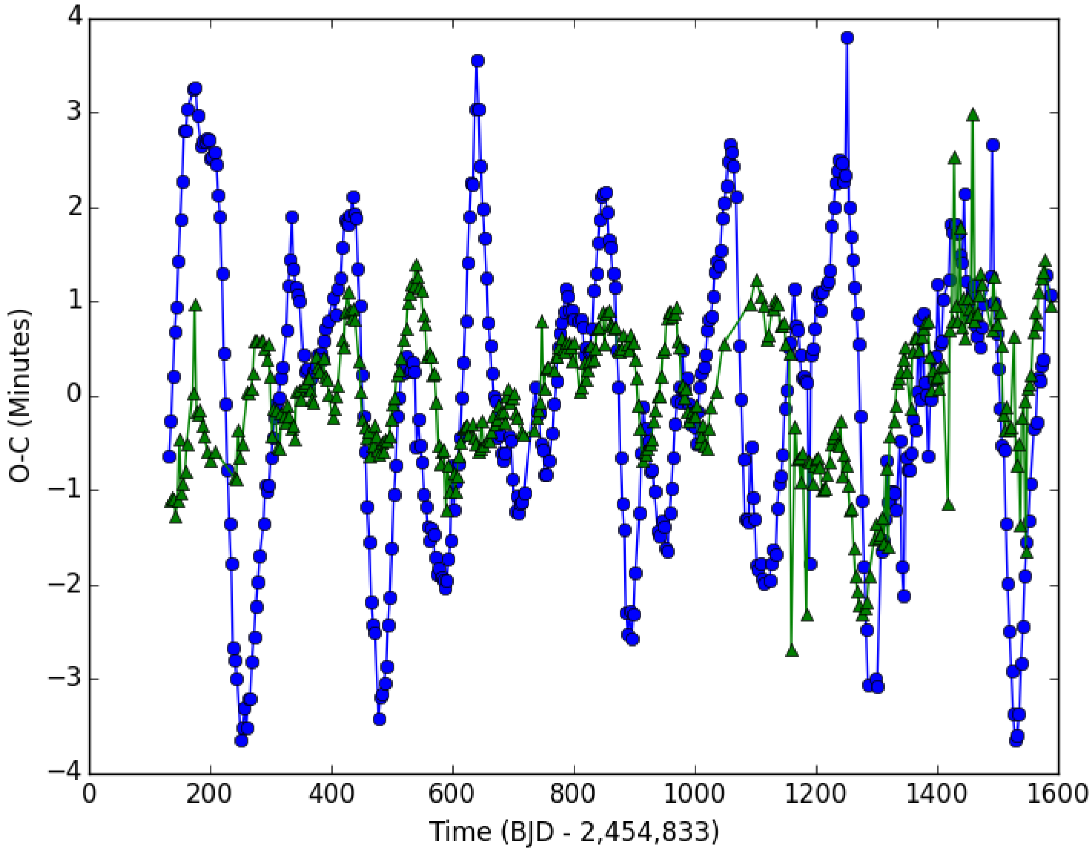

Figure A.1: O-C diagram for KIC 4908495 showing observed eclipse time - calculated eclipse time vs time. Irregular variations seen in the primary eclipses (blue circles) and secondary eclipses (green triangles) may be due to the presence of star spots.

A.2 Periodic Variations

A type of variation that was seen when visually analysing the produced O-C diagrams was periodic variation or variations that appear to re-occur periodically. Fig. A.2 shows an example of an O-C diagram that displayed periodic variability. The variability in the eclipse times repeats at regular intervals while the amplitude of the variability remains approximately the same. The variability in the secondary eclipses (green triangles) can be seen to track the variability in the primary eclipses (blue circles). The variability has amplitude of approximately 10 minutes with a period of approximately 91 days. O-C variations that are strictly periodic may be due to apsidal motion of the binary orbit (which may itself be due to a third body) or due to the presence of an additional body (Beuermann et al. 2010). If a third body is confirmed, the period of the variations is likely to be the orbital period of a third body. As such, a third body which can produce the variations seen in Fig. A.2 would have an orbital period of approximately 91 days.

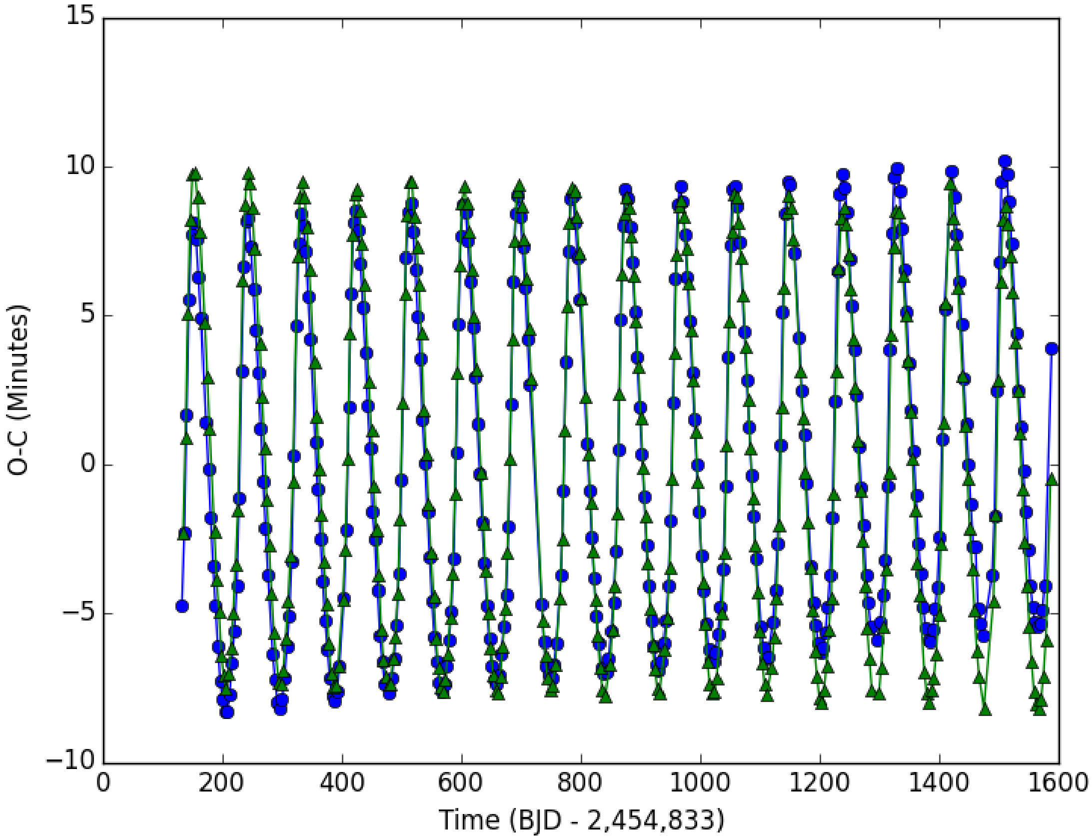

Figure A.2: O-C diagram for KIC 6545018 showing observed eclipse time - calculated eclipse time vs time. The periodic variations that appear in both the primary eclipses (blue circles) and secondary eclipses (green triangles) may be due to the presence of a third body. Third bodies may be stars or planets.

A.3 Sudden Period Flips

As discussed in Chapter 3, there were a small number of systems where the O-C diagram showed large eclipse time variations along with sudden changes in the system's orbital period. Fig. A.3 shows the O-C diagram for the eclipsing binary system KIC 12356914. The secondary eclipses (shown by the green triangles) can be seen to move opposite to the primary eclipses (shown by the blue circles).

Over the approximately 4 year period that was observed, the primary eclipse O-C rapidly changes from positive (i.e. the eclipse occurring later than calculated) to negative (i.e. the eclipse occurring earlier than calculated) over a relatively short period of approximately 200 days. The amplitude of the variability stays consistent until the times of rapid period change when the magnitude of the variability changes. The magnitude of the variability changes from approximately 10 minutes to approximately 30 minutes within the primary eclipses and a change from approximately 10 minutes to approximately 40 minutes in the secondary eclipses.

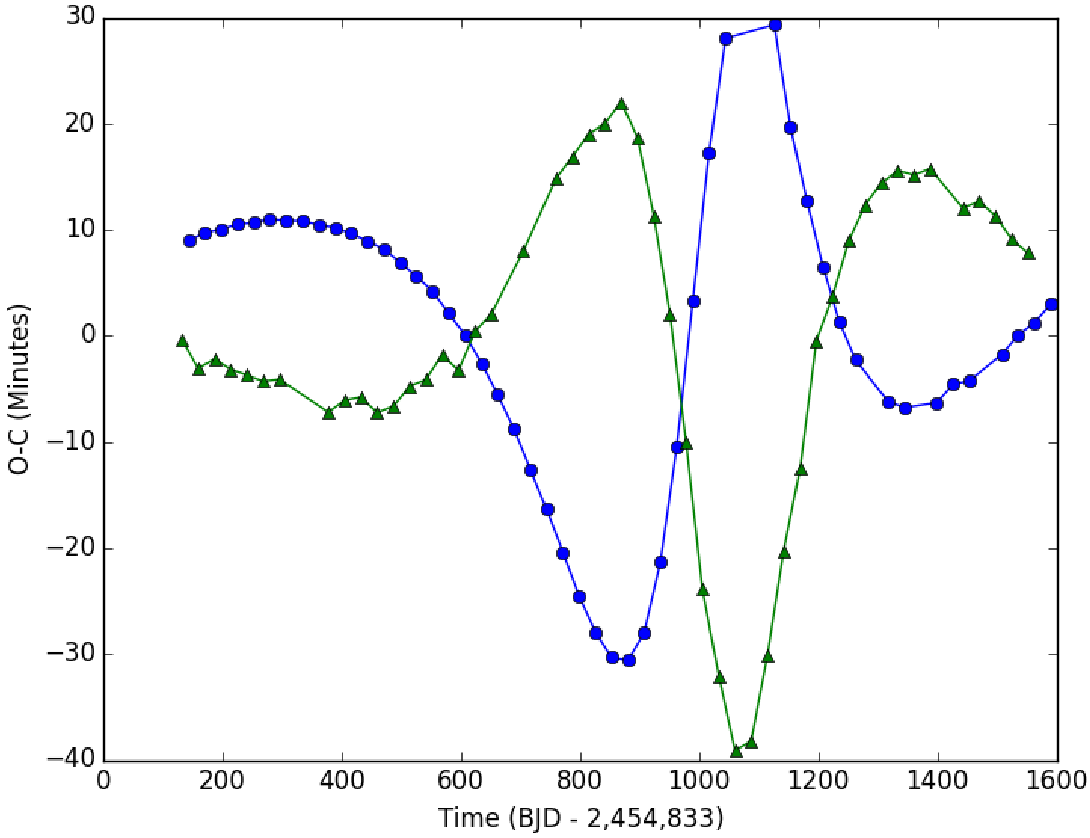

Figure A.3: O-C diagram for KIC 12356914 showing observed eclipse time - calculated eclipse time vs time. A rapid change in period takes approximately 200 days to occur. The sudden period change appears in both the primary eclipses (blue circles) and the secondary eclipses (green triangles) however move in opposite directions to each other. The source of this variability may be a combination of geometrical effects (such as light travel time or the effect of a third body on the orbit of the binary) and dynamical effects such as the interactions between all the bodies in the system causing apsidal motion.

A.4 Long Term Trends

A large number of systems were found to exhibit long term trends in their O-C diagrams. This trend would be seen if the period of the O-C variability was longer than the approximately four year period the systems were observed for.

Fig. A.4 shows the O-C diagram for the system KIC 8701327 which exhibits a long term trend in the O-C variability. The secondary eclipse times (green triangles) follows the primary eclipse times (blue circles) with an amplitude of the variability between approximately three and six minutes.

Long term trends do not necessarily indicate third bodies present in the system but may be apsidal motion i.e. the rotation of the system's orbit (Orosz 2015). There are a number of sources of apsidal motion including mutual tidal deformation of the components, deformation of the components due to axial rotation and relativistic effects (Petrova and Orlov 2002). Masses of the objects need to be known in order to determine relativistic effects while the radii are needed to determine the tidal motion. Axial rotation data is required to estimate rotational deformation. If this information can be determined it will be possible to determine if the O-C variability is due to apsidal motion internal to the binary system or if it is due to some other source such as a third body.

Systems that have long term trends in their O-C diagrams may actually be O-C variability of a different type however the observation period wasn't enough to see the full characteristics of the variability.

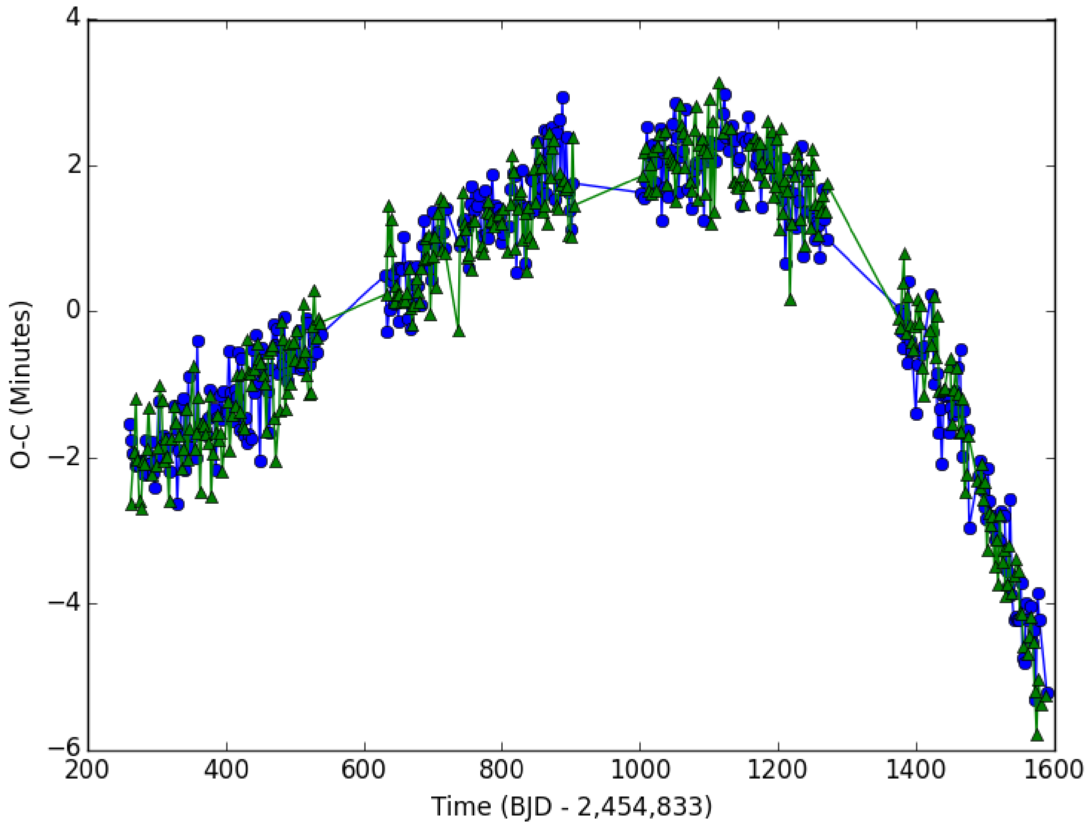

Figure A.4: O-C diagram for KIC 3248019 showing observed eclipse time - calculated eclipse time vs time. A long term trend appears in both the primary eclipses (blue circles) and the secondary eclipses (green triangles). The primary eclipse trend and secondary eclipse trend follow each other. The source of this variability may be due to apsidal motion caused by tidal effects and/or general relativity.

A.5 Out of Phase Long Term Trends

Some of the systems found during the analysis had O-C diagrams that exhibited linear trends with the primary and secondary eclipses having opposite slopes. The O-C diagram for KIC 4544587, can be seen in section A.4 and shows an example of linear trends with opposite slopes. The crossed linear trends only appear when the best-fit for the period of the primary and secondary eclipses is locked to a common value (in this case the best-fit period was 2.189114 days). When fitting the primary and secondary eclipses separately the trends go from linear (with opposite slopes) to long term trends with the primary and secondary eclipses being out of phase with each other by half a period. The O-C diagram for the 'unlocked' period fits for KIC 4544587 can be seen in Fig. A.6. The best-fit period for the primary eclipses was found to be 2.189098 days while the period for the secondary eclipses was found to be 2.189130 days (a difference of approximately 2.7 seconds). The average of the two separate periods is the same as the common period.

As the O-C variability exhibits long term trends such as that seen in Fig. A.4 the source of the variability is not necessarily from the presence of a third body but apsidal motion (Orosz 2015).

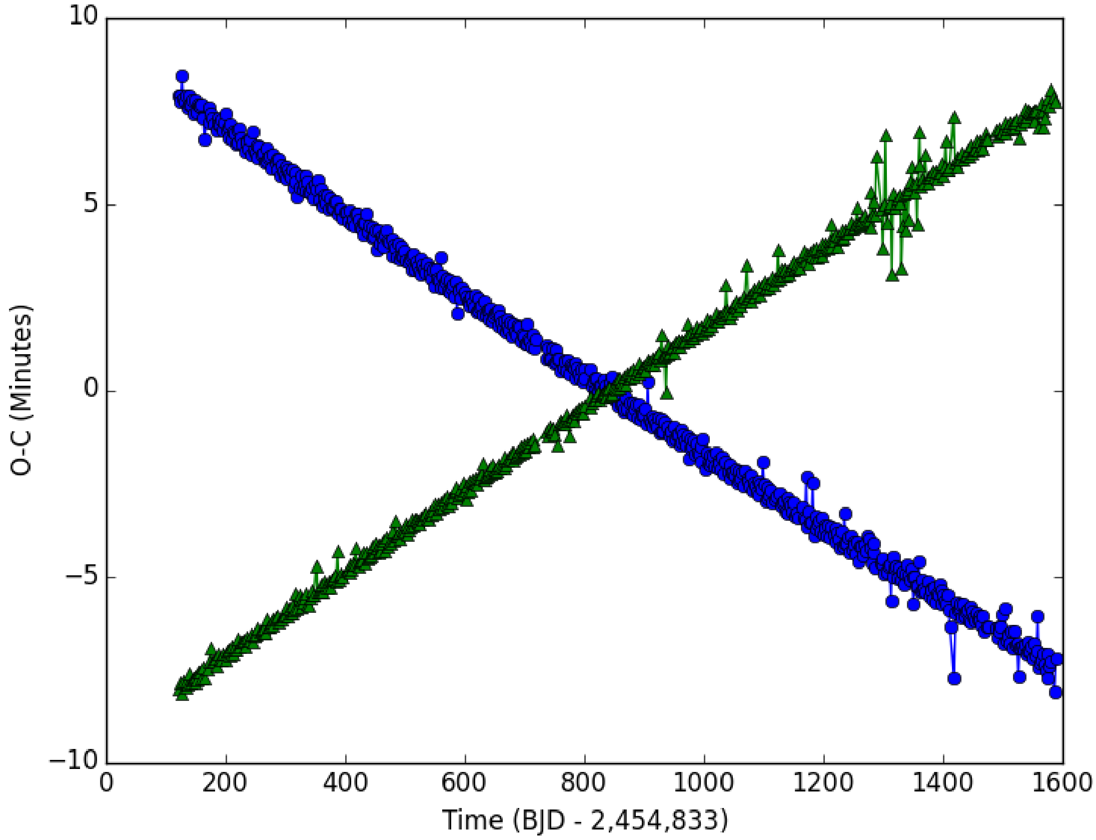

Figure A.5: O-C diagram for KIC 4544587 showing observed eclipse time - calculated eclipse time vs time. The primary eclipses (blue circles) and the secondary eclipses (green triangles), with a common period, show approximately linear trends with opposite slopes. The source of this variability may be due to apsidal motion caused by tidal effects and/or general relativity as when the period of the primary and secondary eclipses is unlocked long term trends appear (Fig. A.6).

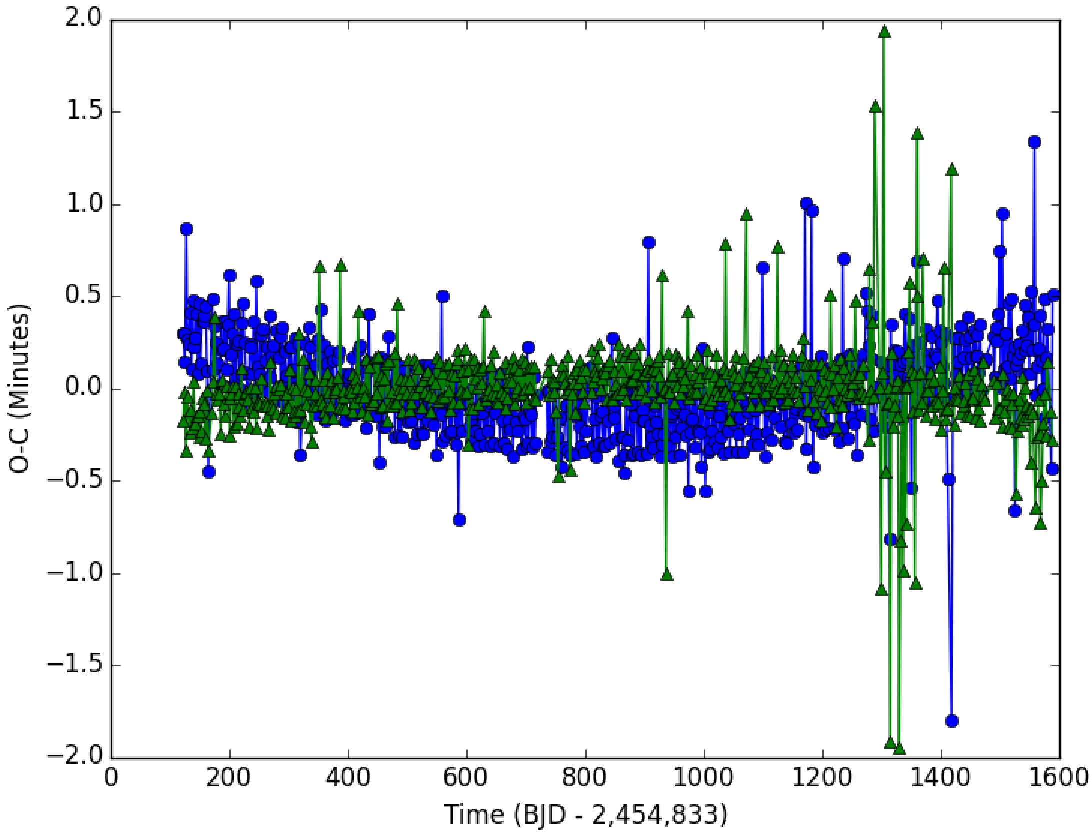

Figure A.6: O-C diagram for KIC 4544587 showing observed eclipse time - calculated eclipse time vs time. The primary eclipses (blue circles) and the secondary eclipses (green triangles), with separate calculated periods, show long term trends with the primary and secondary eclipses being out of phase. The source of this variability may be due to apsidal motion caused by tidal effects and/or general relativity.

APPENDIX B

Binary Eclipse Timings (BET)

Binary Eclipse Timings, or BET, was created based on the software Transit Analysis Package, or TAP (Gazak et al. 2012). BET was written in C++ so that no licenses would be needed to use the program and was created to accept FITS and TXT files to allow data to be input in multiple formats. By allowing a more generic file support, rather than a single file type and format, the program can handle future data structures and not just current ones. Two limitations of TAP (and its companion autoKep to convert Kepler FITS files to a format usable in TAP) are that the program is restricted to v1 of the Kepler format and requires an IDL license to run the programs.

BET is capable of detecting and processing eclipses from a single KEPLER FITS file or a folder of FITS files. While individual eclipses can be selected, automated eclipse detection is the default. Automatic eclipse detection allows whole systems to be processed much quicker than individually selecting eclipses. Each eclipse is located by flux data points that fall below two standard deviations of the average flux value. To ensure an entire eclipse is processed (rather than just the section that falls below the average minus two standard deviations line), the data points equivalent to two located eclipse widths either side of the found eclipse are included for processing. Two standard deviations was selected during testing of the program as if the value is too small, variations in the light curve (that aren't eclipses) get detected as eclipses. If the value is too large, eclipses get discarded as variability within the system and aren't processed. Future revisions of BET may change how eclipses are detected and as a result may be able to pick up eclipses that are “hidden” within variability without the need for manual intervention.

A least-squares best fit is performed using the C version of MPFIT (Markwardt 2009) using the functions from Mandel and Agol (2002) in order to model the light curve obtained from KEPLER and determine the mid-eclipse time for each eclipse that is found in the data. Each eclipse is fit individually in order to determine the mid-eclipse time so that eclipse time variability isn’t “averaged out” or accidentally removed.

APPENDIX C

KIC 5095269: ARTIST'S IMPRESSION

To coincide with the publication of Getley et al. (2017), an artist's impression of KIC 5095269 was created by USQ Media Design and appears in figure C.1.

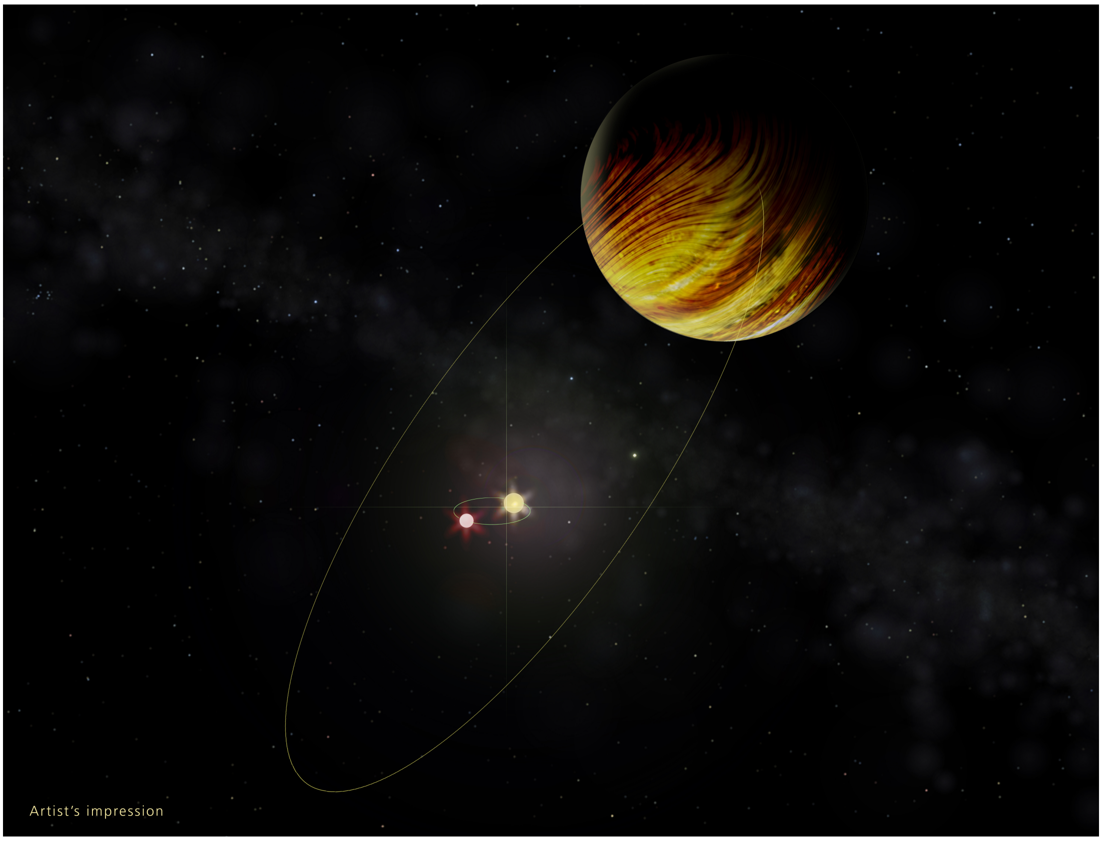

Figure C.1: Artist's impression of KIC 5095269. Credit: USQ Media Design